

**JUNE 2022**

**HASAN KALYONCU UNIVERSITY  
INSTITUTE OF GRADUATE STUDIES**

**DESIGN AND MECHANICAL PROPERTIES OF  
GEOPOLYMER PERVIOUS CONCRETE  
PAVEMENT CURED BY AMBIENT CONDITION**

**Ph.D. THESIS  
IN  
CIVIL ENGINEERING**

**Ph.D. in Civil Engineering**

**Rafah Rasheed Abdulmajeed**

**BY  
RAFAH RASHEED ABDULMAJEED**

**JUNE 2022**

**Design and mechanical properties of geopolymer pervious concrete pavement  
cured by ambient condition**

**Ph.D. Thesis  
In  
Civil Engineering  
Hasan Kalyoncu University**

**Supervisor  
Prof. Dr. Mehmet KARPUZCU**

**Co-supervisor  
Assist. Prof. Dr. Dillshad khidhir Bzeni**

**By  
Rafah Rasheed Abdulmajeed**

**JUNE 2022**

© 2022 [Rafah Rasheed Abdulmajeed]



**INSTITUTE OF GRADUATE STUDIES PhD  
ACCEPTANCE AND APPROVAL FORM**

Civil Engineering Department, Civil Engineering PhD (Philosophy of Doctorate) programme student **Rafah Rasheed Abdulmajeed** prepared and submitted the thesis titled **Design and Mechanical Properties of Geopolymer Pervious Concrete Pavement Cured by Ambient Condition** defened successfully at the VIVA on the date of 30.06.2022 and accepted by the jury as a PhD thesis.

<u>Position</u>	<u>Title, Name and Surname</u> <u>Department/University</u>	<u>Signature</u>
<b>Supervisor</b>	Prof. Dr. Mehmet KARPUZCU Civil Engineering Department/ Hasan Kalyoncu University	
<b>Jury Member</b>	Prof. Dr. Hanifi ÇANAKÇI Civil Engineering Department/ Hasan Kalyoncu University	
<b>Jury Member</b>	Assoc. Prof. Dr. Nildem TAYSI Civil Engineering Department/ Gaziantep University	
<b>Jury Member</b>	Assoc. Prof. Dr. Mehmet Tolga GÖĞÜŞ Civil Engineering Department/ Gaziantep University	
<b>Jury Member</b>	Assoc. Prof. Dr. Adem YURTSEVER Civil Engineering Department/ Hasan Kalyoncu University	

**This thesis is accepted by the jury members selected by the institute management board and approved by the institute management board.**

**Prof. Dr. İbrahim Halil GÜZELBEY  
Director**

**I hereby declare that all information in this document has been obtained and presented in accordance with academic rules and ethical conduct. I also declare that, as required by these rules and conduct, I have fully cited and referenced all material and results that are not original to this work.**

**Rafah Rasheed Abdulmajeed**

## ABSTRACT

### DESIGN AND MECHANICAL PROPERTIES OF GEOPOLYMER PERVIOUS CONCRETE PAVEMENT CURED BY AMBIENT CONDITION

ABDULMAJEED, Rafah Rasheed

Ph.D. in Civil Engineering

Supervisor: Prof. Dr. Mehmet KARPUZCU

Co-supervisor: Assist. Prof. Dr. Dillshad Khidhir BZENI

June 2022, 106 pages

The major binding material required to produce concrete is Portland cement. Portland cement contributes significantly in the global climate change, as the manufacture of 1 ton of cement generates nearly 1000 m<sup>3</sup> of carbon dioxide. Geopolymer concrete is produced through the alkaline activation of alumino-silicates and it has an amorphous to semi-crystalline structure. A pervious concrete pavement absorbs and stores runoff before it infiltrates into the subsoil, and it may have an underlying stone reservoir. This study aims to use both materials together due to the good properties that both materials have for producing geopolymer pervious concrete by developing an appropriate mix quantity, also by determining the characteristics of the geopolymer pervious concrete. This study also aims at developing geopolymer pervious concrete mixtures that contain coarse aggregate. The study was conducted in five phases. In the first- phase and second the key factors affecting the performance of geopolymer pervious concrete were investigated; focusing on the aforementioned parameters using natural coarse aggregate (max. size 14 mm and 20 mm) then the results in order to reach decent mix proportions of the reference mix. In this step a total of 26 mixes were prepared with different proportions of materials. For economical purpose, the Erbil slag was used instead of imported slag in the third fourth and fifth phase, and natural coarse aggregate was used (maximum size 14 mm), which resulted in a total of four mixes with varied proportions of components. This mechanical feature is derived from (compressive strength). After selecting the best mix of geopolymer pervious concrete, a total of 10 mixes of geopolymer pervious concrete were prepared to obtain the best mix proportion with regard to the compressive strength and type (pervious or non- pervious). Finally, after obtaining the best mix proportions from the geopolymer pervious concrete. Then the mechanical properties were founded such as Flow test, Void %, dry density, compressive strength, modulus of elasticity, splitting tensile strength, and flexural strength and infiltration rate and then the second part the design of structural and hydrological by Pervious Pave v1.0. program. The result of geopolymer pervious concrete show that slag content, alkaline -to-slag ratio NaOH molarity and Na<sub>2</sub>SiO<sub>3</sub>-to-NaOH ratio of 325 Kg/m<sup>3</sup>,0.25,12, and 1 respectively gave the best result. The compressive strength was achieved the maximum of 40.17 MPa at age of 28 days, void % 15.37, oven dry density 1858 kg/m<sup>3</sup>, flexural strength 3.37 MPa splitting strength 3.56 MPa, modulus of elasticity 4.2 Gpa and infiltration rate 3545 mm/h.

**Keywords:** Geopolymer, Pervious Concrete, Pervious Pave

## ÖZET

### ORTAM ŞARTLARINA GÖRE KÜRLENEN GEOPOLİMER GEÇİRİMLİ BETON YOLLARIN TASARIMI VE MEKANİK ÖZELLİKLERİ

ABDULMAJEED, Rafah Rasheed

Doktora Tezi, İnşaat Mühendisliği Anabilim Dalı

Tez Danışmanı: Prof. Dr. Mehmet KARPUZCU

Eş Danışman: Dr. Öğr. Üyesi Assist. Prof. Dr. Dillshad Khidhir BZENİ

Haziran 2022, 106 Sayfa

Beton üretmek için gerekli olan ana bağlayıcı malzeme portland çimentosudur. Portland çimentosu, küresel iklim değişikliğine önemli ölçüde katkıda bulunur, çünkü 1 ton çimento üretimi yaklaşık 1000 m<sup>3</sup> karbondioksit üretir. Geopolimer beton, alümino-silikatların alkali aktivasyonu ile üretilir ve amorf ila yarı kristal bir yapıya sahiptir. Geçirgen bir beton kaplama, akışı toprağa sızmadan önce emerek depolar ve altında bir taş rezervuarda saklayabilir. Bu çalışma, uygun bir karışım miktarı geliştirerek geopolimer geçirimli beton üretmek için her iki malzemenin sahip olduğu iyi özelliklerden dolayı her iki malzemenin bir arada kullanılmasını ve ayrıca geopolimer geçirimli betonun özelliklerini de belirlemeyi amaçlamaktadır. Bu çalışma aynı zamanda iri agrega içeren geopolimer geçirimli beton karışımlarının geliştirilmesini de amaçlamaktadır. Çalışma beş aşamada yürütülmüştür. Birinci ve ikinci aşamada, geopolimer geçirimli betonun performansını etkileyen temel faktörler, yukarıda belirtilen parametrelere odaklanarak, doğal iri agrega (en fazla 14 mm ve 20 mm) kullanılarak araştırılmış, ardından referans karışımın uygun karışım oranlarına ulaşmak için sonuçlar incelenmiştir. Bu adımda, farklı oranlarda malzeme ile toplam 26 karışım hazırlanmıştır. Ekonomik amaçla, üçüncü dördüncü ve beşinci aşamada ithal edilen cüruf yerine Erbil cürufu kullanıldı ve doğal iri agrega kullanılmış olup (maksimum boyut 14 mm), bu da çeşitli oranlarda bileşen içeren toplam dört karışım ile sonuçlanmıştır. Bu mekanik özellik (basınç mukavemeti)'den türetilmiştir. En iyi geopolimer geçirimli beton karışımı seçildikten sonra, basınç dayanımı ve türü (geçirgen veya geçirimsiz) açısından en iyi karışım oranını elde etmek için toplam 10 geopolimer geçirimli beton karışımı hazırlanmıştır. Son olarak geopolimer geçirimli betondan en iyi karışım oranları elde edildikten sonra, akış testi, Boşluk yüzdesi, kuru yoğunluk, basınç dayanımı, elastisite modülü, yarmada çekme dayanımı ve eğilme dayanımı ve sızma hızı gibi mekanik özellikler belirlenmiş ve sonra ikinci kısımda Pervious Pave v1.0. programı kullanılarak yapısal ve hidrolojik tasarım yapılmıştır. Geopolimer geçirgen betonun sonucu, sırasıyla 325 kg/m<sup>3</sup>, 0,25,12 ve 1'lik cüruf içeriği, alkalın-cüruf oranı NaOH molaritesinin ve Na<sub>2</sub>SiO<sub>3</sub>-NaOH oranının 1 olduğunu göstermektedir. Basınç dayanımı 28 günlükken maksimum 40,17 MPa, boşluk % 15,37, fırın kuru yoğunluğu 1858 kg/m<sup>3</sup>, eğilme dayanımı 3.37 MPa yarma dayanımı 3,56 MPa, elastisite modülü 4,2 GPa ve sızma hızı 3545 mm/saat olarak elde edilmiştir.

**Anahtar Kelimeler:** Geopolymer, Geçirimli Beton, Geçirimli Kaldırım

To

Soul of my Father

My Mother

My Sisters

My Husband and All my Children my love

This work wouldn't even be possible without them

## ACKNOWLEDGEMENTS

Thanks to Allah who gave me a power and patient to complete this PhD works successfully.

Worm express and appreciations then goes to my supervisor Prof. Dr **Mehmet Karpuzcu** My local supervisor Assist. Prof. Dr. **Dillshad Khidhir Bzeni** for their regular support, guidance throughout the fulfillment of this study. Great thanks go to Assoc. Prof. Dr. **Adem YURTSEVER** for his regular support. Special thanks to the staff in my University Erbil Technical Engineering College. Represented by the Dean and Head of the Civil Engineering Department.

Special thanks to the Dr. **Mohamed Moafak Arbili** and Eng. **Parwar Rasheed** Special thanks and gratitude's to my family, in particular my husband (Eng. **Mustafa BAJALAN**) for their continuous support to overcome all difficulties and problems throughout conducting this study.

Finally, I would like to dedicate this work to my mother andI would like to dedicate this work to the spirit of my father, God bless him.

## TABLE OF CONTENTS

	<b>Pages</b>
<b>ABSTRACT</b> .....	<b>V</b>
<b>ÖZET</b> .....	<b>VI</b>
<b>ACKNOWLEDGEMENTS</b> .....	<b>VIII</b>
<b>TABLE OF CONTENTS</b> .....	<b>IX</b>
<b>LIST OF TABLES</b> .....	<b>XIII</b>
<b>LIST OF FIGURES</b> .....	<b>XIV</b>
<b>LIST OF SYMBOLS AND ABBREVIATIONS</b> .....	<b>XVII</b>
<b>CHAPTER 1</b> .....	<b>1</b>
<b>INTRODUCTION</b> .....	<b>1</b>
1.1 Background .....	1
1.2 Aim of the Research.....	5
1.3 The Research Layout.....	6
<b>CHAPTER 2</b> .....	<b>7</b>
<b>LITERATURE REVIEW</b> .....	<b>7</b>
2.1 Pervious Concrete .....	7
2.2 Advantages and Disadvantages of Using Geopolymer Concrete .....	8
2.2.1 Advantages of pervious concrete. ....	8
2.2.2 Disadvantages of pervious concrete.....	8
2.3 History of Geopolymer .....	9
2.4 History of Geopolymer Concrete .....	9
2.5 Investigation.....	10
2.6 Ground Granulated Blast Slag (GGBS).....	11
2.7 Dissolution Process .....	12
2.8 Polymerisation Process .....	12
2.9 Growth .....	12
2.10 Advantages and Disadvantages of Using Geopolymer Concrete. ....	13
2.10.1 Environmental.....	13
2.10.2 Economical.....	13

2.10.3 Chemical resistance.....	14
2.10.4 Pozzolanic composition analysis.....	14
2.10.5 Workability .....	14
2.11 Hydration Reaction .....	15
2.11.1 Alkaline activators .....	15
2.11.2 Sodium hydroxide (NaOH).....	15
2.11.3 Sodium Silicate (Na <sub>2</sub> SiO <sub>3</sub> ).....	16
2.12 Binder Constituent Proportioning .....	17
2.12.1 Activator concentration.....	17
2.12.2 Pozzolanic / activator ratio.....	18
2.12.3 Sodium silicate and hydroxide activator ratio.....	18
2.13 Curing Geopolymer Method .....	18
2.14 Strength Development of Alkaline-Activated Concrete .....	19
2.15 Analytical Methods .....	20
2.16 Factors Affect Geopolymer Binder/Concrete .....	22
2.17 Geopolymer Concrete .....	23
2.18 Geopolymer Pervious Concrete .....	27
<b>CHAPTER 3 .....</b>	<b>30</b>
<b>MATERIALS AND EXPERIMENTAL PROCEDURES.....</b>	<b>30</b>
3.1 Introduction.....	30
3.2 Materials.....	30
3.2.1 GGBFS Slag.....	30
3.2.2 Iron blast-furnace slag.....	31
3.2.3 Chemical and mineralogic composition.....	31
3.2.4 Erbil steel slag .....	33
3.2.5 Erbil steel steam condenser.....	34
3.2.6 Composition of brick materials .....	34
3.2.7 Sodium silicate solution (Na <sub>2</sub> SiO <sub>3</sub> ).....	35
3.2.8 Sodium hydroxide (NaOH).....	36
3.2.9 Super plasticizer and water .....	37
3.2.10 Coarse aggregates.....	37
3.3 Mix Proportions .....	37
3.4 Experimental Program .....	41
3.4.1 Preparation of the alkaline activator solutions .....	41

3.4.2	Mixing procedure .....	42
3.4.3	Casting and preparing the samples.....	42
3.4.4	Curing.....	44
3.5	Testing of Geopolymer Pervious Concrete. ....	44
3.5.1	Flow table test .....	44
3.5.2	Compressive strength test .....	45
3.5.3	Modulus of elasticity test .....	45
3.5.4	Splitting tensile strength test .....	46
3.5.5	Flexural strength test.....	46
3.5.6	Surface infiltration rate test.....	47
3.5.7	Density (unit weight) test.....	47
3.5.8	Voids content test.....	47
<b>CHAPTER 4</b>	.....	<b>49</b>
<b>RESULTS AND DISCUSSION</b>	.....	<b>49</b>
4.1	Introduction.....	49
4.2	Factors Affecting Geopolymer Paste and Concrete .....	50
4.2.1	Effect of alkali / GGBFS ratio .....	51
4.2.2	Effect of molarity of NaOH .....	53
4.2.3	Effect of sodium silicate to sodium hydroxide (SS/SH) ratio.....	55
4.2.4	Statistical model.....	57
4.3	Functional and Mechanical Properties .....	60
4.3.1	Compressive strength and splitting strength .....	61
4.3.2	Compressive strength and modulus of elasticity.....	63
4.3.3	Compressive strength and flexural strength.....	64
4.3.4	Flexural strength and splitting strength.....	65
4.3.5	Compressive strength and infiltration rate .....	66
4.3.6	Void ratio and oven dry density .....	68
4.3.7	Infiltration rate and void ratio .....	69
4.3.8	Effects of types of compactions .....	70
4.4	Partial Replacement of GGBFS by Waste Products .....	72
<b>CHAPTER 5</b>	.....	<b>74</b>
<b>STRUCTURAL AND HYDROLOGICAL DESIGN BY PERVIOUS PAVE v1.074</b>		
5.1	Description .....	74
5.2	Application.....	75

5.3 Limitations .....	76
5.4 Design theory .....	76
5.5 The Design process involves two design criteria.....	77
5.5.1 Structural design.....	77
When the FD total reaches 100%, the limiting structural design requirement, PerviousPavev1.0 increases the pervious concrete pavement thickness while computing the FD total for each axle type and load group.....	78
5.5.2 Hydrological design .....	78
5.6 Design by Pervious Pave V1.0 Software .....	80
5.6.1 Pervious pave software .....	81
5.6.2 Research study .....	82
5.6.3 Data base for the study .....	83
5.6.4 Design steps by pervious pave v1.0 .....	85
5.6.5 Results analysis .....	85
5.7.6 Design chart .....	90
5.7.7 Examples.....	92
<b>CHAPTER 6 .....</b>	<b>94</b>
<b>CONCLUSIONS AND RECOMMENDATIONS.....</b>	<b>94</b>
6.1 Conclusions .....	94
6.2 Recommendations .....	97
<b>REFERENCES .....</b>	<b>98</b>

## LIST OF TABLES

	<b>Pages</b>
<b>Table 3.1</b> Major Chemical Constituents in Blast Furnace Slag.....	32
<b>Table 3.2</b> Chemical and mineralogic composition of Erbil steel slag.....	33
<b>Table 3.3</b> Chemical and mineralogic composition of Erbil steam condenser.....	34
<b>Table 3.4</b> Mix proportion of geopolymer pervious concrete (max. size 20 mm).....	39
<b>Table 3.5</b> Mix proportion of geopolymer pervious concrete (max. size 14 mm).....	40
<b>Table 3.6</b> Mix proportion of geopolymer pervious concrete (Erbil Steel Slag; Erbil Steam Condenser; Brick Powder).....	41
<b>Table 3.7</b> shows the compressive strength of the above three methods of casting concrete .....	43
<b>Table 3.8</b> The selected mix from trial mixes depending on the largest compressive strength and types (pervious or non-pervious).....	48
<b>Table 4.1</b> Average compressive strength and perviousness of geopolymer pervious concrete after 28 days of ambient curing made with maximum size 14 mm aggregate .....	51
<b>Table 4.2</b> Effect of Alkali//GGBFS ratio on compressive strength of GPPC .....	52
<b>Table 4.3</b> Effect of NaOH Molarity on compressive strength of GPPC .....	54
<b>Table 4.4</b> Effect of SS/SH ratio on the compressive strength of GPPC.....	55
<b>Table 4.5</b> Empirical obtained from the Reaggregation Analysis. ....	58
<b>Table 4.6</b> Showing the Statistical Analysis the goodness of Models .....	58
<b>Table 4.7</b> Effect of the product of molarity and SS/SH ratio on the Compressive strength and void content of GPPC specimen.....	58
<b>Table 4.8</b> Effect of type of compaction .....	72
<b>Table 4.9</b> Mix proportion of geopolymer pervious concrete (Erbil Steel Slag; Erbil Steam Condenser; Brick Powder) .....	73
<b>Table 5.1</b> Laboratory test results on pervious concrete samples: $f_c$ , $r_p$ , and $M_r$ .....	83
<b>Table 5.2</b> Traffic load spectrum .....	84

## LIST OF FIGURES

	<b>Pages</b>
<b>Figure 2.1</b> XRD spectra (a) un-reacted fly ash;(b) alkali-activated fly ash 20 h at 85 °C (Van et al., 1999). .....	21
<b>Figure 2.2</b> Micrographs of alkali-activated PFA geopolymer fracture surface. Fe <sub>2</sub> O <sub>3</sub> is denoted by an arrow (Jiminez et al. 2004) .....	21
<b>Figure 2.3</b> Micrographs of alkali-activated PFA geopolymer fracture surface. (Jiminez et al. 2004).....	22
<b>Figure 2.4</b> Micrographs of alkali-activated PFA geopolymer fracture surface exhibiting PFA particle with reaction shells as well as unexplained spherical assemblages (Jiminez et al. 2004).....	22
<b>Figure 2.5</b> Micrographs of alkali-activated fracture surface. (Jiminez et al. 2004) ..	22
<b>Figure 2.6</b> Geopolymer formation conceptual model (Faris et al., 2017b).....	25
<b>Figure 3.1</b> GGBFS Slag. ....	31
<b>Figure 3.2</b> Erbil steel slag.....	33
<b>Figure 3.3</b> Sodium silicate solution.....	35
<b>Figure 3.4</b> Super Plasticizer .....	36
<b>Figure 3.5</b> Sodium hydroxide.....	36
<b>Figure 3.6</b> Grading curves for coarse aggregate (gravel).....	37
<b>Figure 3.7</b> Compaction by jack hummer .....	43
<b>Figure 3.8</b> Flow Table Test .....	44
<b>Figure 3.9</b> Compressive Strength Test .....	45
<b>Figure 3.10</b> Modulus of Elasticity Test.....	45
<b>Figure 3.11</b> Splitting Tensile Strength Test .....	46
<b>Figure 3.12</b> Flexural strength test.....	46
<b>Figure 3.13</b> Surface Infiltration rate test .....	47
<b>Figure 4.1</b> Effect of Alk/GGBFS ratio on compressive strength .....	53
<b>Figure 4.2-a</b> Effect of NaOH molarity on compressive strength of GPPC.....	54
<b>Figure 4.2-b</b> Effect of NaOH molarity on the percentage of voids.....	55
<b>Figure 4.3-a</b> Effect of SS/SH ratio on compressive strength .....	56

<b>Figure 4.3-b</b> Effect of SS/SH ratio on the percentage of voids.....	57
<b>Figure 4.4-a</b> the effect of (Molarity X SS/SH) on the Compressive Strength of GPPC produced with maximum size of 14 mm, Alk/GGBFS ratio of 0.25 and GGBFS content 325 kg/m <sup>3</sup> .....	59
<b>Figure 4.4-b</b> The effect of (Molarity X SS/SH) on the percentage of voids of GPPC produced with maximum size of 14 mm, Alk/GGBFS ratio of 0.25 and GGBFS content 325 kg/m <sup>3</sup> .....	60
<b>Figure 4.5</b> Relationship between Void ratio and 28 day compressive strength of GPPC made with maximum size 14 mm .....	61
<b>Figure 4.6</b> Compressive strength and Splitting Strength.....	62
<b>Figure 4.7</b> Compressive strength and Modulus of Elasticity .....	64
<b>Figure 4.8</b> Compressive strength and Flexural Strength .....	65
<b>Figure 4.9</b> Flexural Strength and Splitting Strength .....	66
<b>Figure 4.10</b> Compressive strength and Infiltration Rate .....	68
<b>Figure 4.11</b> Void Ratio and Oven Dray Density .....	69
<b>Figure 4.12</b> Infiltration Rate and Void ratio.....	70
<b>Figure 4.13</b> Compressive Strength and Types of Compactions .....	71
<b>Figure 5.1</b> Typical cross-section of pervious concrete paver units .....	75
<b>Figure 5.2</b> Application Pervious concrete pavements.....	76
<b>Figure 5.3</b> Atypical section of the pervious concrete pavement. ....	76
<b>Figure 5.4</b> Mathematical Model for Pervious Concrete Pavement .....	77
<b>Figure 5.5</b> show the screen menu of the Previous Pav v1.0.....	81
<b>Figure 5.6</b> Final step of design by Previous Pave v1.0 .....	82
<b>Figure 5.7</b> Pervious concrete pave model for the study .....	83
<b>Figure 5.8</b> Pervious pave and open graded sub-base thickness vs. pave concrete compressive strength for various traffic load.....	87
<b>Figure 5.9</b> Open graded layer thickness vs. rain intensity for various concrete compressive strength for parking lots area of Traffic A (ADTT=2).....	87
<b>Figure 5.10</b> Pervious pave and open graded sub-base thickness vs. pave concrete compressive strength for various traffic category and rain intensity 70 mm. ....	88
<b>Figure 5.11</b> Pervious pave and Open graded sub-base thickness vs. pave concrete compressive strength for various traffic category under rain intensity 70 mm.....	89
<b>Figure 5.12</b> Rain intensity vs. Entire water volume infiltrated and calculated infiltration time by soil and drain pipes. ....	90

<b>Figure 5.13</b> Design flow chart.....	91
<b>Figure 5.14</b> Mathematical model .....	92

## LIST OF SYMBOLS AND ABBREVIATIONS

ACI	American concrete institute	
ASTM	American society for testing and materials	
Alk	Alkali solution	
GGBFS	Granular Ground blast Furnace Slag	
GPPC	Geopolymer pervious concrete	
MPa	Megapascal $N/mm^2$	
Gpa	Gigapascal (1000 Mpa)	
$Al_2O_3$	Aluminum oxide	
CaO	Potassium hydroxide	
KOH	Potassium oxide Calcium oxide	
$K_2O$	Potassium oxide	
$CO_2$	Carbon dioxide	
$C_3A$	Aluminate	
$Fe_2O_3$	Iron oxide	
$H_2S$	Hydrogen sulphide	
NaOH	Sodium hydroxide	
$Na_2O$	Sodium oxide	
ADTT	average daily truck traffic	
Symbol	Factor	Unite
hp	pervious pave thickness	mm
rp	void ratio for pervious pave	%
hs	open graded sub-base thickness	mm
rs	void ratio for open graded sub-base	%
I	rain intensity	mm
Vw	entire volume of water	$m^3$
k	infiltration rate of subgrade soil	m/hr
Tc	calculated time for full infiltration	hr
Tmax	maximum time of infiltration	hr
Ap	area of pervious pave zone	$m^2$

Ab	area of non-pervious pave zone	m <sup>2</sup>
hcrub	curb stone height	mm
fc	compressive strength of pervious concrete	Mpa
Mr	rupture strength of pervious concrete	Mpa
R	resilient modulus of open graded subbase	Mpa
C.B.R	California bearing ratio	%
PC	Portland Cement	
GGBS	Ground Granulated Blast Furnace Slag	
CA	Coarse Aggregate.	
BMPs	Best Management Practices	
EPA	Environmental Protection Agency	
UHI	Urban Heat Island.	
PFA	pulverized Fly Ash	
SS/SH	Sodium Silicate to Sodium Hydroxide Ratio.	
FD <sub>total</sub>	Total fatigue damage	%
FD <sub>single</sub>	fatigue damage from single axle loads	%
FD <sub>tandem</sub>	fatigue damage from tandem axle loads	%

# CHAPTER 1

## INTRODUCTION

### 1.1 Background

Concrete as manufacture material shows a vital role wide-reaching, which is composed of cement, aggregate and water. Cement, which is a main component of concrete, produces a significant quantity of CO<sub>2</sub> into the environment during manufacturing. It is predicted that each 1000 m<sup>3</sup> of ordinary Portland cement PC products releases one ton of CO<sub>2</sub>. which causes it to be the second largest producer of greenhouse (Jamal, 2019; Arafa et al., 2017).

One ton of CO<sub>2</sub> is predicted to be discharged into the environment for each ton of synthetic Portland cement. To extract raw minerals, the method involves high temperatures 1400–1500 °C and quarry demolition, and it releases greenhouse gases such as CO<sub>2</sub>. (Fernandez-Jimenez et al., 2006; Arafa et al., 2017). For this reason, engineers are researching continuously to invention a different material or materials for Portland cement that is not harmful for our environment and gives the same advantages.

Optional pozzolanic components, such as slag Palm oil fuel waste, fly ash, and rice husk, are used to reduce the development of Portland cement PC. When compared to PC production, ash is utilized as an alternative cementitious material to exchange a portion of Portland cement. These materials are made from items from modern processes and hence use less energy to produce (Chindaprasirt et al., 2007; Tangchirapat et al., 2009; Malayali et al., 2020). The impact heaters used to manufacture iron produce ground granulated blast furnace slag GGBFS. These operate at a temperature of roughly 1500 degrees Celsius and are powered by a well-balanced blend of iron ore, coke, and limestone. Only a small amount of GGBFS is used only (Huang et al., 2010; Malayali et al., 2020). Its high void content allows it to be used in a variety of purposes, including thermal insulation, acoustic absorption,

solid bed for vegetation or living beings, and water refining. (Yang et al., 2003; Malayali et al. 2020; Kim, 2010).

As a result, pervious concrete is good for the environment. The permeable compacted blend is prepared up of protection material, coarse total, nearly no fine totals, water, and some admixture, if required. Furthermost situations, Portland cement is employed as a required material in pervious concrete, and there is currently a lack of emphasis on alternate constraining materials, for example geopolymer fasteners, in pervious concrete. Slag GGBFS is now commonly utilized in the manufacturing of geopolymer concrete. Geopolymer, a mineral polymer, is created when aluminosilicate rocks react with alkaline fluids (Chindaprasirt et al., 2008). Many excellent properties of geopolymer have been demonstrated, including exceptional confrontation to acid and sulfate assaults, high primary strength, and moral concert at high temperatures (Malayali et al., 2019; Deo et al., 2010). Geopolymer eliminates the need for cement, lowering greenhouse gas emissions by 44–64 percent. Additionally, dissipates and byproducts like blast furnace slag and fly ash are good sources of aluminosilicate, which is utilized to make geopolymer. Geopolymers have a lesser environmental impact than other forms of concrete binders because they are manufactured from waste materials (Rahmat et al., 2017; Nawy, 2008; Arafa et al. 2017).

The main purpose of this research is to develop a type of concrete that permits water to distribute through it pervious concrete. Pervious concrete can also be utilized as a temporary rainfall and pavement storage area. This kind of pavement can help users stay safe while reducing skid resistance. Pervious concrete is a kind of concrete with voids and a high-water permeability when assessed to standard concrete. It was created as a green material for permeable pavement, water purification, thermal insulation, acoustic absorption, and other civil and architectural uses (Kevern et al., 2009; Kim et al., 2010).

Pervious concrete has a void content ranging from 15% to 35%, with connected pore sizes ranging from 2 mm to 8 mm in diameter and compressive strengths ranging from 2.8 MPa to 28.0 MPa. The high porosity comes from a significantly connected void content. Pervious concrete with a high void content allows water to drain naturally at rates ranging from 81 to 730 L/min/m<sup>2</sup>, obviating the need for

conventional surface-water drainage infrastructure, reducing runoff, and allowing ground water recharge where conventional concrete does not ACI 522-2010. It is suitable for pedestrian pathways, park spaces, tennis courts, greenhouses, low-traffic zones, and other civil engineering and architectural projects ACI522-2010 (Tyner et al., 2009b). CA, binder, and admixture are the most common components of pervious concrete. In most cases, Portland cement is applied as the requisite material in pervious concrete such as geopolymer binders, in pervious concrete is immobile needed (Arafa et al., 2017).

Every street pavement is designed to facilitate traffic flow while also providing drainage. The objective of having a drainage system on the street is to ensure that water, that flows on the street surface, may be collected and transferred underground to another stormwater drainage system (Valiev and Kosimov, 2019). As a result, it is critical to stress the necessity of ensuring that the drainage system, particularly the stormwater inlet, is well-designed and operates efficiently to handle large amounts of stormwater. In general, academics have conducted a number of studies on stormwater inlets. The hydraulic behavior of stormwater inlets has been discovered to be difficult to comprehend (Zakaria et al. 2004; Sathonsaowaphak et al.,2009).

As a result, experimental and numerical research on stormwater inlets have been conducted, with a focus on inlet performance and efficiency (Fernandez-Jimenez et al., 2006; Nawy 2008; Zakaria et al., 2004; Park et al., 2010; Mahboub et al., 2009). Based on prior studies, it could be decided that insurrection the inlet spacing or amount of inlets would improve the hydraulic performance of stormwater inlets. Modifications to the stormwater inlet design could be altered in terms of dimension, grate geometry, or both (Kevern et al., 2009).

However, it appears that improving the stormwater inlet's performance is insufficient to prevent water ponding and increase the pastoral stormwater drainage system's managing. As a different, pervious road pavement technology has been extensively applied. It has been designated as one of the Best Management Practices (BMPs) for long-term stormwater management to reduce road flooding by the Environmental Protection Agency EPA. This technology allows stormwater to seep straight through the pavement apparent into sub drainage, consequential in considerable stormwater management and environmental benefits (Duxson et al. 2007; Chindaprasirt et al.,

2008). Many research has been done on pervious street pavement to see how it performs, how durable it is, and how it could be improved (Tho-in et al., 2012; Luck et al. 2009).

However, completely adopting pervious street pavement is difficult since the pavement's construction presents more difficulties than conventional pavement because it has more requirements to meet. As recently stated by, there are numerous obstacles to overcome and factors to consider (Neithalath et al., 2006). There is still a scarcity of knowledge and skills in the field of pervious pavement, among other things. As a result, rather than using pervious street pavement, which is extra difficult, expensive, and large-scale, this research will use an original sustainable technology named pervious curb as an alternative. The most common material used to construct pervious curbs is pervious concrete, as well identified as porous concrete or high permeability concrete (Park et al., 2004; Chokkalingam et al., 2018). The components consumed in this concrete are identical to those used in impermeable concrete, with the exception that it contains little or no small particles, resulting in large spaces that allow water to pass. (Haselbach et al., 2006; Lian et al., 2010).

The major purpose of implementing the pervious road curb concept is because it is extremely usual to see excess rainwater runoff gathered and concentrated between the street curb and gutter during a storm. Despite the fact that the roadway curb has a stormwater intake, it still has restrictions and is unable to totally eliminate water ponding. Stormwater was predicted to be proficient to completely infiltrate into the side surface of the pervious curb after pervious concrete was applied to the street curb. This novel solution, rather of depending exclusively on the impermeable roadside curb as a barrier, might be integrated into the stormwater drainage system. It has a high chance of increasing stormwater removal rates and, as a result, reducing water ponding on the road. As a result, the goal of this investigation is to explain a new infiltration rate test that is tailored to pervious concrete installations on road curbs. While doing so, the infiltration rate and flow net of the concrete will be studied (Valiev and Kosimov, 2019).

## 1.2 Aim of the Research

The aim of the first section of this investigate is to determine the optimum mix proportion of geopolymer pervious concrete which is composed with geopolymer paste and coarse aggregate. The objectives are listed as follows:

Fifty-four mixes of geopolymer pervious concrete are prepared, the samples were preserved at ambient curing situations. The impacts of ground granulated blast furnace slag GGBFS content ranging from 300 to 450 kg/m<sup>3</sup>, alkaline solution to slag (Al/GGBFS) ratio by mass of 0.25, 0.3 and 0.35, NaOH concentration Molarity of 8,10,12,14,16, sodium silicate solution to sodium hydroxide solution (SS/SH) ratio by mass of 1.0, 1.5, 1.75, 2,2.25,2.5,2.75,3.0) and two aggregate sizes of 14 and 20 mm on compressive strength and its performance whether they are pervious or not pervious, are studied.

The optimal geopolymer pervious concrete mixture proportion, in addition to their physical and mechanical characterise, are investigated. Compressive strength, modulus of rupture, tensile splitting strength, and modulus of elasticity, as well as percentage of void content, bulk density, and infiltration rate, are determined, these are all important properties for the design of concrete pavement to carry traffic loads and infiltrate a significant amount of surface water during floods.

For economic reasons and ensuring long-term sustainability various waste products that are abundant in our region as industrial by products, such as Erbil steel slag, Erbil slag steam condenser, and waste fired clay products are utilized as a partial replacement. These materials have never been the subject of any prior research. The major goal is to use these materials as a partial replacement for GGBFS-slag, which is commonly imported into our region. To see if these materials could be used to make geopolymer pervious concrete. Different percentages from 25 % to 100 % of these waste products are employed as a partial substitute.

The impacts of various forms of compaction on the compressive strength and void content of Geopolymer pervious concrete samples are studied, such as compaction with a tamping rod, compaction by Jack hammer with a base plate, and compaction with a vibrating table.

The goal of second part dealt with the structural and hydrologic design of pervious concrete pavements using pervious pave-version 1.0, in which the relevant properties of the best mixture proportion of geopolymer pervious concrete were used as input data and a reasonable value of CBR of the compacted subgrade soil was handled to estimate the thickness of the pavement slab, thickness of open graded subbase required based on the traffic category and the intensity of rain water, as well as the total infiltrated water volume.

### **1.3 The Research Layout**

- Chapter One: provides a brief background of the geopolymer pervious concrete.
- Chapter Two: displays a literature review on Pervious concrete, geopolymer concrete and geopolymer Pervious concrete.
- Chapter Three: provides a detailed presentation of the materials, mix proportions, experimental program, and the tests applied on geopolymer pervious concrete.
- Chapter Four: presents the outcomes and examination of the research and comparison of separate outcomes is performed.
- Chapter Five: Then along with the second part the design of structural and hydrological. By Pervious Pave v1.0. program.
- Chapter six: describes the concluding points and recommendations for further study.

## **CHAPTER 2**

### **LITRATURE REVIEW**

#### **2.1 Pervious Concrete**

Pervious concrete has been used in many countries for more than 30 years, mainly in England and the United States (Kevern et al. 2005; Tho-in et al., 2012). Pervious concrete also called porous concrete or water-permeable concrete is a type of concrete with a high void content that allows air or water to pass through it. Many countries have conducted field investigations of pervious concrete sidewalks, parking lots, and recreation squares (Chandrappa and Biligiri, 2016; Sun et al., 2018). It can be used to build park areas, light-traffic areas, pedestrian walkways, tennis courts, greenhouses, and other civil engineering and architectural project work (Chen et al., 2013; Tyner et al., 2009a; Tho-in al., 2012).

Its high vacuum content allows it to be used in a variety of other applications, including thermal insulation, sound absorption, a concrete substrate for plants or organisms, and water purification. (Yang and Jiang, 2003; Kim et al., 2010; Tho-in et al., 2012). Because of its high voids content, it can be used for a variety of purposes, including heat insulation, sound absorption, solid bed for plants or organisms, and water purification. (Yang and Jiang, 2003; Kim et al., 2010). Among the many environmental advantages of a former concrete pavement are the elimination of stormwater run-off, the reduction of the urban heat island (UHI) effect, the removal of water pollutants, and the maintenance of groundwater levels (Chandrappa and Biligiri, 2016; Ibrahim et al. 2014; Sun et al.,2018).

The connected pore size ranges from 2 to 8 mm, the void content is from 18 to 35 percent, and the compressive strength is from 2.8 to 28.0 MPa, which is typical for ex-concrete (Tho-in et al. 2012). The former concrete is lightweight and consists of coarse aggregate, Portland cement and water. Standard airspaces for pre-mix concrete in the United States are between 14 and 13 (Chokkalingam et al.,2018; Tho-in et al., 2012). The carefully measured amount of cement paste covers and binds the aggregate together, which may also comprise additional cementitious materials (SCM) and chemical admixtures (Chen et al., 2013; Sun et al., 2018).

Pervious concrete is lightweight concrete with voids that allow water to pass through. Groundwater recharge, tire noise reduction, rainwater run-off prevention and rainwater scattering during rainy seasons are all advantages of using pervious concrete (Tennis et al., 2004; Babu and Babu, 2017). All of these factors combine make pervious concrete a low-impact paving approach that is ecologically friendly growth (Luck et al., 2008; Sun et al., 2018). Waterproofing is aided by the higher porous content of the precast concrete, but at the cost of a significant reduction in mechanical strength (Sonebi et al., 2016; Chandrappa and Biligiri, 2016).

## **2.2 Advantages and Disadvantages of Using Geopolymer Concrete**

### **2.2.1 Advantages of pervious concrete.**

- • Assists in the effective management of rainwater.
- • Helps drain rainwater to the ground and prevent waterlogging.
- • It is also useful in areas of low rainfall to increase the level of groundwater.
- • Reduces runoff.
- • Reduces the risk of flooding.
- • Ensures pedestrian safety because it dries quickly.

### **2.2.2 Disadvantages of pervious concrete**

- The compressive strength of pervious concrete is lower than that of conventional concrete.
- Because of water intrusion, it requires routine maintenance.
- Pre-concrete cannot be applied to roads with heavy traffic.
- The durability of the pervious concrete is lower.

- Because of the water-absorbing property, there may be a problem with corrosion of the rebar.
- Because of the loose aggregate, there is a chance of transferring on the surface.

### **2.3 History of Geopolymer**

Following a series of devastating fires in France between 1970 and 1973, Davidovits began researching fire-resistant materials. J.P. Latapie and M. Davidovics, a team of ceramicists, proved in 1972 that water-resistant ceramic tiles could be made at temperatures lower than 450°C without firing. Besson et al. produced hydrosulfite from diffraction patterns in 1969. this geological synthesis the ability of the aluminum particle to produce crystallographic and chemical changes in a silica backbone is critical for geosynthesis. The word "geopolymer" was coined by Davidovits in 1979 (Davidovits, 2002). Many novel materials have been developed thanks to geopolymer technology. Similar to organic polymers made from oil, geopolymers go through polycondensation and solidify quickly at low temperatures, in only a few minutes. that is, inorganic, solid, non-flammable, and stable at temperatures as high as 1250 °C. These characteristics greatly accelerated invention and advancement. (Davidovits, 1994).

### **2.4 History of Geopolymer Concrete**

Davidovits developed an alternative theory concerning the construction of the Great Pyramids in the 1980s. The Egyptians did not drag the blocks to the pyramids; instead, they made them one by one and placed them on the pyramids. The blocks, according to Davidovits, were made by pouring an ancient concrete into wooden molds, which he dubbed geopolymer. Some workers would be required to transport sacks of wet geopolymer concrete to wooden forms precisely where each block was needed. As a compacted moist blend hardens against surrounding blocks, joints between poured concrete blocks would always be exactly accurate. The geopolymer concrete, according to Davidovits, was constructed using crushed limestone, clay, water, and a strongly alkaline opposite of acidic activator that caused the crushed limestone mixture to reconstitute into a man-made stone form (Davidovits, 2008).

Balaguru et al. (1997) revealed the utilization of geopolymer composites for strengthening concrete structures as well as geopolymer coating to protect the transportation infrastructures. The researchers wanted to see if geopolymer could be used instead of organic polymers to secure carbon fabrics to concrete. Their findings revealed that geopolymer has great adhesion to both the concrete surface and the interlaminar planes of textiles, implying that geopolymer composites can be used to efficiently strengthen reinforced concrete beams. Geopolymer outperformed organic polymers in terms of adhesion, fire resistance, and ultraviolet light durability, and it didn't include any harmful elements (Jamal, 2019).

## **2.5 Investigation**

Commonly utilized with PC in buildings are GGBS and PFA. Technical advantages of using such materials in concrete include improved long-term strength, durability, and workability. Geopolymers are not employed in fast-track construction because their strength develops at a much slower rate than PC-based concrete at an early age. The biggest disadvantage of employing geopolymers rather than PC is this. Fast-track concrete mixes with excellent early-age strength are required in today's construction industry. As a result, elements like cementitious additives play a role. Early on, it is critical to think about the curing temperature and mix proportions that effect strength. The amount of PFA and GGBFS that can be used as a PC substitute material in concrete is determined by the required early strength. It is necessary to explore the role of PFA and GGBFS in the hydration of total binder content in concrete.

Geopolymer concrete's early strength development is problematic because its strength is mostly affected by the concrete's mix balance and the environment in which it cures. Unfortunately, the majority of data and procedures for predicting the strength of geopolymer concrete were only described on a computer. Due to the lack of precision, the conclusions are occasionally wrong when the methodologies are applied to estimate geopolymer strength growth. To help contractors recognize the precise early-age strength development of geopolymer concrete, a specific method for estimating strength growth of geopolymer concrete is necessary. (Safari, 2016).

## **2.6 Ground Granulated Blast Slag (GGBS)**

Ground Granulate Blast Furnace Slag is mostly composed of alumina-silicates, magnesium, and calcium, and it is created in a molten state in a blast furnace with pig iron during the reduction of iron ore. The slag is separated into different types depending on how it is cooled. When Granulate Blast Furnace Slag is showered with iron to generate granules with an amorphous structure, it achieves the maximum cementing capabilities. GGBFS is the fine powder generated by grinding and drying this substance (Imbabi et al., 2012). GGBFS is a semi-cementitious material that will harden with time. Even yet, between 10% and 90% of GGBFS is routinely combined with PC, which produces both sulphate and hydroxide ions, speeding up the GGBFS's strengthening benefit (Bone et al., 2004).

PFA and GGBFS both improve the workability and mobility of concrete with the same water content. These substances are also less expensive than PC. The volume of fine powder rises with fly ash and GGBFS due to the decreased density of the replacement, resulting in greater cohesion. When PFA is used in concrete, there is less bleeding, however GGBFS can increase bleeding for bigger volume replacements. In the concrete mix, PFA and GGBFS will increase setting durations by 1 to 4 hours over PC. Because the heat produced within the concrete is less long-lasting in the winter, extra vigilance is essential when utilizing Fly Ash and GGBFS. The addition of GGBFS and PFA causes the strengthening process to take longer, but if the curing period is extended enough, greater final strengths can be produced (King, 2012).

PFA and GGBFS boosted sulphate resistance while decreasing alkali-silica attack. When up to 70% of the cement is replaced, the heat of hydration is reduced, and thermal stress is reduced. However, such results could be explained by decreased creep, and the tensile strain capacity could be lower (King 2012). Slag materials can be used in a variety of methods, but when used as partial PC replacements, they are usually blended with a 3.5/5.5 percent (by mass) sodium hydroxide or sodium silicate solution (Shen et al., 2006). This alkali activation produces a calcium silicate hydrate gel with a high amorphousness and low basicity (C-S-H). Alkali-activated slag is a term used to describe this mixture, but it is becoming less common (Pacheco-Torgal et al. 2008).

The saturated GGBFS blend has a much more porosity and chemical shrinkage than the PC blend, which is a real issue during the setting process. The hydration process causes drying shrinkage, which has been proven to increase with increased alkali modulus and sodium silicate-based activator dosages (Fernández-Jiménez et al., 2007). Increasing the alkaline concentration in the mix, on the other hand, improves the microstructure characteristics of the C-S-H constituents while reducing pore volumes (Fernández-Jiménez et al., 2007)

## **2.7 Dissolution Process**

When an alkaline solution dissolves the aluminum silicate found in pozzolanic minerals like fly ash or GGBFS, this stage happens quickly. At this stage, covalent connections between oxygen, aluminum, and silicon atoms can dissolve as well as ionic contacts within species. The amount of PFA and GGBFS employed, along with the pH of the activated solvent, dictate the solubility range (Xie et al., 2001).

## **2.8 Polymerisation Process**

A powerful chemical reaction on Si-Al minerals in alkaline settings produces a three-dimensional polymeric of Si-O-Al-O linkages (Škvára et al., 2005). The deficit charges associated with replacing aluminum with silicon are neutralized by the alkaline cations in the generated gel (Xie et al., 2001). These gels show the formation of 3D textures that form the cementitious component that binds together the unreacted fly ash spheres. Si is defined as a form of Q4 (nAl) in this aluminum silicate gel, where n varies from 0 to 4 and depends on the processing conditions and type of activator (Fernandez-Jimenez et al., 2006). The Q unit is used to represent many silicate atoms in silicate systems. However, this notation falls short of the main components of zeolite or aluminosilicate frameworks. When each silicate is surrounded by four silicate or aluminate units in zeolite systems, the Q units are usually Q4 (Szostak, 1989).

## **2.9 Growth**

This process exhibits a progressive increase in crystalline components when the polymerized gel's core approaches a substantial size. From the first stage of dissolving to the polymerization stage, in which the three-dimensional aluminosilicate is coated, the last phase of polymerization and setting is the many

elements of the microstructure of the final setting that geopolymer produces. These factors will have an impact on the physical characteristics of the created glue (Fernandez-Jimenez et al., 2006).

## **2.10 Advantages and Disadvantages of Using Geopolymer Concrete.**

### **2.10.1 Environmental**

In two respects, the manufacture of geopolymers reduces the impact of the computer on the environment. Carbon dioxide emissions generated during the manufacture of CO<sub>2</sub> products could be eliminated if a commercially viable alternative to CO<sub>2</sub> could be developed. One ton of PC concrete produces approximately one ton of carbon dioxide in the atmosphere during manufacturing (Škvára et al., 2005). This amount of computers requires 2.8 tons of raw materials, including gasoline and other ingredients, and the process produces 5% to 10% of all airborne dust (Khale and Chaudhary, 2007b). In addition, the use of cement products would reduce the harmful raw waste of these compounds in the environment. Currently, unclaimed PFA and GGBFS are deposited in landfills, posing a risk of mineral intrusion into groundwater. On a global scale, the production of geopolymer cement will reduce or eliminate this threat (Puertas et al., 2003).

### **2.10.2 Economical**

The production of geopolymers reduces the demand for clinker, an expensive component used in personal computers. The high cost of PC production is due to the large amount of energy required to manufacture the material. Computer manufacturing is an expensive and energy-intensive process due to the high temperatures (1400-1500°C) required (Fernandez-Jimenez et al., 2006). It is a realistic choice because the pozzolanic components used in geopolymer cements are readily available as waste from coal power plants (Fernández-Jiménez et al., 2007). Only 30-40% of the viable PFA was used, according to the study, with the rest dispersed in environmentally controlled ways to reduce the risks of air pollution, leaching, and potential contamination of inland and marine waters. Reusing the resources used in industrial manufacturing will be economically and environmentally responsible in the face of this growing challenge (Sumajouw and Rangan, 2006).

### **2.10.3 Chemical resistance**

Geopolymer paste has been shown to be highly resistant to sulfates and a variety of acids. The PC deterioration caused by the sulfate attack is attributed to the buildup of broad gypsum and etherite, which causes cracking and spalling of the concrete. A decrease in the calcium concentration in the source material is associated with an increase in the synthesis of geopolymer components under acidic conditions. Since geopolymer cement does not have a gypsum or extranet structure, there is no sulfate charging mechanism in low-calcium, heat-treated, fly ash-based geopolymer cements. (Škvára et al., 2005).

### **2.10.4 Pozzolanic composition analysis**

The chemical structure and particle mass distribution must be validated before using the PFA and GGBF (Škvára et al., 2005). The mechanics of hard geopolymers are inextricably linked to the mineralogical structure of pozzolana. The characteristics of the final binder are significantly influenced by small changes in these components. The physical properties of the finished product and the reaction route are significantly influenced by the amount and distribution of calcium in the raw materials. (Haddad, 2016).

Prior to activation, a micro-analysis of the pozzolanic is required to identify the existing minerals and their sizes in proportion to the overall mass. This will help you figure out which activating agent to use and at what concentration to get the greatest results. The proportion of iron varies significantly, with silica content ranging from 40% to 60% of the ash material, 20% to 30% alumina, and silica presence ranging from 40% to 60% of the ash substance (Khale and Chaudhary 2007b).

### **2.10.5 Workability**

Geopolymer paste and PC concrete have different rheological properties. Pozzolanic-based geopolymers have higher static and dynamic viscosities than PC-based geopolymers, therefore vibration efforts should be able to eradicate air holes in fresh paste. (McDonald and Thompson, 2018).

## 2.11 Hydration Reaction

Within these process intervals, the thermodynamic and kinetic parameters for gel formation and reaction degree are established. The level of reactivity detected in a blended geopolymer paste is influenced by a number of variables. The cementitious properties of hardened cement are defined in the following states, depending on how these elements influence the polymerization process. The element size division and mineral structure of the PFA or GGBFS have an impact on the rate of the activation reaction and the chemical structure of the reaction output. (Fernandez-Jimenez et al., 2006).

### 2.11.1 Alkaline activators

Sodium Hydroxide (NaOH), Sodium Sulphate ( $\text{Na}_2\text{SO}_4$ ), Sodium Carbonate ( $\text{Na}_2\text{CO}_3$ ), and Sodium Silicate are the most often employed activators ( $\text{Na}_2\text{SiO}_3$ ). Alkali-activated concrete and cement commonly use alkaline salts or caustic alkalis as alkali activators (Glukhovskiy et al., 1980). These are arranged into six groups according to their chemical structures as follows, where M is an alkali ion (Pacheco-Torgal et al. 2008) :

- Alkalis with a Caustic Base (MOH)
- Weak acid salts of non-silicate ( $\text{M}_2\text{CO}_3$ ,  $\text{M}_2\text{SO}_3$ ,  $\text{M}_3\text{PO}_4$ , MF)
- Silicates ( $\text{M}_2\text{O nSiO}_3$ ) are a kind of silicate.
- $\text{M}_2\text{O nAlO}_3$  aluminates.
- Aluminosilicate ( $\text{M}_2\text{O nAl}_2\text{SO}_3 (26) \text{SiO}_2$ ) is a kind of aluminosilicate.
- Strong acid salts that aren't silicate ( $\text{M}_2\text{SO}_4$ ).

NaOH,  $\text{Na}_2\text{CO}_3$ ,  $\text{nSiO}_2\text{Na}_2\text{O}$ , and  $\text{Na}_2\text{SO}_4$  are the most commonly used cost-effective and easily accessible chemicals. Potassium hydroxide, on the other hand, has been used in a few experiments, although it is difficult to use due to cost and availability. Furthermore, as the characteristics of potassium and sodium are comparable, using potassium as an alkali activator in geopolymer production is not cost effective (Kong et al., 2008).

### 2.11.2 Sodium hydroxide (NaOH)

Since sodium cations are smaller than potassium (+) ions, sodium hydroxide (NaOH) is widely used as an alkaline activator in the production of geopolymer. This

conserves energy by facilitating the transfer of cations through the adhesive network. In addition, NaOH has a high charge density, which helps in the formation of zeolites. (ME and Shimpale, 2019). The amount and molarity of this specific activating solution cause the characteristics of the putty. The use of a large amount of NaOH during the linker development process can accelerate dissolution and reduce the formation of ettringite and CH (Khale and Chaudhary, 2007b). Larger NaOH concentrations also increase the intensity of the reaction in its initial phases. Only the stabilizing strength of the ancient materials is greater. This is because there is too much OH in the solution, which contributes to the end product's undesirable form and irregularity. (McDonald and Thomson). Other advantages of utilizing NaOH dopants include enhanced crystallization and increased endurance in corrosive settings with acids and sulfates. (García-Lodeiro et al. 2007).

Moreover, the use of sodium hydroxide (NaOH) as an activator maintains the pH of the pore solutions, regulates the hydration activity, and directly changes the composition of the C-S-H product in geopolymer cement. The amount of heat generated and the NaOH concentration have a linear relationship. The reaction of these acid molecules requires more heat energy as the acid concentration rises because there are more acid molecules in the same volume. Although there is an inverse relationship between the concentration of NaOH and the peak water temperature (Imbabi et al., 2012).

### **2.11.3 Sodium Silicate ( $\text{Na}_2\text{SiO}_3$ )**

High-pressure fumes dissolve sand ( $\text{SiO}_2$ ) into a semi-viscous fluid known as waterglass when it is fused with sodium carbonate or sodium-potassium ( $\text{Na}_2\text{CO}_3$  or  $\text{K}_2\text{CO}_3$ ) at a very high temperature of  $1100^\circ\text{C}$  (Fernandez-Jimenez et al., 2006). Because it has the activation potential to initiate the pozzolanic reaction on its own, waterglass is rarely used as an independent activating agent. To boost alkalinity and develop general sample strength, it is usually mixed with sodium hydroxide (NaOH) as a fortifying component. The most common alkaline liquid used in polymerization is a mixture of potassium hydroxide (KOH) or sodium hydroxide (NaOH) and sodium silicate ( $\text{Na}_2\text{SiO}_3$ ) (McDonald and Thompson). Commercially accessible sodium silicate solutions come in a variety of grades and types. When comparing the

powdered and liquid forms of waterglass, it is worth noting that the powdered version has a lesser performance (Kong et al., 2008).

Furthermore, the activation solution should be prepared 24 hours before the match for best results. (Škvára et al., 2005). The major distinguishing feature of this product is the mass ratio of  $\text{SiO}_2$  to  $\text{Na}_2\text{O}$ , which ranges from 1.5 to 3.2 on a commercial scale (Fernandez-Jimenez et al., 2006). Due to the solubility of silicates, alkaline saturation in pore solutions is reduced, allowing the pozzolanic components and aggregates to better bind the molecules together. Activated solutions containing little or no soluble silicates have significantly lower compressive strength in mortar and concrete than those with higher doses of solvent silicate, according to tests. The surface bonding between the coarse aggregate and the geopolymer slurry can also be improved by including the aforementioned silicate component. Several studies have found that when temperatures rise, samples containing aqueous glass lose their strength compared to those containing only a basic activator, despite the fact that water glass usually gives a higher strength. However, more research is needed to fully understand the effects of adding water glass to samples (Fernandez-Jimenez et al., 2006).

## **2.12 Binder Constituent Proportioning**

The type, rates, and concentrations of blend components have a big impact on geopolymer binder qualities. Individual constituents, as well as the variables associated with them, have a crucial role in limiting the qualities of the final product (Song 2007).

### **2.12.1 Activator concentration**

Alkali activator plays an important role in forming strong geopolymers and developing high compressive strength. Regardless of the rating of the activator, increasing the concentration increases reaction speed and grade to a few more acceptable and stronger cement components. For PFA-based procedures, increasing the doping and increasing the concentration leads to an increase in the size of smaller holes and a decrease in the overall porosity, thus enhancing the initial strength of the slurry samples (GangaRao et al., 2006).

With time, the effect of activator concentration grows. PFA and GGBFS combinations have a minimum molarity of 2 to 10 molar. Furthermore, when the concentration reaches its maximum level, greater strength is achieved (Song, 2007). Capabilities of greater strength Higher concentrations may have an effect; all activators have a maximum concentration. As a result, exceeding the restriction will have an impact on the outcome. Because alkaline concentration increases setting time, it can be used to postpone polymer formation. The severe ion barrier, fluidity, and the potential for mixing by reactive types are all factors to consider. As a result, in a geopolymer mix, the concentration must be clearly addressed (Khale and Chaudhary, 2007b).

### **2.12.2 Pozzolanic / activator ratio**

The ratio of PFA, GGBFS, and calcined clays to the selected activator influences some important characteristics of the geopolymer base. Power is significantly impacted by this factor. The proposed ratio of an alkaline liquid to a PFA by mass is used on a scale of 0.3 to 0.45. (Kevern et al. 2005). For the geopolymer's overall strength and fire resistance, the PFA to activator ratio appeared to be the most important factor. (Fernández-Jiménez et al. 1999).

### **2.12.3 Sodium silicate and hydroxide activator ratio**

Adding sodium silicates to the process enhances mechanical characteristics beyond what can be achieved with just a hydroxide activator. The rate of each ingredient, on the other hand, must be administered and maintained with caution. The mass ratio of sodium silicate to sodium hydroxide solution should be fixed at 2.5, according to some books. (Fernández-Jiménez et al. 1999).

## **2.13 Curing Geopolymer Method**

In synthesizing PFA-based geopolymers, Puertas and Fernández-Jiménez found that they did not set at 23°C. The achievement of acceptable mechanics at ambient temperatures is a difficulty for strong geopolymer mortar. The geopolymers reaction is more easily accomplished by increasing the alkaline activity of the pozzolanic materials using an external heat source. A study was conducted to examine geopolymer designs, which included the ability to harden strongly at room

temperature. However, nothing is known about the strategies for a large-scale ambient geopolymer cure (Škvára et al., 2005).

#### **2.14 Strength Development of Alkaline-Activated Concrete**

Investigated was how the clinker chemistry affected the GGBFS mixture's early strength development. The early ages saw a change in the rate of hydration of cement-based mixes due to the process through which clinker delivers calcium and alkali. (Gee 1979). To improve the C-S-H gel in the bond, GGBFS reacts with water in alkaline environments, and then with calcium hydroxide formed by hydration of cement in pozzolanic materials. (Siddique, 2007). The hydration result  $\text{Ca}(\text{OH})_2$  begins the hydration of C-S-H in the GGBFS mix with a low  $\text{CaO}/\text{SiO}_2$  ratio.

Due to the low levels of  $\text{Ca}(\text{OH})_2$  and C-S-H in a GGBFS mix, the pozzolanic effect can enhance the C/S ratio to around 1.7 (Siddique, 2007; Khan et al., 2011). Mindess et al (1981) reported that when the water-binder ratio remained the same, compressive strength increased more slowly in concrete mixes containing 40–60% GGBFS than PC for the first three days. However, they did remark that, particularly for concrete with a 40 percent GGBS content, the enhanced strength of GGBFS concrete after three days was more than that of PC-only concrete. (Popovics, 1982). It was also discovered that the improvement in concrete strength of 20-60% GGBFS did not occur until 28 days, whereas strength became balanced with that of concrete using only PC after an equal or extended period of time. Compressive strength analyses have been used as a tool to track the progress of repolymerization in a number of investigations. Given that identifying strength progress is a key means of monitoring the efficiency of materials at different stages of construction, the low-purity of compressive strength measurement has also been investigated. (Provis et al., 2005).

The compressive strength of geopolymers is determined by a number of factors, including the gel state strength, the gel state, the arrangement of the undissolved Al-Si particles, the hardness of the undissolved Al-Si particles, the type of amorphous geopolymer or the number of crystallizations, and the external interaction of the gel state and Al particles -Si undissolved. (Li and Li 2003; Xu et al., 2000b). Since the undissolved particles remain bound in the matrix after geopolymerization, the maximum compressive strength has a positive effect on the hardness of the minerals

(Xu and Van Deventer, 2000b). With the geopolymerization of common minerals, after the introduction of aggregates, for example, or granular sand into the geopolymer mixture, the compressive strength increase (Xu et al., 2000b).

The maximum compressive strength of the material is affected by the amount of methacholine in the geopolymer matrix, as well as the concentration of potassium hydroxide (KOH) and the addition of sodium silicate (Na<sub>2</sub>SO<sub>3</sub>) Swanepoel. Fernández-Jiménez et al (1999) showed that adding more meta kaolinite boosts strength because it can change how much Al gel formed, which is more common in systems with higher levels of polymerization. Some studies claim that the density and amorphous state of the meta-kaolinite geopolymer, in which sodium hydroxide (NaOH) concentration rises from 4 to 12 mol/L, determine the compressive strength. This is because, in the presence of highly concentrated NaOH, the dissolution of kaolinite super-particles increases and the monomer concentration accelerates. (Wang). et al. 2005; Revie, 2011). On cementitious materials, the effects of alkaline activation of sodium silicate and sodium hydroxide solutions were investigated. The materials exhibit greater mechanical strength than those activated just with NaOH, according to their 32 findings.

## 2.15 Analytical Methods

Geopolymerization mechanisms can be elucidated using a variety of methods, both advanced and basic. Specific surface area measurements, which indicate the amount of surface area that participates in distinct processes in a solid–fluid system, may predetermine the ability of Al–Si crystals to facilitate geopolymerization (Van et al., 1999; Jaarsveld, 1999).

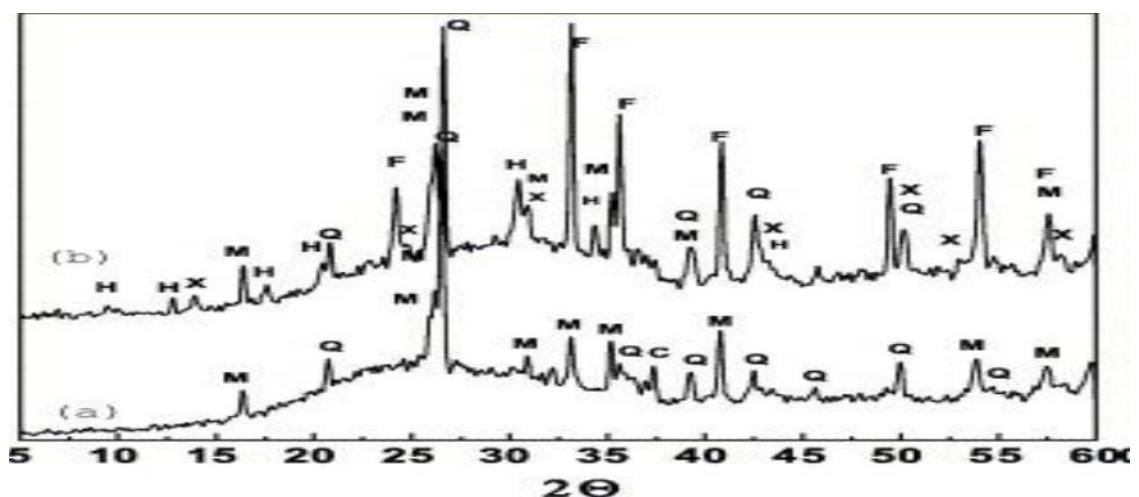


**Figure 2.1** XRD spectra (a) un-reacted fly ash;(b) alkali-activated fly ash 20 h at 85 °C (Van et al., 1999).

Microscopy can disclose remarkable microstructure characteristics since it presents results based on the physical quantity and design of distinct geopolymer components. For elemental investigation of Al–Si crystals, X-ray fluorescence (XRF) spectroscopy works very well. Although X-ray diffraction (XRD) may be a valuable tool, the amount of data that can be acquired is limited due to the massive amorphous nature of the geopolymer. The extent to which crystalline origin materials have reacted will be presented using this method (Van et al., 1999). Figure 2.7 shows the XRD model of a geopolymer made from PFA and cured at 85°C for 20 hours after being begun with a NaOH (8M) solution (Fernández-Jiménez et al., 2007). In order to obtain an absolute topography report on the physical and mechanical requirements of the microstructures of crystalline and amorphous substances that cannot be observed using other techniques, SEM enables visual analysis of results in millimeters to micrometers. (Duxson et al., 2007; Bone et al., 2004).

Geopolymer microstructures (Figures 2.8–2.11) have been described as a variety of morphologies in a wide range of hydration outcomes that are largely featureless (i.e., alumina-silica gel). Due to the heat approach employed during activation, mechanical destruction during specimen preparation, or shrinking caused by drying in the electron microscope's vacuum, cracking in these items is infrequent. The number of distinct component stages is depicted in Figures (2.2) and (2.3), whereas low magnification local item growth is depicted in Figures (2.4) and Figures (2.5).

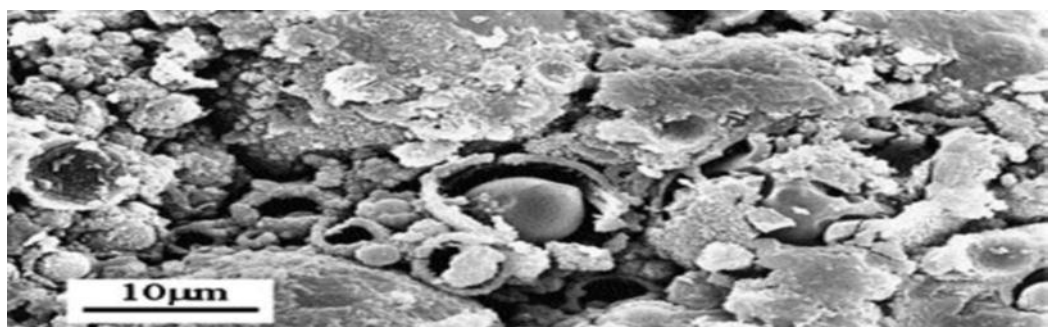


**Figure 2.2** Micrographs of alkali-activated PFA geopolymer fracture surface.  $\text{Fe}_2\text{O}_3$  is denoted by an arrow (Jiminez et al. 2004)

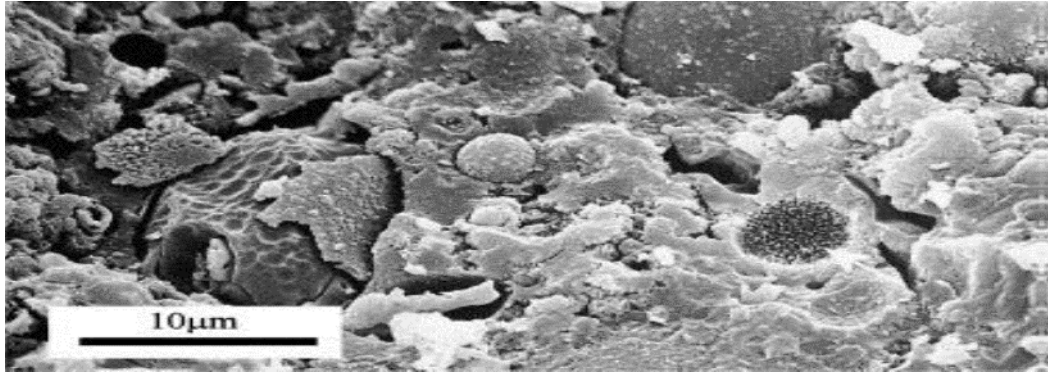


**Figure 2.3** Micrographs of alkali-activated PFA geopolymer fracture surface. (Jiminez et al. 2004)

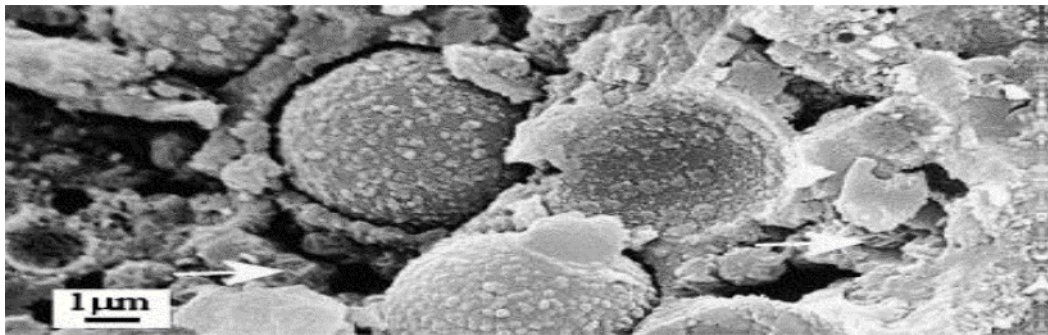


**Figure 2.4** Micrographs of alkali-activated PFA geopolymer fracture surface exhibiting PFA particle with reaction shells as well as unexplained spherical assemblages (Jiminez et al. 2004)

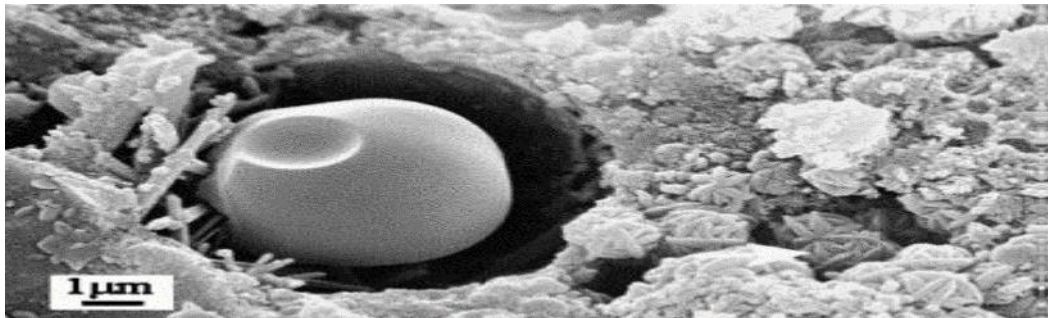


**Figure 2.5** Micrographs of alkali-activated fracture surface. (Jiminez et al. 2004)

### 2.16 Factors Affect Geopolymer Binder/Concrete

There are many factors affect geopolymer binder, some of these factors that have significant effect are:

- The mass ratio of the activator solution to the source material (fly ash, GGPFS, etc.).
- NaOH solution concentration.

- The mass ratio of sodium silicate  $\text{Na}_2\text{SiO}_3$  solution to sodium hydroxide NaOH solution; the effect of this parameter is dependent on the sodium silicate solution composition.
- Curing temperature.
- Curing period.
- Water content.

### **2.17 Geopolymer Concrete**

The production of cement contributes to environmental pollution, which is currently the biggest problem facing the planet. One of the most popular building materials is concrete. The manufacturing of Portland cement contributes significantly to  $\text{CO}_2$  emissions. A new generation of concrete, such as geopolymer concrete, has been developed to reduce the requirement for cement (GPC). Geopolymer is an excellent substitute for cement concrete since it is made from industrial by-products like fly ash and GGBS. In concrete, it can completely replace cement. (Juenger et al., 2011). The researchers found that the degree of workability increases along with the GGBFS level. They also found that the strongest concrete had the highest compressive, split tensile, and flexural strength ratings when it contained 75% slag. (Zende, 2015).

The freshly formed geopolymer mixtures were cohesive, and as the alkaline solution ratio was increased, so did their workability. They also discovered that the strength of geopolymer concrete is improved by lowering the water/binder and aggregate/binder ratios. The achieved compressive strength lies between 20.64 and 60  $\text{N/mm}^2$ . Three to four and a half to nine  $\text{N/mm}^2$  is the obtained split tensile strength. P.S. (Madheswaran et al., 2014). The combinations were found to be very workable (225-250 mm slump). After 28 days of casting, the mixture compressive strength was found to be in the range of 30 to 44 MPa (Nath and Sarker, 2014).

Researchers have looked into the effects of geopolymer concrete that hasn't been heated. Fly ash (class F type), an activator made from a combination of sodium hydroxide and sodium silicate solutions, and a tiny amount of granular blast furnace slag were used to create geopolymer concrete (GGBFS). It was determined through the workability, setting, and compressive strength tests that fly ash-based geopolymer with GGBFS is an effective binder for the construction of low to

medium strength concrete under ambient curing conditions because it does not require heat treatment. (Srinivasan et al., 2017). As GGBFS content increases, compressive strength continuously increases. The 15M Alkaline Solution is mixed with Coal Ash and GGBFS to produce a total replacement of about 30% and a greater compressive strength of 57Mpa. Although GGBFS with Geopolymer costs 7% more than PC, it is nearly three times stronger after seven days. (Hardjito et al., 2008).

Meininger presented a study of GGBFS totally replaces Portland cement in geopolymer concrete, and the components are attached to sodium hydroxide and sodium silicate in the alkaline liquid. Different molarities of NaOH solutions, such as 3M, 5M, 7M, and 9M, are taken into consideration. Higher molarities of NaOH increase the geopolymer's strength. (Meininger 1988). In one study, five different ratios of slag were substituted for low-calcium fly ash to test the tensile properties of geopolymer concrete. Higher GGBFS (slag) concentrations in geopolymer concrete result in more compressive strength. 90% of pressure resistance is attained in just 14 days. (Morsy et al., 2014).

The experimental investigation is offered. Fly ash and GGBFS are utilized equally (50 percent each). The geopolymer concrete increases its compressive strength by 60–70% in just 7 days. (Keerthan, 2018). Slag is used as a fine aggregate, partially or fully swapping out sand for the mixture. We employ the following ratios: 0, 15, 30, 50%, and 100%. The best results are obtained with replacement ratios of 30–50% for tensile strength and 15–30% for compressive strength. (Srinivasan et al. 2017). In contrast to conventional concrete, which uses a hydrated calcium silicate binder system, geopolymer concrete (GPC) is an unique type of concrete that uses an alumino-silicate binder system. They are an environmentally friendly and long-lasting alternative to conventional Portland cement concrete because they provide quick strength growth, no requirement for water curing, and exceptional mechanical and durability properties. (Ahmed et al., 2020).

In a solid alkaline solution such as sodium hydroxide, potassium hydroxide, sodium silicate, or potassium silicate, several aluminosilicate minerals are activated, creating geopolymer. Byproducts like fly ash and geologically obtained minerals like metakaolin are examples of potential source materials. (Faris et al., 2017a). Conceiç

(2019) provided a generic model to define and explain these materials' activation reactions, noting three key stages:

- Destruction of coagulation.
- Coagulation-condensation.
- Condensation-crystallization.

Conceição (2019) represented these in a conceptual model, as illustrated in Figures (2.1) There are three major stages that may or may not occur simultaneously.

- Si and Al atoms are dissolved from the source material.
- Precursor ions are oriented or condensed into monomers.
- Polycondensation or setting of monomers into polymeric structures.

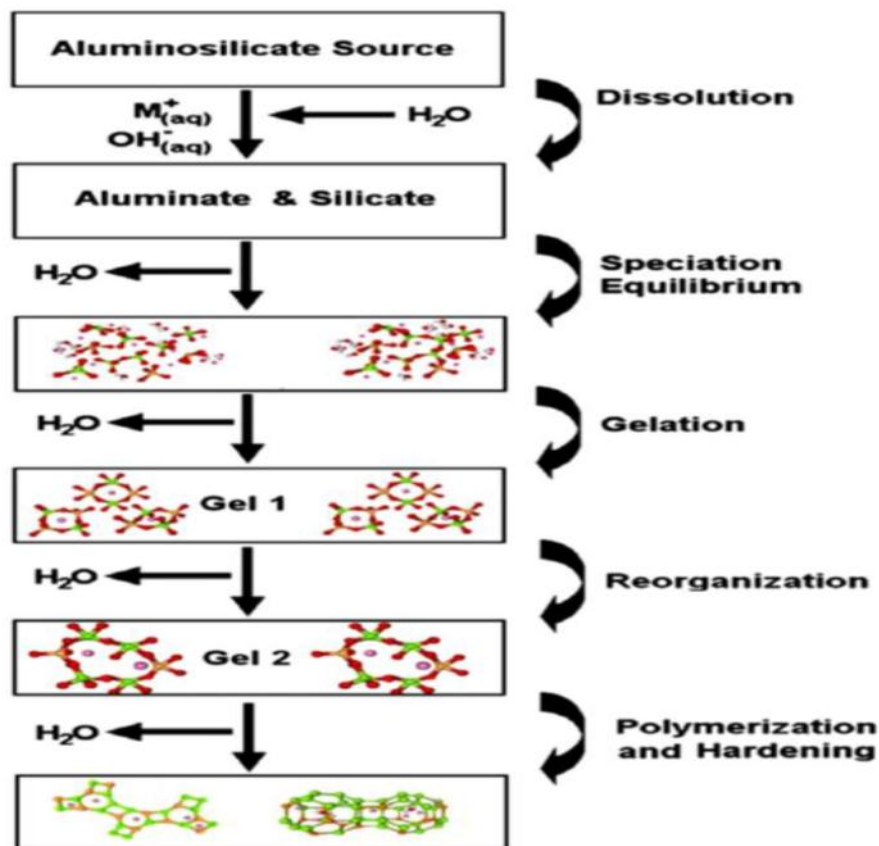


**Figure 2.6** Geopolymer formation conceptual model (Faris et al., 2017b)

By exchanging all oxygen atoms between two tetrahedral units, aluminosilicate materials dissolve in alkaline solutions to create free  $\text{SiO}_4$  and  $\text{AlO}_4$  tetrahedral units, which link together to form polymeric precursors. The continual connecting of these precursors results in the formation of the amorphous Geopolymer. As the process



treatment (Olivia and Nickraz, 2012). Sodium silicate to NaOH ratios of 1.5-2.5 have been shown to be sufficient (Wallah et al., 2005). Another important component in the composition of geopolymers is the amount of sodium hydroxide in the solution. The use of a higher concentration of NaOH in the aqueous phase of the geopolymer system increases the solubility of the source material and accelerates the geopolymerization reaction (Temuujin et al., 2009).

## **2.18 Geopolymer Pervious Concrete**

Portland cement (PC) output has been constantly expanding over the world, with no indications of slowing down. A large number of common assets are required in the production of PC, including limestone, nonrenewable energy sources, power, and petroleum gas, resulting in a high temperature record in the production of PC, resulting in a large amount of carbon dioxide CO<sub>2</sub> emissions into the environment in Thailand, estimated at around 33 million tons (Swain et al., 2015; Malayali et al., 2020). To minimize PC growth, pozzolanic materials such as slag Palm oil fuel waste, fly Ash, and rice husk are being employed. When compared to the manufacturing of Portland cement, ash is used as an alternate cementitious material to replace a portion of it. Because these materials are manufactured via current technologies, they take less energy to manufacture. (Chindaprasirt et al., 2007; Tangchirapat et al., 2009; Malayali et al. 2020).

Water does not sift underground in conventional hard asphalt due to its lack of water porosity and air permeability, and plants have a hard time developing naturally (Yang and Jiang, 2003; Malayali et al., 2020). According to the research, solid porosity, water-cement ratio (w/cm), glue brand, volume and volume of coarse aggregates material are the most important features that determine the previous solid quality (Chindaprasirt et al., 2008; Crouch et al., 2007; Malayali et al., 2020). The mechanical properties of ex-cement can be greatly improved by using appropriate solid components and mixing ranges (Sumanasooriya and Neithalath, 2011; Huang et al., 2010; Malayali et al., 2020).

Iron is made with impact heaters that create ground granulated blast furnace slag (GGBFS). These are fueled by a finely balanced blend of iron ore, coke, and limestone and run at a temperature of roughly 1500 degrees Celsius. GGBFS is utilized in a very small amount. (Malayali et al., 2019; Malayali et al. 2020). The

polymerization reaction is known as the polymerization process, and the paste is known as geopolymer. Chemicals are not used in the production of geopolymer concrete. A type of cement is Portland cement (Babu and Babu, 2017). Geopolymer is an inorganic polymer formed when aluminosilicate minerals combine with alkaline fluids (Kong et al., 2007; Arafa et al., 2017).

Many great geopolymer qualities have been established, including superior acid and sulfate resistance, high early strength, and high temperature performance (Kong and Sanjayan, 2008; Awal et al., 2017; Arafa et al., 2017). Geopolymer removes the need for cement, resulting in a 44–64 percent reduction in greenhouse gas emissions. Blast furnace slag and fly ash, for example, are great sources of aluminosilicate, which is used to manufacture geopolymer. Because geopolymers are created from by-product materials, they have a lesser environmental impact than other types of concrete binders (Rahmat et al., 2017; Eduok, 2016; Arafa et al., 2017). Pervious concrete uses Portland cement as a binding material, and more study into the use of other binding materials, such as geopolymer binders, is still needed (Arafa et al., 2017).

The present work used granulated blast furnace slag (GGBFS) as a solid precursor to synthesize the surrounding process binders. A high ratio of aggregate to binder was used to check the suitability of these bonds to create the improved precast concrete. Compressive strength, density, total porosity and other qualities are affected by the overall volume. As a result, the focus of this research is on the use of a geopolymer binder for precast concrete made from granulated blast furnace slag (GGBFS), sodium silicate, sodium hydroxide solution and coarse aggregate. The physical and mechanical properties of the material were examined. The information obtained will certainly be useful in the future for the use of granulated geopolymer blast furnace slag (GGBFS) in the creation of precast concrete, resulting in reduced cement consumption and environmental issues.

Pervious concrete has been the subject of a lot of research and development on a global scale. However, from an international perspective, it has been noted that a significant amount of work has been done in the area of pervious concrete. However, research on geopolymer pervious concrete is limited, and it must be strengthened by conducting research in the relevant field. This is a research paper about Pervious concrete that has been the subject of a lot of research and development on a global

scale. However, the main goal is to develop geopolymer pervious concrete using GGBFS as the raw material and sodium hydroxide and sodium silicate as the activator solution, as well as to investigate its mechanical and permeability.

The goal of this study is to see if slag-based geopolymer cement may be used as a binding ingredient in ambient-curing geopolymer pervious concrete (GPPC) (No heat curing and No water curing). Some essential parameters connected to the geopolymer binder are investigated in this research to examine how they affect GPPC's key properties. On a global scale, pervious concrete has been the focus of extensive research and development. There are several parameters to consider, including compressive strength, total permeability void content, and bulk density.

## **CHAPTER 3**

### **MATERIALS AND EXPERIMENTAL PROCEDURES**

#### **3.1 Introduction**

In this chapter a comprehensive outline of the materials used and methods adopted for preparing geopolymer pervious concrete, are described including the standards followed and properties of materials used, the mix proportions and the various types of tests carried out during this research. In addition to the types of equipment used in this study are presented as well. This chapter consists three sections; the first section covers the materials and the equipment used in this study including the physical and chemical features of the materials. The second section explains details of the geopolymer pervious concrete mixes including; mix proportion. The third and the last section of this chapter explains the experimental works and procedures including; the mixing process and the performed flow test, Void ratio, density, compressive strength, splitting test, flexure test, Modulus of Elasticity and infiltration Rate, and, the curing regimes ambient curing.

#### **3.2 Materials**

##### **3.2.1 GGBFS Slag**

Slag from the iron and steel industries is often misclassified as industrial waste and is generally misunderstood. In fact, these by-products are useful and flexible building materials. Since the Roman Empire, when slag shredded from primitive iron formations of that time was used in the construction of bases, slag was used in road construction. Orders were erratic until the previous century, when large quantities came into use for a number of purposes. The need to expand the use and recycling of by-products and recovered waste materials for economic and environmental reasons has led to a rapid increase in the use of slag in recent years. In some places, almost all iron and steel slag is already used, and in other places the use is increasing rapidly.

These sections will cover the composition, properties, and applications of iron blast furnace slags and steelmaking slags. The expertise gained in the United States will,

of course, be the basic foundation, with applications in other countries mentioned. Other slags may be used on occasions, but only the major slags produced by the iron and steel industries will be considered.



**Figure 3.1** GGBFS Slag.

### **3.2.2 Iron blast-furnace slag**

The non-metallic product consists predominantly of calcium and other silicates and aluminosilicate bases that are “manufactured in a molten state in conjunction with iron in a blast furnace,” according to the American Society for Testing and Materials. The conversion of iron oxides to molten metallic iron is commonly performed in blast furnaces. It is constantly fed with supplies of iron oxide (ores, pellets, sintering, etc.), flux stone (limestone, dolomite), and fuel (coke). The furnace floats over liquid slag. On a regular basis, both are drawn from the furnace. Fusing iron ore impurities (mainly silica and alumina) with calcium and magnesium oxides from flux stone to form slag. It comes out of the furnace as a liquid at temperatures around 1500°C, it will contain sulfur and ash from coke. It is a man-made molten rock similar to lava in many ways.

### **3.2.3 Chemical and mineralogic composition**

Chemical analyses show that the four principal oxides (lime, magnesia, silica, and alumina) account for roughly 95% of the total in blast-furnace slags. Sulfur, iron, manganese, alkalis, and trace amounts of several additional elements are minor elements. The compositions of the majority of blast-furnace slags generated in the United States fall within the ranges indicated below.

**Table 3.1** Major Chemical Constituents in Blast Furnace Slag

Constituent	Weight Percent
Lime (CaO)	32 to 45
Magnesia (MgO)	5 to 15
Silica (SiO <sub>2</sub> )	32 to 42
Alumina (Al <sub>2</sub> O <sub>3</sub> )	7 to 16
Sulfur (S)	1 to 2
Iron Oxide (Fe <sub>2</sub> O <sub>3</sub> )	0.1 to 1.5
Manganese Oxide (MnO)	0.2 to 1.0

The majority of slag produced in other countries appears to have similar or close composition ranges. The chemical composition of the slag is determined by the nature of the iron ores, flux stones and available fuel, as well as the quantities required for efficient operation of the furnace. If the grade of iron produced is consistent, the blast furnace should be charged with uniform raw materials. This approach also maintains slag composition homogeneity, resulting in a minor variation in slag composition from a single source. Where different raw materials are used, as seen in the overall ranges above, there may be larger variances between sources. When slag is rapidly cooled after leaving the furnace, it becomes noncrystalline and glassy. A number of minerals crystallize as a result of slower cooling; the most prevalent ones are listed in Table 3.1. Melilite is the most frequent mineral in slag, and it refers to a continuous series of solid solutions made up of akermanite and gehlenite. The presence or absence of minor minerals is determined by the relative proportions of the principal oxides in the slag; normally, slags include no more than four minerals. When the mineral dicalcium silicate forms in high-lime slags and changes from one crystalline form to another after cooling, it disintegrates due to a volume increase. Sulfur sulfides of calcium, iron, and manganese are common in slow-cooled slag (Piemonti, 2021).

### 3.2.4 Erbil steel slag

Chemical and mineralogic composition of Erbil steel slag Shown in table 3.2.

**Table 3.2** Chemical and mineralogic composition of Erbil steel slag

Constituent	Weight Percent
Na <sub>2</sub> O	0.03%
MgO	0.34%
Al <sub>2</sub> O <sub>3</sub>	3.23%
SiO <sub>2</sub>	11.04%
P <sub>2</sub> O <sub>5</sub>	0.66%
SO <sub>3</sub>	0.14%
K <sub>2</sub> O	0.01%
CaO	22.27%
MnO	2.04%
Fe <sub>2</sub> O <sub>3</sub>	27.51%



**Figure 3.2** Erbil steel slag

### 3.2.5 Erbil steel steam condenser.

Chemical and mineralogic composition of Erbil steam condenser shown in table 3.3

**Table 3.3** Chemical and mineralogic composition of Erbil steam condenser

Constituent	Weight Percent
Na <sub>2</sub> O	0.12%
MgO	0.06%
Al <sub>2</sub> O <sub>3</sub>	0.22%
SiO <sub>2</sub>	4.08%
P <sub>2</sub> O <sub>5</sub>	0.67%
SO <sub>3</sub>	0.97%
K <sub>2</sub> O	1.53%
CaO	9.43%
MnO	1.29%
Fe <sub>2</sub> O <sub>3</sub>	30.07%

### 3.2.6 Composition of brick materials

The components of good brick material are as follows: Alumina is the main ingredient in all types of clay. Alumina content should be between 20% and 30% in a good brick. This component gives the clay plasticity, allowing it to be shaped. If there is too much alumina and not enough sand, the raw bricks shrink and bend during drying/burning and become excessively hard when burned. Silica is found in clay in two forms: free and mixed. It is mechanically combined with clay as free sand. It exists in a chemical composition with alumina in its combined form. A good brick material should have a silica content of 50 to 60 percent. The presence of this component protects uncooked bricks from breaking, shrinking, and warping. As a result, the bricks will have a consistent shape. The proportion of silica in the brick composition affects brick durability. The bricks become brittle as a result of the excess silica's damage to particle cohesion.

Lime: In good brick material, a tiny amount of lime (less than 5%) is preferable. Because even little particles the size of a pinhead promote flaking of the bricks, it should be present in a highly powdered state. Lime stops uncooked bricks from shrinking. The sand is infusible on its own. However, in the presence of lime, it somewhat ignites at kiln temperature. For brick particles, fused sand acts as a stiff

cementing medium. The brick melts as a result of the extra lime, and its shape is lost. After being burned, the lime lumps become fast lime, which slakes and expands in the presence of moisture. Bricks are fractured into bits as a result of this motion. Iron oxide: In good brick material, a modest amount of iron oxide (about 5 to 6 percent) is ideal. As a lime, it aids in the fusion of sand. It also gives the bricks a red hue. The bricks are dark blue or blackish due to an overabundance of iron oxide. If the amount of iron oxide in the bricks is comparably low, the bricks will be yellowish in hue. Magnesia: A minor amount of magnesia in brick material gives the bricks a yellow color and reduces shrinkage. Excess magnesia, on the other hand, causes bricks to deteriorate.

### 3.2.7 Sodium silicate solution ( $\text{Na}_2\text{SiO}_3$ )

Sodium Silicate is available commercially in liquid gel form, as shown in Fig. 3.5 and it was used for this study, the chemical composition of sodium silicate was:  $\text{Na}_2\text{O}$  13.4%,  $\text{SiO}_2$ -32.5%, and Water-54.1%.



**Figure 3.3** Sodium silicate solution

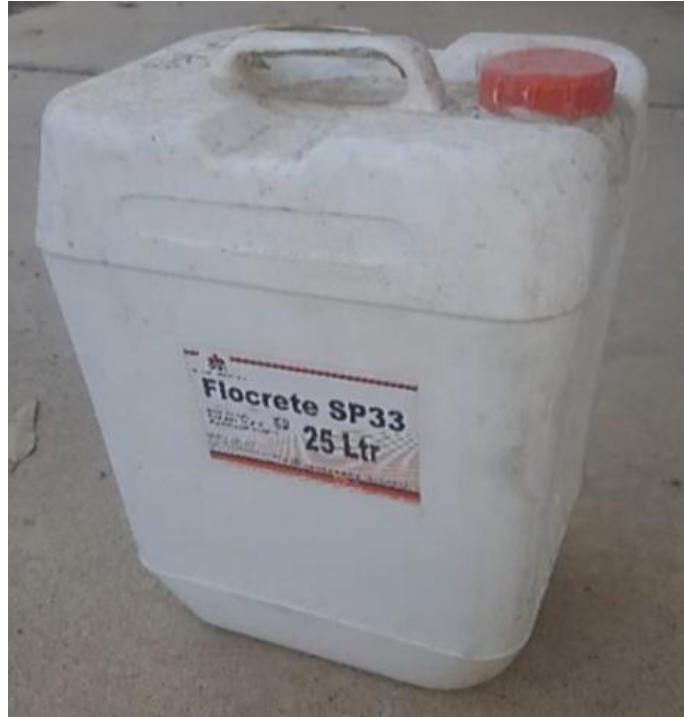


**Figure 3.4** Super Plasticizer

### **3.2.8 Sodium hydroxide (NaOH)**

Commercially, Sodium hydroxide is present in flakes shape and pellets shapes. For the present observe, Sodium hydroxide pellets with 98% purity have been liquefied in water to make NaOH solution with distinctive Molarity, which is ordered from Don Construction Products (DCP) Company as shown in Figure. 3.6.



**Figure 3.5** Sodium hydroxide

### 3.2.9 Super plasticizer and water

Sulphonated Naphthalene is a type of sulphonated naphthalen Condensed polymerization of naphthalene, sulphonic acid, and formaldehyde produces formaldehyde (SNF) (Figure. 3.2). The distribution of cement grains induced by the negative charge left on the admixture adsorbed cement particle, which repels other cement particles, was exploited in this study to improve concrete workability. Extra water, washing, mixing, and curing of conventional Portland cement concretes were all done with potable drinking water.

### 3.2.10 Coarse aggregates

Aggregates were obtained from Great Zab River quarry which is commonly used in Erbil. The coarse aggregate used in the concrete mixes with a nominal maximum size of 14 mm and with Bulk specific gravity of 2.76 and (clean, well-graded). Grading of coarse aggregates are shown in Fig. 3.1 with the limits specified with (ASTM 1999) (ASTM C33-9)

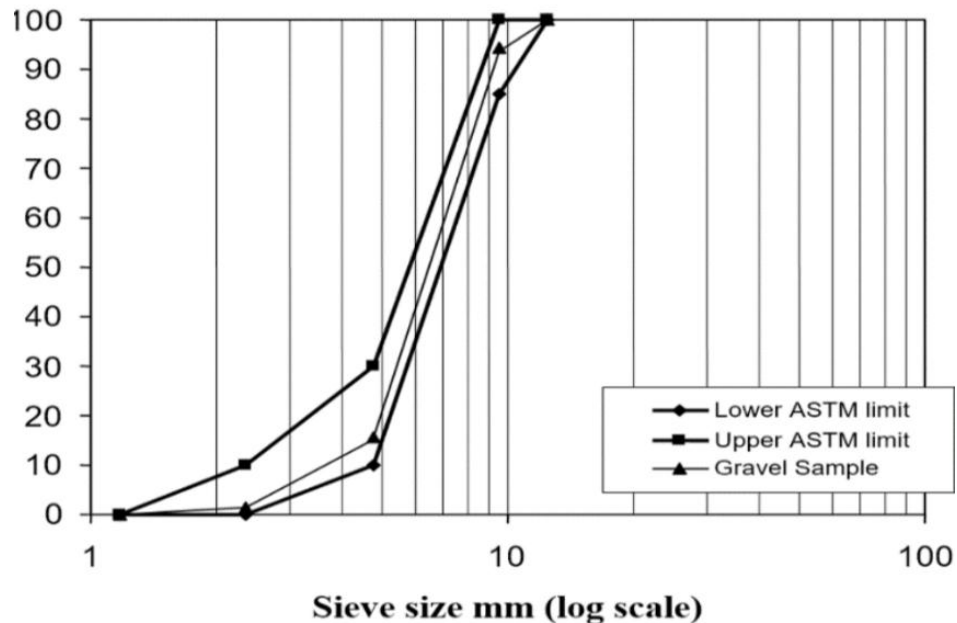


Figure 3.6 Grading curves for coarse aggregate (gravel)

### 3.3 Mix Proportions

Since preparing the geopolymer pervious concrete don't depend on a specific standard, therefore all the mixes in this study were prepared by the classic method of trial and error. Consequently, to prepare a geopolymer pervious concrete batch there

are many parameters that need to be considered, such as, amount of the binder, superplasticizer amount, or the calculation of the aggregate content. about preparing geopolymer pervious concrete mix, all other attempts for making geopolymer pervious concrete are trial and error. Furthermore, we can list the parameters that affect the geopolymer pervious concrete follows as: -

- The ratio of sodium silicate to sodium hydroxide.
- The sodium hydroxide solution's concentration (molarity).
- The ratio of alkaline to binder (Alk/GGBFS).
- The superplasticizer's kind (not all types are suitable) Those that are based on naphthalene are recommended.
- The impact of the largest aggregate size.

In the first- phase, the key factors affecting the performance of geopolymer pervious concrete were investigated; focusing on the aforementioned parameters using natural coarse aggregate (max. size 20 mm) then the results were as shown in the table no. (3-4) in order to reach decent mix proportions of the reference mix. In this step a total of 26 mixes were prepared with different proportions of materials. Out of this mechanical property (compressive strength)

**Table 3.4** Mix proportion of geopolymer pervious concrete (max. size 20 mm)

Mix designation	GGBFS content	Na OH molarity	Alk/GGBFS	Na <sub>2</sub> SiO <sub>3</sub> /Na OH	Compressive Strength. (mpa) -1-	Compressive Strength. (mpa) -2-	Compressive Strength. (mpa) -3-	Compressive Strength. (mpa)	Type.
GPPC 20-1	450	14	0.35	2.50	10.15	11.25	10.55	10.65	Pervious.
GPPC 20-2	450	14	0.35	2.00	9.61	10.71	10.01	10.11	Pervious
GPPC 20-3	450	14	0.35	1.50	9.38	10.48	9.78	9.88	Pervious
GPPC 20-4	450	14	0.35	1	8.27	9.37	8.67	8.77	Pervious
GPPC 20-5	450	14	0.3	1	7.51	8.61	7.91	8.01	Pervious
GPPC 20-6	350	14	0.35	1	7.48	8.58	7.88	7.98	Pervious
GPPC 20-7	350	14	0.25	1	6.61	7.71	7.01	7.11	Pervious
GPPC 20-8	350	14	0.3	1	6.43	7.53	6.83	6.93	Pervious
GPPC 20-9	350	14	0.35	1	5.83	6.93	6.23	6.33	Pervious
GPPC 20-10	350	14	0.25	1	5.41	6.51	5.81	5.91	Pervious
GPPC 20-11	300	16	0.25	1	4.72	5.82	5.12	5.22	Pervious
GPPC 20-12	300	16	0.25	1	6.04	7.14	6.44	6.54	Pervious
GPPC 20-13	350	16	0.25	1	6.83	7.93	7.23	7.33	Pervious
GPPC 20-14	325	14	0.25	1	11.04	12.14	11.44	11.54	Pervious
GPPC 20-15	325	12	0.25	1	19.62	20.72	20.02	20.12	Pervious
GPPC 20-16	325	10	0.25	1	11.04	12.14	11.44	11.54	Pervious
GPPC 20-17	325	8	0.25	1	8.16	9.26	8.56	8.66	Pervious
GPPC 20-18	325	12	0.25	1.50	16.26	17.36	16.66	16.76	Pervious
GPPC 20-19	325	12	0.25	1.75	12.48	13.58	12.88	12.98	Pervious
GPPC 20-20	325	12	0.25	2.00	13.27	14.37	13.67	13.77	Pervious
GPPC 20-21	325	12	0.25	2.25	12.93	14.03	13.33	13.43	Pervious
GPPC 20-22	325	12	0.25	2.50	11.95	13.05	12.35	12.45	Pervious
GPPC 20-23	325	12	0.25	2.75	11.51	12.61	11.91	12.01	Pervious
GPPC 20-24	325	12	0.25	3.00	11.48	12.58	11.88	11.98	Pervious
GPPC 20-25	325	12	0.25	3.25	11.16	12.26	11.56	11.66	Pervious
GPPC 20-26	325	12	0.25	3.50	10.48	11.58	10.88	10.98	Pervious

In the second phase, the key factors affecting the performance of geopolymer pervious concrete were investigated; focusing on the aforementioned parameters using natural coarse aggregate (max. size 14 mm) then the results were as shown in the table no. (3-5) in order to reach decent mix proportions of the reference mix a total of 26 mixes were prepared with different proportions of materials. Out of this mechanical property (compressive strength).

**Table 3.5** Mix proportion of geopolymer pervious concrete (max. size 14 mm)

Mix designation	GGBFS content	Na OH molarity	Alk/GGBFS	Na <sub>2</sub> SiO <sub>3</sub> /Na OH	Compressive Strength (mpa) -1-	Compressive Strength (mpa) -2-	Compressive Strength (mpa) -3-	Compressive Strength (mpa)	Type.
GPPC 20-1	450	14	0.35	2.50	45.66	46.76	46.06	46.16	Non-Pervious
GPPC 20-2	450	14	0.35	2.00	36.05	37.15	36.45	36.55	Non-Pervious
GPPC 20-3	450	14	0.35	1.5	42.24	43.34	42.64	42.74	Non-Pervious
GPPC 20-4	450	14	0.35	1	38.00	39.10	38.40	38.50	Non-Pervious
GPPC 20-5	450	14	0.30	1	29.51	30.61	29.91	30.01	Non-Pervious
GPPC 20-6	350	14	0.35	1	31.17	32.27	31.57	31.67	Non-Pervious
GPPC 20-7	350	14	0.25	1	28.12	29.22	28.52	28.62	Pervious
GPPC 20-8	350	14	0.30	1	15.53	16.63	15.93	16.03	Non-Pervious
GPPC 20-9	350	14	0.35	1	16.76	17.86	17.16	17.26	Non-Pervious
GPPC 20-10	350	14	0.25	1	12.72	13.82	13.12	13.22	Pervious
GPPC 20-11	300	16	0.25	1	9.79	10.89	10.19	10.29	Pervious
GPPC 20-12	300	16	0.25	1	19.39	20.49	19.79	19.89	Pervious
GPPC 20-13	350	16	0.25	1	23.62	24.72	24.02	24.12	Pervious
GPPC 20-14	325	14	0.25	1	25.15	26.25	25.55	25.65	Pervious
GPPC 20-15	325	12	0.25	1	39.67	40.77	40.07	40.17	Pervious
GPPC 20-16	325	10	0.25	1	19.68	20.78	20.08	20.18	Pervious
GPPC 20-17	325	8	0.25	1	19.27	20.37	19.67	19.77	Pervious
GPPC 20-18	325	12	0.25	1.50	36.61	37.71	37.01	37.11	Pervious
GPPC 20-19	325	12	0.25	1.75	36.38	37.48	36.78	36.88	Pervious
GPPC 20-20	325	12	0.25	2.00	35.93	37.03	36.33	36.43	Pervious
GPPC 20-21	325	12	0.25	2.25	35.03	36.13	35.43	35.53	Pervious
GPPC 20-22	325	12	0.25	2.50	34.27	35.37	34.67	34.77	Pervious
GPPC 20-23	325	12	0.25	2.75	32.92	34.02	33.32	33.42	Pervious
GPPC 20-24	325	12	0.25	3.00	32.02	33.12	32.42	32.52	Pervious
GPPC 20-25	325	12	0.25	3.25	30.11	31.21	30.51	30.61	Pervious
GPPC 20-26	325	12	0.25	3.50	29.15	30.25	29.55	29.65	Pervious

In the third phase, Erbil slag was used instead of imported slag to reduce the cost and using natural coarse aggregate (max. size 14 mm) then the results were as shown in the table no. (3-6) In this step a total of 4 mixes were prepared with different proportions of materials, out of this mechanical property (compressive strength). In the fourth phase, Erbil slag steam condenser was used instead of imported slag to reduce the cost and using natural coarse aggregate (max. size 14 mm) then the results were as shown in the table no. (3-6) In this step a total of 4 mixes were prepared with

different proportions of materials. out of this mechanical property (compressive strength).

In the fifth phase, brick powder was used instead of imported slag to reduce the cost and using natural coarse aggregate (max. size 14 mm) then the results were as shown in the table (3-6) In this step a total of 4 mixes were prepared with different proportions of materials. out of this mechanical property (compressive strength).

**Table 3.6** Mix proportion of geopolymer pervious concrete  
(Erbil Steel Slag; Erbil Steam Condenser; Brick Powder)

Mix No.	GGBFS (%)	Compressive Strength MPa	Replacement material %		NaOH Molarity	Maximum size of aggregate
1	0	8.34	Erbil Steel Slag	100	12	14
2	25	11.98		75		
3	50	15.18		50		
4	75	24.11		25		
5	0	8.44	Erbil Steam Condenser	100		
6	25	11.98		75		
7	50	17.32		50		
8	75	25.31		25		
9	0	6.57	Fired clay bricks	100		
10	25	9.48		75		
11	50	11.81		50		
12	75	19.76		25		

### 3.4 Experimental Program

In this section, the details of the way of preparing the materials used in this study is presented. It including the steps of mixing the ingredients of the concrete mixtures, the details of the handling of the concrete casting, samples and curing, and the details of the standard tests for fresh and hardening properties.

#### 3.4.1 Preparation of the alkaline activator solutions

The solution or liquid that used in this research for the activation of the binder is a mixture of two solutions (liquids);  $\text{Na}_2\text{SiO}_3$  solution. Such type of alkaline liquid is

the most common used liquid in geopolymer concrete as was found in the literature. To prepare the alkaline solution (liquid), NaOH flakes were added to water and mixed by stirring the solution to dissolve the flakes of NaOH, then left for one hour to cool down. As the molecular weight of the NaOH is 40 g/mol, the mixing of the NaOH with water was kept for 24 hours to complete the reaction prior to adding it to the mixer pan.

### **3.4.2 Mixing procedure**

Similar mixing procedure was used for both types of mixtures. For the mixing process, an electrical mixer was used, which has paddles and mixing bowls specified in (ASTM 2020) (ASTM C305). The mixing procedure can be explained in the following steps: -

- The mixer homogenized the binder (GGBFS) and aggregates (Dry mix) for 45 seconds.
- The alkaline solution was poured into the mixer, and the contents were mixed together for one minute.
- After the SP had been integrated, the appropriate water was added and blended for another minute. Finally, the mixture was halted for 200 seconds before being emptied into containers.

### **3.4.3 Casting and preparing the samples**

Three types of samples were used for the different properties examined in this research. These were cubes, prisms and cylinders. The dimensions of the cubes were (150\*150\*150) mm the size of the prisms was (150\*150\*750) mm. While the dimensions of the cylinders were (300\*150) mm. When the mixing of the fresh concrete has finished, it was poured into cubes, prisms and cylinders, the fresh GPPC were placed on a vibration table. When we used the vibrating table, it caused segregation in the concrete and thus the mix failed, so we thought of another way to place the concrete, which is to use the jack hammer after turning its head as shown in the Figure 3.7, where it was applied on three layers, each layer 15 seconds then left for 24 hours at room temperature to prepare for the curing.



**Figure 3.7** Compaction by jack hummer

**Table 3.7** shows the compressive strength of the above three methods of casting

Mix no.	Compressive Strength. (MPa)/placed concrete with Hammer jack	Compressive Strength. (MPa)/Placed concrete with Tamping rod	Compressive Strength. (MPa)/ placed concrete with vibration table
GPC14-15	40.17	28.3	3.98
GPC14-18	37.11	25.24	2.88
GPC14-19	36.88	25.01	2.82
GPC14-20	36.43	24.56	2.80
GPC14-21	35.53	23.66	2.77
GPC14-22	34.77	22.9	2.79
GPC14-23	33.42	21.55	2.73
GPC14-24	32.52	20.65	2.68
GPC14-25	30.61	18.74	2.55
GPC14-26	29.65	17.78	2.51

concrete

### 3.4.4 Curing

The processing methods for this study are explained in the following sections, based on previous studies, samples were left for 24 h before processing. The samples were placed in the laboratory at room temperature between 30 to 40 degrees Celsius, for the required period until the day of the test, and the room humidity was also measured, the minimum humidity was 10% and the maximum humidity was 21% inside the laboratory where the samples were kept during the four months of processing for all samples for all Mixtures.

### 3.5 Testing of Geopolymer Pervious Concrete.

#### 3.5.1 Flow table test

The flowability of new geopolymer mortar was assessed using a flow table test, which was carried out in accordance with the manufacturer's instructions. (ASTM 2013a) (C1437) for all of the mixes as shown in Figure 3.8.



**Figure 3.8** Flow Table Test



**Figure 3.9** Compressive Strength Test

### **3.5.2 Compressive strength test**

A hydraulic testing machine was used to conduct a compressive strength test on hardened geopolymer pervious concrete. (ASTM 2002a C109/C109M) as shown in Figure 3.8. Three 150 mm cubes were tested for each mix. The results given in various figures are the mean of these values. The loading rate used was 0.9 kN/s.

### **3.5.3 Modulus of elasticity test**

For measuring modulus of elasticity, the geopolymer pervious concrete was cast in 150x300 mm cylinders. The modulus of elasticity and the Poisson's ratio test were carried out in accordance with the guidelines. (ASTM 2002b) (C469/C469M, 2002) as shown in Figure 3.9.



**Figure 3.10** Modulus of Elasticity Test

### 3.5.4 Splitting tensile strength test

For testing splitting tensile strength, the geopolymer pervious concrete was cast in 150x300 mm cylinders. The tensile strength test for splitting was carried out in accordance with (ASTM 2017 C496/C496M) as shown in Figure 3.10.



**Figure 3.11** Splitting Tensile Strength Test

### 3.5.5 Flexural strength test

The geopolymer pervious concrete was cast in 150x150x750 mm prisms for testing flexural toughness. The flexural strength test was performed according to the criteria below.: (ASTM 2015) (C78/C78M) as shown in Figure 3.12



**Figure 3.12** Flexural strength test

### 3.5.6 Surface infiltration rate test

For evaluating the Infiltration Rate, 1. meter squares of geopolymer pervious concrete were cast. The Infiltration Rate test was done in accordance to (ASTM 2013b) (C1781/C1781M – 2013) as shown in Figure 3.13



**Figure 3.13** Surface Infiltration rate test

### 3.5.7 Density (unit weight) test

The density of pervious concrete is an important parameter since it has a direct link with the void content., Density (unit weight) in accordance with (ASTM 2018 C-16887).

### 3.5.8 Voids content test

The (ASTM 2014 C-1688) The void content is measured according to ASTM C1688. The void content is measured as follows.

$$\text{Void content (\%)} = (T - D) / T * 100$$

$$D = (M_c - M_m) / V_m$$

$$T = M_s / V_s$$

where,

$M_c$  = measure filled with concrete (mass)

$M_m$  = measure (mass)

$V_m$  = measure (volume)

$M_s$  = total mass of all materials batched

$V_s$  = sum of absolute volume of each ingredient equal to the quotient of mass of that ingredient divided by the product of its specific gravity times the density of water sample.

Calculation plastic void content must be determined and compared to the void percentage needed by the hydraulic design. The void content must be between 15 and 25 percent unless otherwise specified. Based on two factors, ten experimental mixtures were chosen from the 64 above. The first step was to assess compressive strength, and the second was to focus on type. The remaining tests, which are mentioned in Tables 3-10, were then completed.

**Table 3.8** The selected mix from trial mixes depending on the largest compressive

Mix no.	Flow %	Void %	Density $Kg/m^3$	Compressive Strength (MPa)	Flexural Strength (MPa)	Splitting Strength (MPa)	Modulus of Elasticity (GPa)	Infiltration Rate (mm/h)
GPPC 14-15	60	15.37	1850	40.17	3.37	3.56	4.2	4218
GPPC 14-18	63	16.73	1851	37.11	3.01	3.22	3.9	3977
GPPC 14-19	65	16.98	1851	36.88	2.93	3.00	3.7	3898
GPPC 14-20	65	17.11	1851	36.43	2.89	2.88	3.1	3861
GPPC 14-21	66	17.43	1852	35.53	2.79	2.76	2.9	3748
GPPC 14-22	67	18.34	1852	34.77	2.74	2.66	2.8	3711
GPPC 14-23	67	19.01	1852	33.42	2.56	2.35	2.6	3650
GPPC 14-24	68	20.00	1853	32.52	2.11	2.16	2.5	3609
GPPC 14-25	69	20.89	1853	30.61	1.98	1.88	2.4	3588
GPPC 14-26	70	21.22	1853	29.65	1.79	1.54	2.3	3545

strength and types (pervious or non-pervious)

## CHAPTER 4

### RESULTS AND DISCUSSION

#### 4.1 Introduction

This chapter consists of two parts, first part involves 26 mixtures proportion of GPPC were the flowability, compressive strength and appearance of the products was investigated. This part is to optimize the composition and select mixture proportions that have given the convenient workability for construction, good compressive strength and pervious performance which allow the water to pass through it. Then 10 mixtures were selected from trial mixes depending on the target compressive strength and type (pervious or non-pervious). The mechanical Properties of the selected mixes of Geopolymer pervious Concrete and the results obtained from the experimental work are interpreted and studied. The effect of several parameters that mostly influence on the compressive strength of GPPC and specifically GPPC are investigated. These parameters are Sodium silicate to sodium hydroxide ratio ( $\text{Na}_2\text{SO}_3/\text{NaOH}$ ), Concentration (Molarity) of the sodium hydroxide solution, alkaline to binder ratio (Alk/GGBFS).

Type of the superplasticizer (not all types are suitable) naphthalene based are preferred, the effect of maximum aggregate size (14 and 20) mm and the effect of type of compaction were examined. Furthermore, to reduce the cost of the product, which necessitated the use of GGBFS, which is not available in every country and has a high demand on this material, made the production of GPPC in general to be expensive. led us to choose an alternative material for GGBFS. As a result, different waste locally industrial products such as: Erbil steel slag, Erbil slag steam condenser and Brick Powder were used as a partial replacement material to GGBFS, the combination of GGBFS and waste materials were used as a source material of geopolymer. The following tests were conducted. Flow table test, void ratio, density, compressive strength, splitting tensile strength, flexural strength, modulus of

elasticity and infiltration rate. GPPC specimens were cured under the ambient condition.

#### **4.2 Factors Affecting Geopolymer Paste and Concrete**

The average compressive strength of geopolymer pervious concrete after 28 days of ambient curing is shown in Table 4.1. A variety of mixtures ranging from GPPC14-1 to GPC14-26 were water impermeable, indicating that either the amount of GGBFS (450, 350, and 300 kg/m<sup>3</sup>) or the ratio of Alk to GGBFS (0.35) was excessively high. This is due to the high concentration of geopolymer paste in these mixtures, which resulted in the appearance of non-pervious performance. Typical pervious concrete has a void ratio of 15 to 25 percent; thus, it is advised that the correct paste content be used in conjunction with a low water-to-cement (w/c) ratio or Alk/GGBFS ratio of 0.20 to 0.25 to create the necessary void structure in pervious concrete applications. GPPC14-7 and GPPC14-10 to GPPC14-26 mixes created with an Alk/GGBFS ratio of 0.25 at GGBFS content of 325 kg/m<sup>3</sup>, this resulted in a reduction in the amount of geopolymer paste used, which resulted in increased compressive strength and improved pervious performance.

A strong relationship was found between the molarity of NaOH, the ratio of SS/SH and GGBFS content in GPC specimens as independent variables, with the compressive strength as a dependent variable. The mix GPPC14-1 has given the highest compressive strength which is 46 MPa, that is due to the presence of 450 kg GGBFS, a 0.35 Alk/GGBFS ratio, and a 2.5 SS/SH ratio. Reduced compressive strength in non-pervious concrete was observed when the SS/SH ratio was reduced from 2.5 to 1.0. This result could also be observed in ordinary concrete if the other parameters were held constant, whereas increased compressive strength in GPPC specimens was observed when the SS/SH ratio was decreased from 3.5 to 1.0

In this section of the study, a statistical analysis was generated to indicate the best relationship between the obtained results of compressive strength with all the parameters investigated. All variable used in this process containing (i) Alk/GGBFS, (ii) Molarity, (iii) SS/SH ratio, and GGBFS content, these were represented by graphs and analyzed with compressive strength.

**Table 4.1** Average compressive strength and perviousness of geopolymer pervious concrete after 28 days of ambient curing made with maximum size 14 mm aggregate

Mix NO.	GGBFS Content Kg/m <sup>3</sup>	NaOH Molarity	Alk / GGBFS	Na <sub>2</sub> SiO <sub>3</sub> / NaOH (SS/SH)	Compressive Strength MPa	Void Content %
GPPC14-15	325	12	0.25	1	40.17	15.37
GPPC14-16	325	10	0.25	1	30.18	16.00
GPPC14-17	325	8	0.25	1	19.77	22.30
GPPC14-18	325	12	0.25	1.5	37.11	16.73
GPPC14-19	325	12	0.25	1.75	36.88	16.98
GPPC14-20	325	12	0.25	2	36.43	17.11
GPPC14-21	325	12	0.25	2.25	35.53	17.43
GPPC14-22	325	12	0.25	2.5	34.77	18.34
GPPC14-23	325	12	0.25	2.75	33.42	19.01
GPPC14-24	325	12	0.25	3.00	32.52	20.00
GPPC14-25	325	12	0.25	3.25	30.61	20.89
GPPC14-26	325	12	0.25	3.50	29.65	21.22

#### 4.2.1 Effect of alkali / GGBFS ratio

Table 4.2 and Figure 4.2 illustrate how the alkaline solution-to-GGBFS ratio affects the compressive strength of GPPC specimens. These samples were created using a 14 molar sodium hydroxide solution and a 1:1 sodium silicate to sodium hydroxide solution ratio. Alk/GGBFS mass ratios of 0.25, 0.3, and 0.35 were chosen because they are about equal to the normal w/cm ratios of pervious concrete made with Portland concrete. To achieve the appropriate workability, pervious concrete should be proportioned with a low w/cm ratio of 0.27 to 0.43. ACI 522-10 [18]. Lower w/c ratios can lead to extremely low workable concrete, but higher w/c ratios induce the paste to flow and are more likely to encourage segregation, which can fill the gaps and minimize GPPC perviousness.

. There seems to be a strong correlation between the Alk/GGBFS ratio and GPPC compressive strength for different GGBFS concentrations. Though the specimens

have different levels of water permeability, the data points have a good correlation—better than 95%. The only specimens that were permeable to water had an Alk/GGBFS ratio of 0.25, while those with a ratio of 0.3 and 0.35 were not. Since increasing the ratio increases the amount of water utilized to create alkaline liquid, it was anticipated that the relationship between Alk/GGBFS ratio and compressive strength would be inversely proportional. However, increasing the ratio also greatly increases the alkaline content. When compared to other ratios, the Alk/GGBFS ratio of 0.35 has the most alkaline liquid and the fastest rate of geopolymerization. As a consequence, after 28 days of curing in ambient conditions, the concrete reached its maximum compressive strength of 46 MPa, although the specimens were not pervious to water.

As a general trend, increasing GGBFS content increased compressive strength, the highest compressive strength was 46 MPa achieved when GGBFS content was 450 kg/m<sup>3</sup> but the product was non pervious to water. The amount of this material should not be high enough to produce high content of geopolymer paste because most voids will be filled by the paste, nor should it be low enough to produce weak geopolymerization. Results showed that the optimal amount was 325 kg/m<sup>3</sup> to generate GPPC with high strength and a sufficient percentage of voids that made it permeable.

**Table 4.2** Effect of Alkali//GGBFS ratio on compressive strength of GPPC

Mix No.	GGBFS Content	Alk/GGBFS ratio	SS/SH ratio	Compressive Strength	Remark
GPPC14-5	350	0.30	1	30.01	Non pervious
GPPC14-6		0.35		31.67	Non pervious
GPPC14-7		0.25		28.62	Pervious
GPPC14-8	300	0.30		16.03	Non pervious
GPPC14-9		0.35		17.26	Non pervious
GPPC14-10		0.25		13.22	Pervious
GPPC14-14	325	0.25		25.65	Pervious

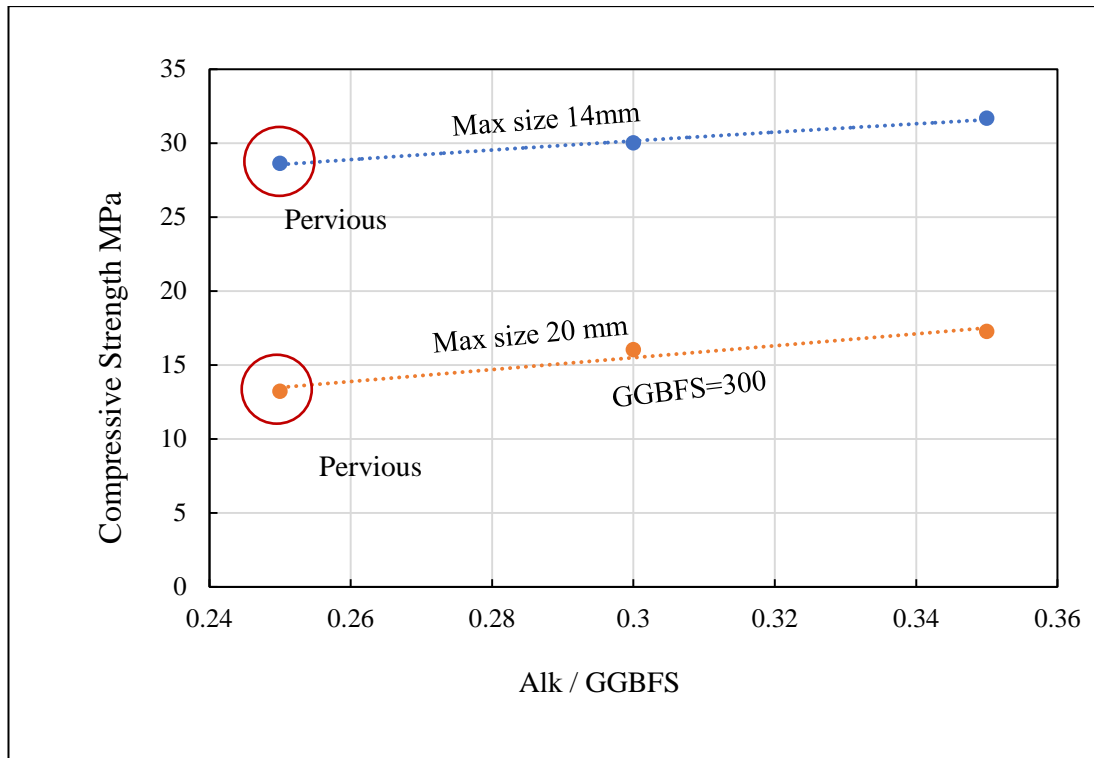


**Figure 4.1** Effect of Alk/GGBFS ratio on compressive strength

#### 4.2.2 Effect of molarity of NaOH

The impact of sodium hydroxide molarity on the compressive strength and percentage of voids of GPPC is depicted in Table 4.3 and Figure 4.3, respectively. It was found that increasing the (NaOH) molarity of GPPC specimens from 8 to 12 increased compressive strength and reduced void ratio, but increasing the molarity above this point decreased compressive strength and increased void ratio. GPP14-1 utilized 450 kg/m<sup>3</sup> GGBFS, an Alk/GGBFS ratio of 0.35, and a molarity of 14 for non-pervious specimens to obtain the greatest compressive strength of GPPC, 46 MPa. However, the greatest compressive strength obtained for the previous specimen was 40 MPa at Molarity 12. Because of the effect of other factors, the growth in molarity from 12 to 14 Molar may enhance or decrease compressive strength, as a general tendency compressive strength decreased. Hardjito claims that (Hardjito,2008). The strength of the fly ash-based geopolymer material is significantly influenced by the molarity of the NaOH solution. Due to a rise in soluble silicate and a higher concentration of reactants, an increase in molarity speeds up the rate of reaction. (Wang, 2005) demonstrated that at the age of 3 days, the highest strength was reached with 12 Molar of NaOH for fly-ash based geopolymer mortar.

**Table 4.3** Effect of NaOH Molarity on compressive strength of GPPC

Mix No.	GGBFS Content	Alk /GGBFS ratio	SS /SH ratio	NaOH Molarity	Compressive Strength N/mm <sup>2</sup>
GPPC14-12	325	0.25	1	16	19.89
GPPC14-14	325	0.25	1	14	25.65
GPPC14-15	325	0.25	1	12	40.17
GPPC14-16	325	0.25	1	10	30.18
GPPC14-17	325	0.25	1	8	19.77

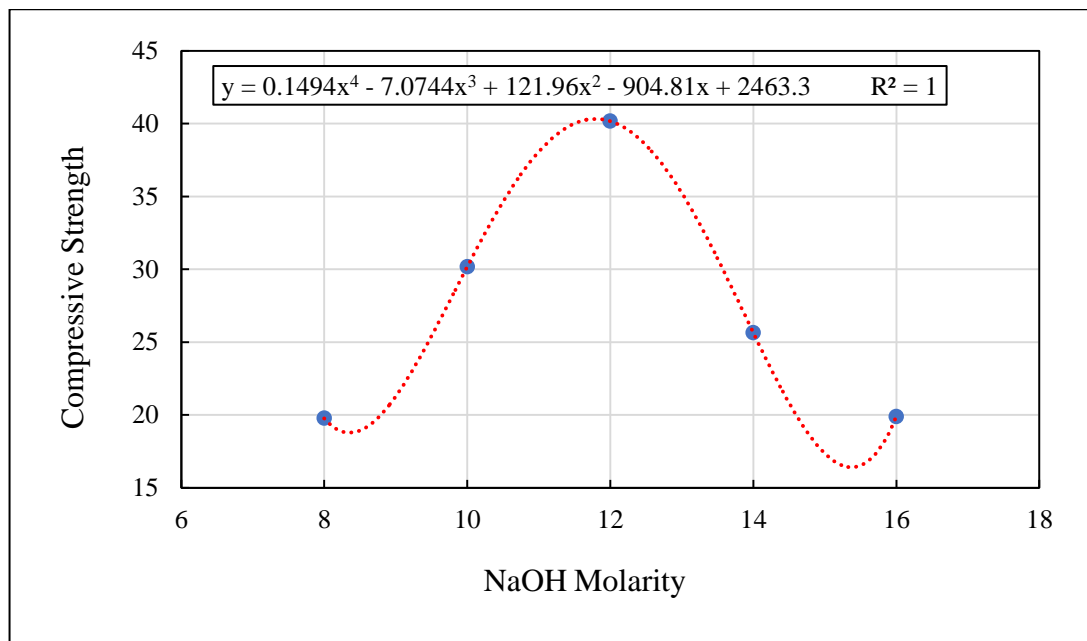


**Figure 4.2-a** Effect of NaOH molarity on compressive strength of GPPC

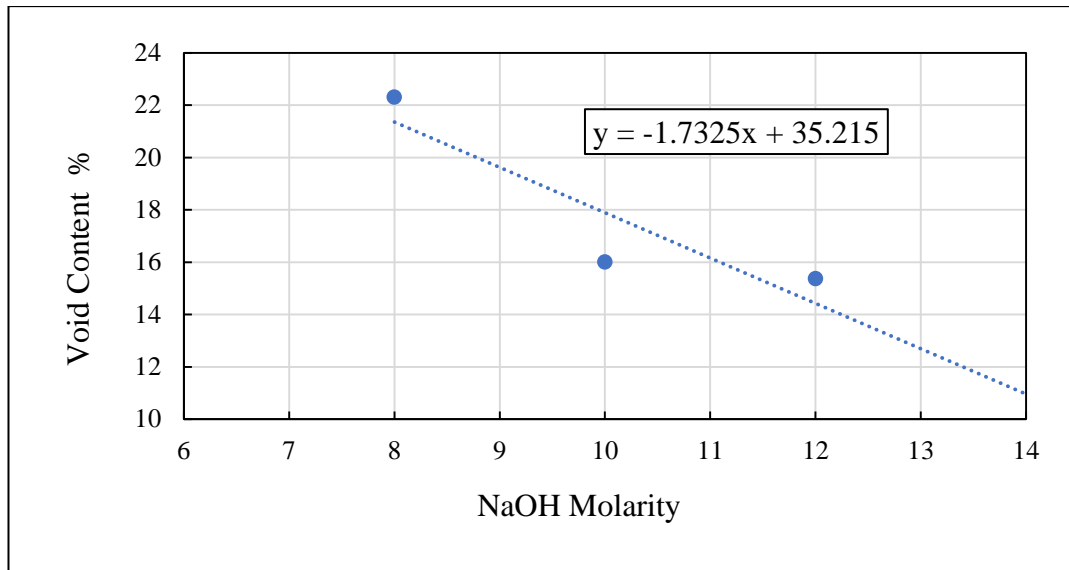


**Figure 4.2-b** Effect of NaOH molarity on the percentage of voids

#### 4.2.3 Effect of sodium silicate to sodium hydroxide (SS/SH) ratio.

Table 4.4 and Figures 4.4 -a and 4.4- b show the influence of the sodium silicate-to-sodium hydroxide solutions ratio on the compressive strength of GPPC and the percentage of voids. With increasing SS/SH ratio from 1 to roughly 2.5, the line showed an increase in compressive strength and a decrease in void ratio, and beyond that point, compressive strength dropped. The greatest compressive strength obtained for non-pervious specimens was 46 MPa at SS/SH ratio 2.5, while the maximum compressive strength obtained for pervious specimens was 40 MPa at SS/SH ratio 1. (Morsy, 2014) According to the study, increasing the SS/SH ratio reduces compressive strength because more sodium silicate in the geopolymer structure limits water evaporation and delays the creation of the geopolymer structure. (Škvára, 2005) from his experimental work on fly-ash-based geopolymer concrete, The SS/SH ratio influences Si and Al leaching; when the SS/SH ratio is low, Si leaching is higher than Al, which is most likely the reason for the maximum geopolymer gel formation with a homogeneous microstructure and the lowest proportion of voids.

**Table 4.4** Effect of SS/SH ratio on the compressive strength of GPPC

Mix No.	GGBFS Content	Alk/GGBFS ratio	SS/SH Ratio	NaOH Molarity	Compressive Strength N/mm <sup>2</sup>	Void content (%)
GPPC14-1	450	0.35	2.50	14	46.16	Very Low And Non-pervious
GPPC14-2			2.00		36.55	
GPPC14-3			1.50		42.74	
GPPC14-4			1.00		38.50	
GPPC14-15	325	0.25	1.00	12	40.17	15.37
GPPC14-18			1.50		37.11	16.73
GPPC14-19			1.75		36.88	16.98
GPPC14-20			2.00		36.43	17.11
GPPC14-21			2.25		35.53	17.43
GPPC14-22			2.50		34.77	18.34
GPPC14-23			2.75		33.42	19.01
GPPC14-24			3.00		32.52	20.00
GPPC14-25			3.25		30.61	20.89
GPPC14-26			3.50		29.65	21.22

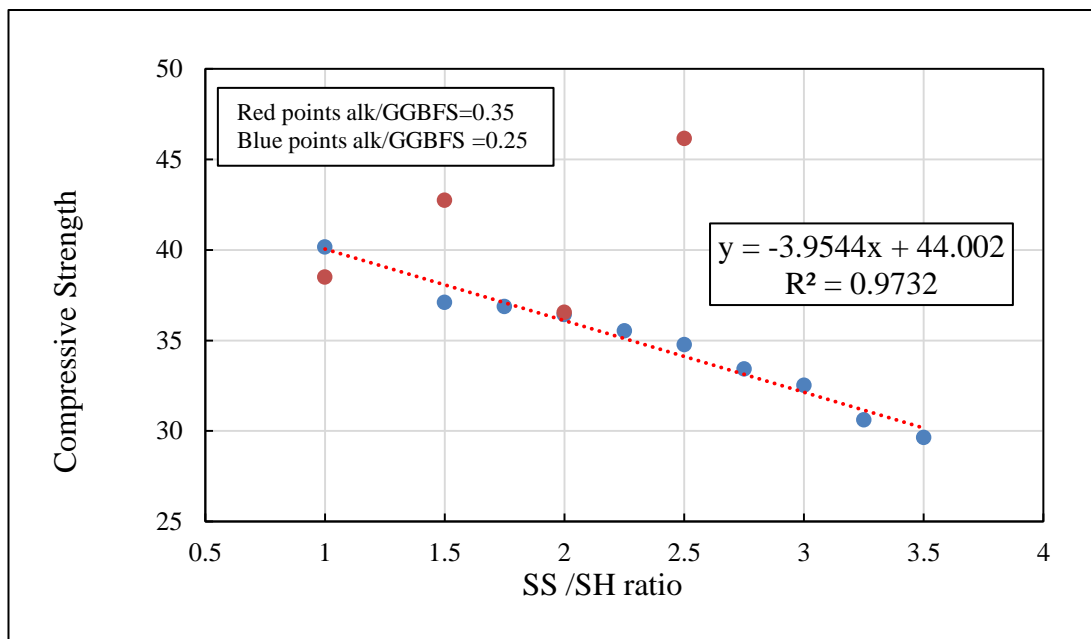


**Figure 4.3-a** Effect of SS/SH ratio on compressive strength

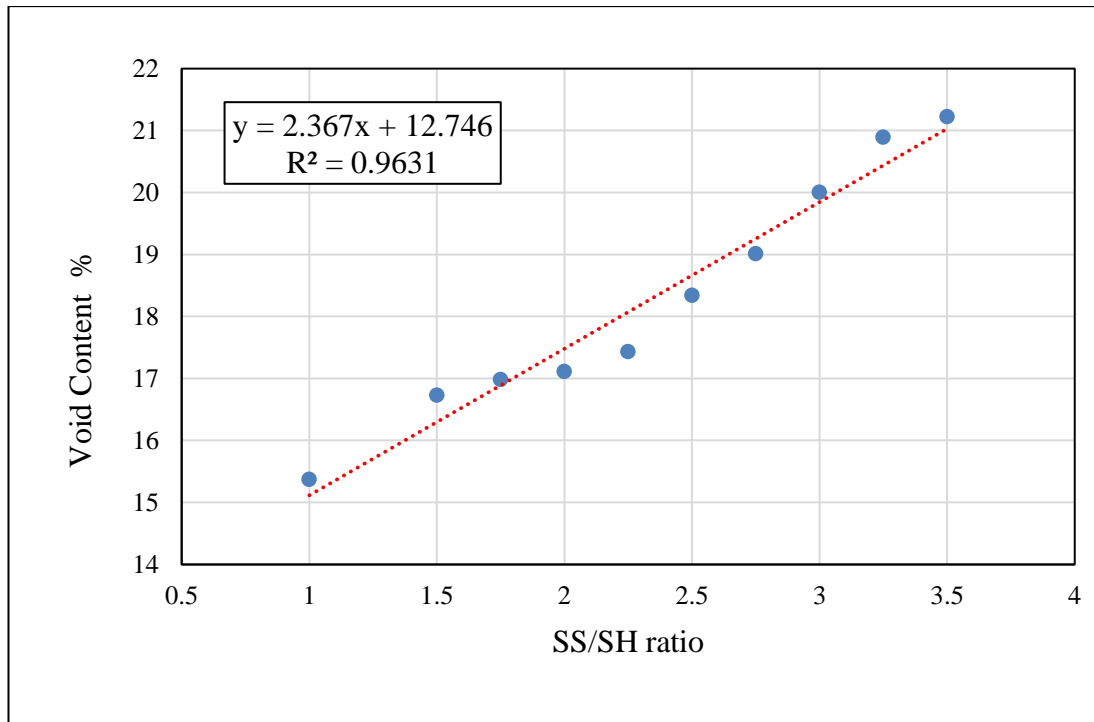


**Figure 4.3-b** Effect of SS/SH ratio on the percentage of voids

#### 4.2.4 Statistical model

Presently compressive strength and the percentage of voids as a dependent variable of GPPC formulated as a function of the product of molarity of NaOH and SS/SH ratio as independent variables. The effect of ALk/GGBFS ratio and GGBFS content was excluded because all data points that showed pervious concrete made with ALk/GGBFS ratio was 0.25, and the best GGBFS kept constant equal to 325 kg/m<sup>3</sup>. While Specimens made by ratios of 0.3 and 0.35 were not pervious. The relation is estimated statistically using computer package (MATLAB version 2017). The best fit non-linear exponential equation used to express the compressive strength and the percentage of voids of GPPC is shown below

$$f_{cube} = a * \exp(b * \mu) + c * \exp(d * \mu) \quad 4.1$$

$$\% Voids = a * \exp(b * \mu) + c * \exp(d * \mu) \quad 4.2$$

Where;

$\mu$ : Is the product of molarity by SS/SH ratio

And a, b, c, d are empirical coefficients were determined statistically for the best fit equation, these Coefficients (with 95% confidence bounds) are shown in table 4.5

**Table 4.5** Empirical obtained from the Reaggregation Analysis.

Coefficients	Equation-1	Equation-2
a	47.14 (40.53, 53.75)	1.599e+04 (-3.395e+04, 6.593e+0)
b	-0.01073 (-0.01536, -0.006106)	-0.9535 (-1.348, -0.5594)
c	-757.7 (-1932, 416.6)	13.28 (12.61, 13.96)
d	-0.4319 (-0.6352, -0.2286)	0.01116 (0.009568, 0.01276)

To determine and estimate the efficiency of the proposed models, the following parameters containing coefficient of determination ( $R^2$ ), sum of square errors and root Mean Squared Error (RMSE), are used as listed in the table 4.6.

**Table 4.6** Showing the Statistical Analysis the goodness of Models

Goodness of fit assessed by	Equation-1	Equation-2
SSE	17.74	0.855
RMSE	1.489	0.327
$R^2$	0.942	0.984
Adjusted $R^2$	0.9203	0.978

**Table 4.7** Effect of the product of molarity and SS/SH ratio on the Compressive strength and void content of GPPC specimen

Mix NO.	NaOH Molarity Col (1)	Na <sub>2</sub> SiO <sub>3</sub> /NaOH (SS/SH) Col (2)	Molarity X SS/SH ratio Col (3)=Col(1)X Col(2)	Compressive Strength MPa	Void Content %
GPPC14-15	12	1	12	40.17	15.37
GPPC14-16	10	1	10	30.18	16.00
GPPC14-17	8	1	8	19.77	22.30
GPPC14-18	12	1.50	18	37.11	16.73
GPPC14-19	12	1.75	21	36.88	16.98
GPPC14-20	12	2.00	24	36.43	17.11
GPPC14-21	12	2.25	27	35.53	17.43
GPPC14-22	12	2.50	30	34.77	18.34
GPPC14-23	12	2.75	33	33.42	19.01
GPPC14-24	12	3.00	36	32.52	20.00
GPPC14-25	12	3.25	39	30.61	20.89
GPPC14-26	12	3.50	42	29.65	21.22

The models presented so far are utilized to predict the compressive strength and percentage of voids of GPPC, gaining a superior prediction value of compressive strength and void content when compared to experimental data. The relationship between compressive strength, void content as a dependent variable and the product of molarity times SS/SH ratio as independent variable are shown in figures 4.5-a and 4.5-b respectively

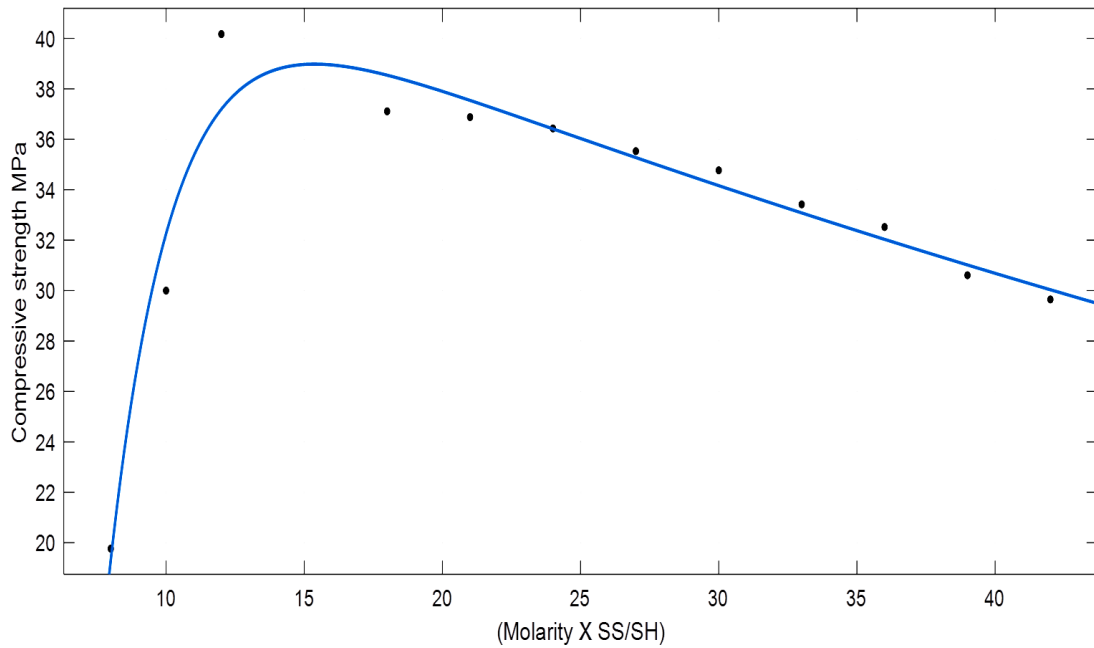


**Figure 4.4-a** the effect of (Molarity X SS/SH) on the Compressive Strength of GPPC produced with maximum size of 14 mm, Alk/GGBFS ratio of 0.25 and GGBFS content  $325 \text{ kg/m}^3$

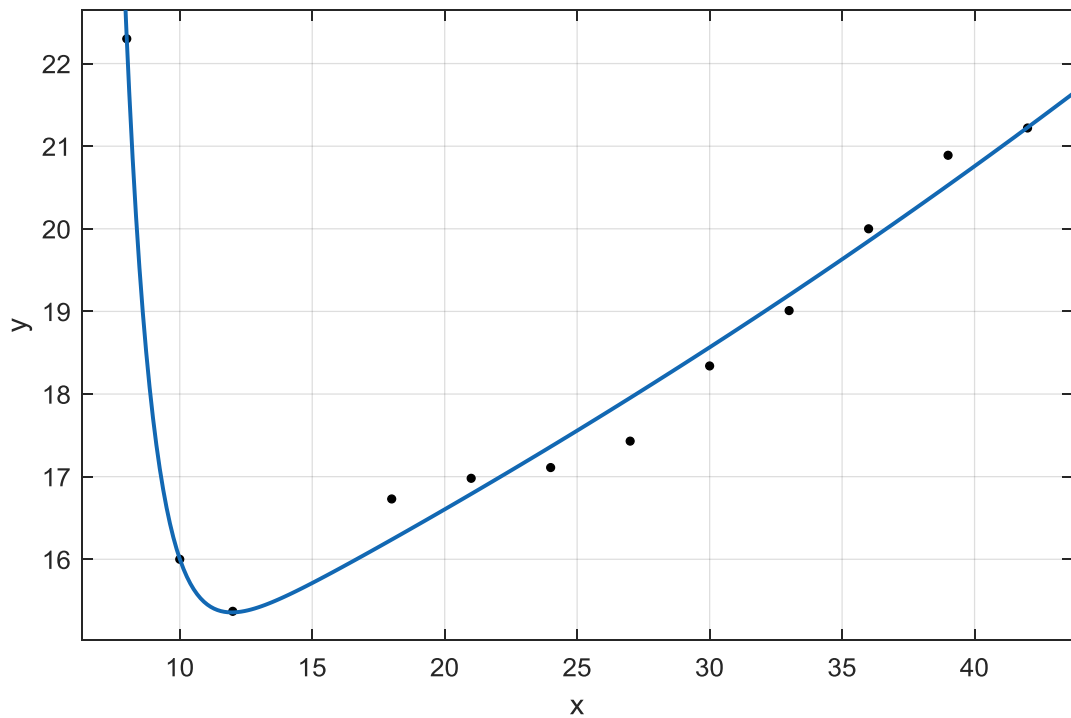


**Figure 4.4-b** The effect of (Molarity X SS/SH) on the percentage of voids of GPPC produced with maximum size of 14 mm, Alk/GGBFS ratio of 0.25 and GGBFS content  $325 \text{ kg/m}^3$

### 4.3 Functional and Mechanical Properties

Ten mix compositions were selected from trial mixtures depending on the target compressive strength and type of GPPC as pervious or non-pervious to water. The mechanical Properties such as compressive strength, flexural strength, splitting tensile strength and modulus of elasticity, and other physical properties such as the density, percentage of voids , and infiltration rate of the selected mixes of Geopolymer pervious Concrete and the results obtained from the experimental work are studied interpreted.

The void ratio of the studied samples ranges between 15 and 21%. According to NRMCA, CIP 38 for pervious concrete, the void content is generally between 15-25% and permeability is generally between 2-30 mm/s. and the typical range of void ratio is between 18- 35 percent, according to ACI, 2010. Aggregate gradation, geopolymer paste composition, and compacting efforts all have a role in the air void ratio. The gradation and maximum aggregate size was set at 14 mm in this study, and the optimal form of compaction, namely the efforts exerted by the jack hammer, was

also kept constant. The geopolymer paste was the only variable that changed. Figure 4.6 depicts the relationship between compressive strength and void %. The curve is the most well-fitting, and the R2 value is the highest (0.9853) The best association between the void ratio and the compressive strength of the 28-day GPPC is:

$$y = -1.6497x + 64.912 \quad 4.3a$$

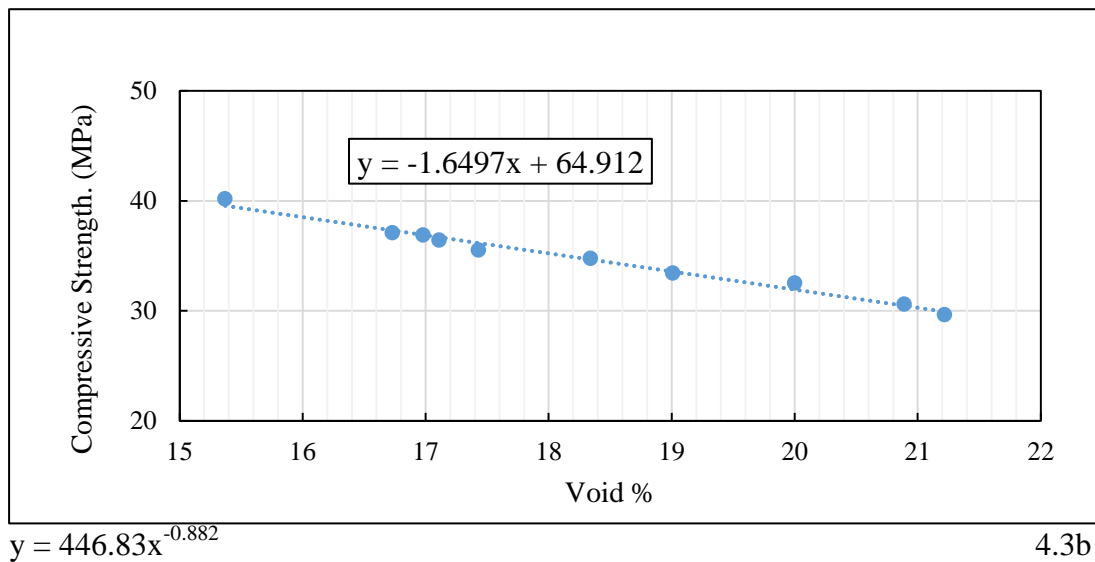


**Figure 4.5** Relationship between Void ratio and 28 day compressive strength of GPPC made with maximum size 14 mm

### 4.3.1 Compressive strength and splitting strength

The quality of the concrete structure is mainly determined by the compressive strength. Compressive strength is more important in structural design, but tensile strength is also important for specific applications. Shear strength and crack resistance are required in the design of road and airport boards. Depending on the strength of concrete, the compressive tensile strength and cleavage are closely related. Since concrete is not usually built to withstand direct tension, tensile strength is used to estimate the load at which cracking may occur. This is due to its effect on the formation and spread of cracks on the tension side of the bending members of reinforced concrete. There is no clear relationship between compressive tensile forces and cleavage. It is found that when the compressive strength increases, the tensile cleavage strength also increases, albeit at a slower rate (Jaber et al., 2018: Lavanya and Jeganm 2015; Hassan et al. 2016) during the cleavage tensile strength test, cylinder samples are loaded to create tangential tension. Due to the high tensile

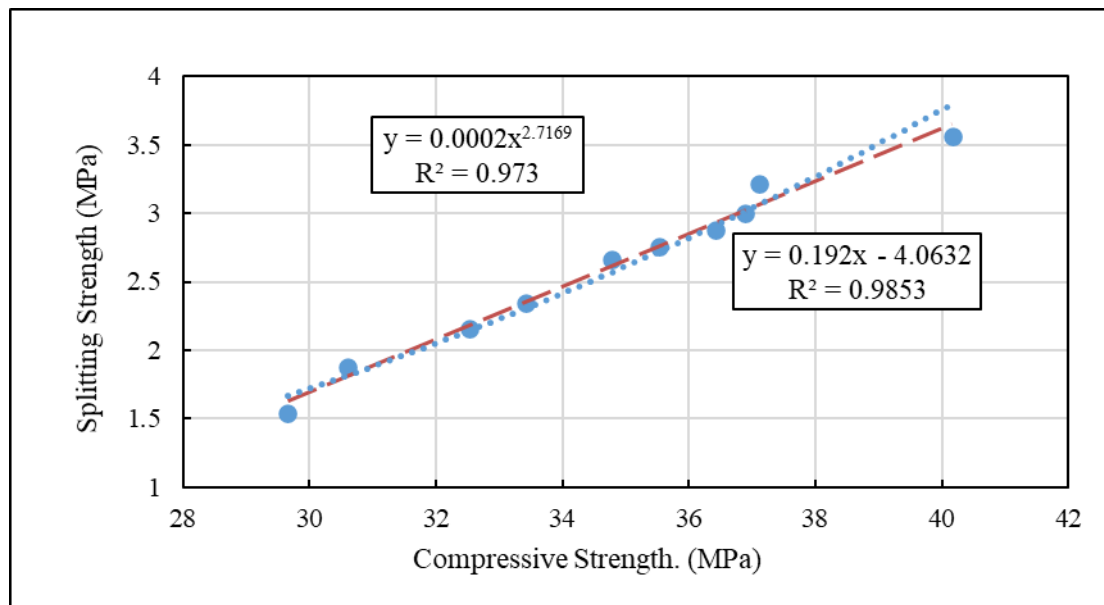
stresses that produce a split of the sample in the vertical plane, two strong parallel plates distribute and compress two diametrically opposite points on the diameter of the cylinder, causing the fractures to spread across the paste (Hassan et al. 2016; Lavanya and Jegan, 2015).

Figure 4.10 shows the compressive strength test at the age of 28 days for all the mixtures, it can be seen that the higher the compressive strength the higher the cleavage strength. The highest compressive strength 40.17 MPa when cleaved was 3.56 MPa and the lowest pressure resistance 29.65 MPa was when the cleavage strength was reported 1.54 MPa (Malayali et al. It can be concluded that the compressive strength and modulus of elasticity for these ten groups of geopolymer fillers were determined by mechanical properties tests, and the compressive strength and splitting strength were fitted linearly and nonlinearly by Excel software, and the internal and external limitations are shown in Fig. 4.10. The compressive strength and cleavage tensile strength of 28 days of GPPC are analyzed by linearity.

As seen from Figure (4.10). the curve has the best fitting effect and the R2 value is (0.9853) and (0.9694) the better relationship between the flexural strength and the compressive strength of the 28 days GPPC can be expressed by

$$y = 0.192X - 4.0632 \tag{4.4a}$$

$$y = 0.0002x^{2.7169} \tag{4.4b}$$



**Figure 4.6** Compressive strength and Splitting Strength

### 4.3.2 Compressive strength and modulus of elasticity

Concrete's modulus of elasticity is commonly stated in terms of compressive strength. While numerous researchers have suggested empirical formulae for predicting modulus of elasticity, only a few are regarded to cover the entire data set. The mechanical qualities of concrete are thought to be significantly reliant on the properties and quantities of binders and particles. The modulus of elasticity of concrete is a crucial factor in determining the modular ratio, which is used to design flexure-resistant sections of members, as well as in estimating the deformation of buildings and members. Based on the fact that the modulus of elasticity of concrete is related to the square root of compressive strength in the standard concrete strength range (Tomosawa and Noguchi, 1993).

Figure 4.12 shows the compressive strength test at 28 days old for all mixtures, it can be seen that the higher the compressive strength the higher the modulus of elasticity. It can be seen that the higher the modulus of elasticity the higher the compressive strength, the higher the compressive strength was 40.17 MPa when the modulus of elasticity was 4.2 Gpa and the lowest compressive strength was 29.65 MPa when the modulus of elasticity was 2.3 Gpa (Malayali et al. 2020; Chokkalingam et al., 2018) that the higher the modulus of elasticity, the higher the compressive strength.

It can be concluded that the compressive strength and modulus of elasticity for these ten groups of geopolymer grouting materials were determined by mechanical properties tests, and the compressive strength and modulus of elasticity were linearly and nonlinearly fitted by Excel software, and the inner and outer limits are shown in Figure (4.11). The compressive strength and bending strength of 28 days of GPPC are analyzed by linear and nonlinear

As shown in Figure (4.11), the curve has the best fit effect and the value of R2 is (0.856), the best relationship between elastic modulus and compressive strength for 28 days GPPC can be expressed by:

$$y = 0.1932X - 3.6641 \quad 4.5a$$

$$y = 0.0016x^{2.1266} \quad 4.5b$$

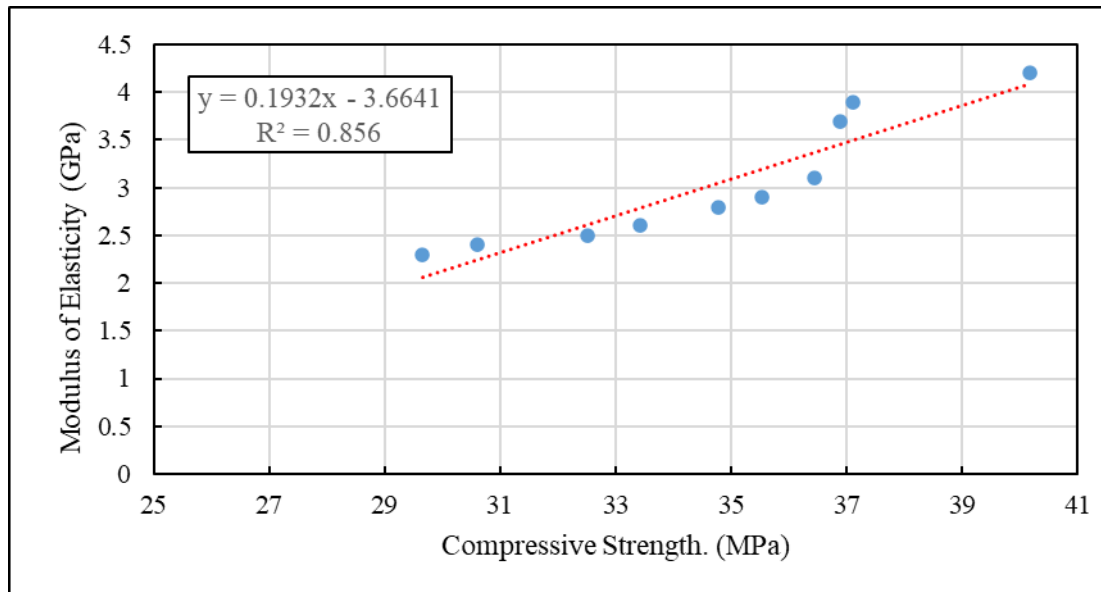


**Figure 4.7** Compressive strength and Modulus of Elasticity

### 4.3.3 Compressive strength and flexural strength

The average compressive strength of geopolymer pervious concrete after 28 days of ambient curing is shown in Table 4.3. A strong relationship was found between the molarity of NaOH, the ratio of SS/SH and GGBFS content in GPPC specimens as independent variables, with the compressive strength and the flexure strength as a dependent variable. The mix GPPC14-15 has given the highest compressive strength which is 40.17 MPa and the highest flexure strength 3.37 MPa, that is due to the presence of 325 kg GGBFS, a 0.25 Alk/GGBFS ratio, and a 1.00 SS/SH ratio. The decrease in compressive strength and bending strength was observed when the SS/SH ratio was reduced from 3.5 to 1.0. While the increase in compressive strength and bending strength was observed in GPPC samples when the ratio of SS/SH decreased from 3.5 to 1.0. It can be concluded that the compressive strength and flexural strength of these ten groups of geopolymer grouting materials were determined by the mechanical properties tests, and the compressive strength and flexural strength were linearly and nonlinearly fitted by Excel software, and the internal and external constraints were shown in Fig. 4.12 on the next page.

The compressive strength and flexural strength of 28days of GPPC are analyzed by linearity and non-linearly

As it is shown in Figure 4.12 the curve has the best fitting effect and the  $R^2$  value are (0.9672 and 0.9543) the better relationship between the flexural strength and the compressive strength of the 28 days GPPC can be expressed by (Malayali et al.,

2020; Chokkalingam et al., 2018 noted that it may be observed that the flexural strength increases with increasing compressive strength. As may be seen, compressive strength increases as flexural strength decreases.

$$y = 0.1545X - 2.7444 \quad 4.6a$$

$$y = 0.0013x^{2.1467} \quad 4.6b$$

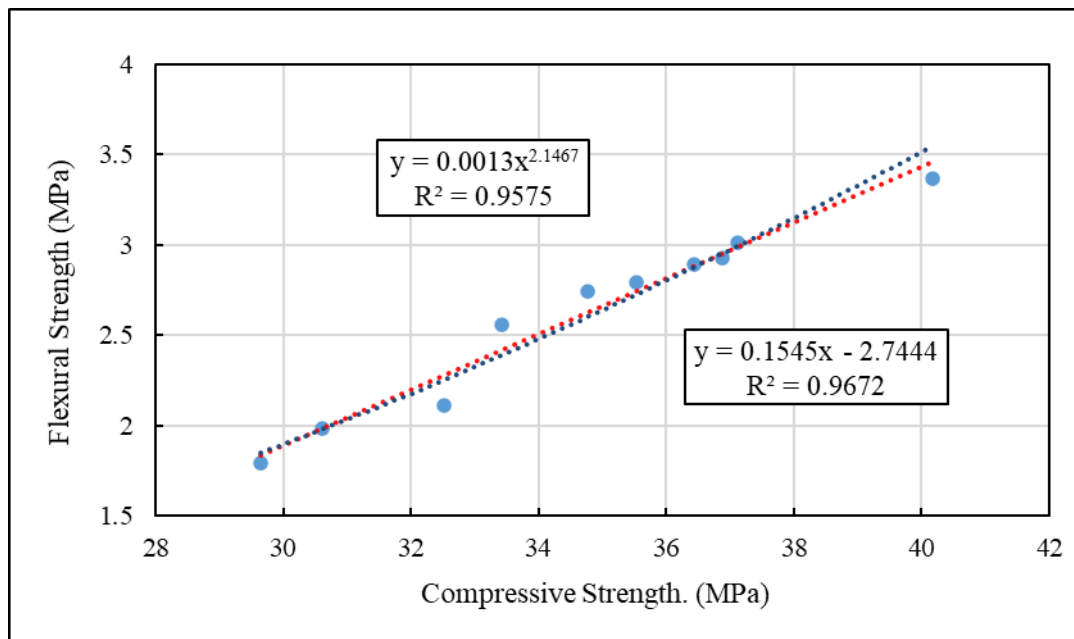


**Figure 4.8** Compressive strength and Flexural Strength

#### 4.3.4 Flexural strength and splitting strength

A few investigations on the relationship between flexural strength and splitting tensile strength have been done (Ramadoss, 2006). Statistical methods were used to investigate the relationship between splitting tensile strength and flexural strength of geopolymer concrete, the relationship, appeared to be linear (Chung and Structures, 2002). A basic test determines splitting tensile strength, while a flexural beam test determines flexural strength. Splitting tensile strength is a basic test, which necessitates a normal cube or cylinder specimen, whereas flexural strength testing necessitates a heavier beam specimen with bigger dimensions than most standards provide. As a result, splitting tensile strength tests with small specimens are clearly more practicable and cost-effective than flexural strength tests. The ability to derive the flexural design strength from the splitting tensile strength requires a correlation between the two measurements of tensile capacity, notably for geopolymer pervious concrete GPPC, which would be used in a pavement construction. This research

proposes a relationship between flexural and splitting tensile strengths for GPPC made from sustainable minerals and industrial by-products instead of using Portland cement. Figure 4.5 shows the Flexural Strength for all the mixes, it can be seen that the higher Flexural Strength the higher is the splitting strength. the highest Flexural Strength obtained was (3.37 MPa) at this point splitting strength is 3.56 MPa and the lowest Flexural Strength was (1.79 MPa) was when the splitting strength 1.54 MPa. The relevant empirical expressions obtained from this study are;

$$f_{st} = 0.78 \cdot f_t^{1.235} \quad 4.7a$$

$$f_{st} = 1.21 \cdot f_t - 0.57 \quad 4.7b$$

Where;  $f_{st}$  is the splitting tensile strength and  $f_t$  is the flexural strength measures both in MPa. A regression analysis showed power equation with high correlation coefficient where the coefficient of determination  $R^2 = 0.97$ . Therefore, by estimating flexural strength from splitting tensile strength, it may be possible to avoid the need for bulky and heavy specimens. It has been stated by (Malayali et al., 2020; Chokkalingam et al., 2018b) that the higher the flexural Strength, the higher is the splitting strength;

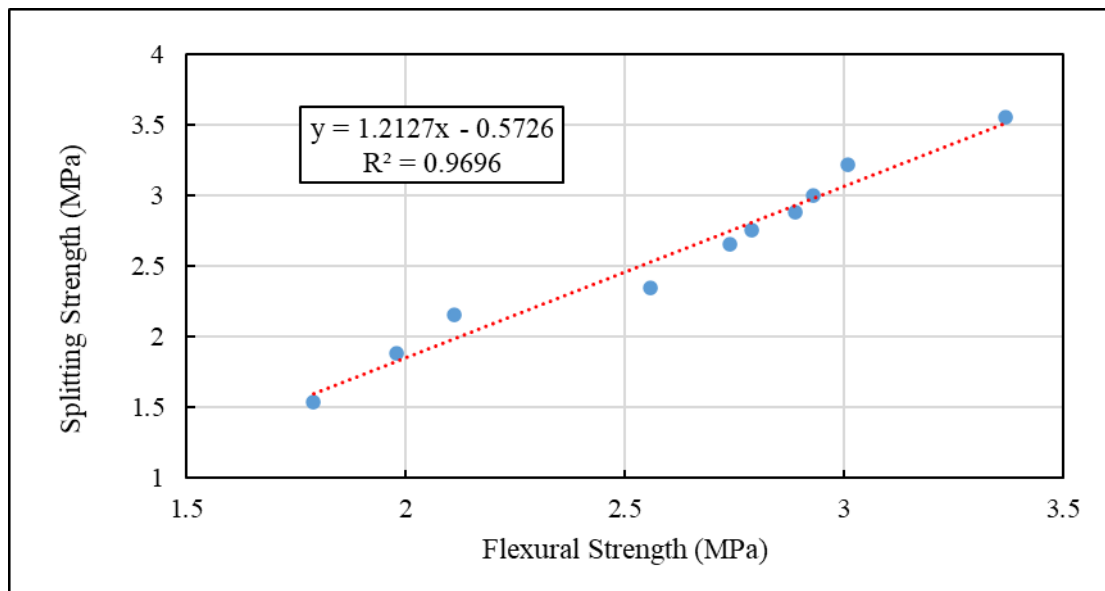


**Figure 4.9** Flexural Strength and Splitting Strength

#### 4.3.5 Compressive strength and infiltration rate

The environmental protection agency has now designated pervious pavement systems as a best management practice (Andersen et al., 1999), as well as the Florida

New storm water bill for the statewide Department of Environmental Protection. Infiltration into the underlying soil is possible due to the rapid passage of water through the joints or the porous structure of this type of paving system. When impermeable pavements are replaced with former pavements, runoff can reach the soil surface, where natural processes can break down pollutants (Cahill et al., 2003). Despite previous developments and experiences, there remains a great deal of uncertainty about infiltration rates over time, infiltrated water quality, and infiltrated water strength, which raises some concerns about its use as an alternative to rainwater management than conventional sidewalks.

This study noted the infiltration rates, regeneration processes, long-term storage of comprehensive components and systems, water purity, and strength characteristics of these berths. Infiltration rates are measured using the built-in ring infiltration meter (Kevern, 2008). A device developed at Stormwater Management Academy (Chopra et al., 2010). Designers and planners can use previous paving solutions to properly control rainwater. By increasing the rate and amount of rainwater intrusion, these rainwater management methods reduce runoff. Reduced runoff from pavement surfaces can reduce the bulk of the pollutants carried by runoff water, reducing non-point source pollution. Figure 4.6 shows the compressive strength test at 28 days for all mixtures; It can be seen that the higher the compressive strength, the lower the infiltration rate; The highest-pressure resistance (40.17 MPa) was achieved when the infiltration rate was 3545 mm / h, and the lowest pressure resistance (29.65 MPa) was achieved when the infiltration rate was 4218 mm / h (Chokkalingam et al., 2018).

According to the data, the lower the compressive strength, the lower the Infiltration Rate. It can be concluded that the compressive strength and Infiltration Rate of these 10 groups of geopolymer grouting material were determined by mechanical characteristics tests, the compressive strength and flexural strength were linearly and non-linearly fitted by axel program, and the internal and exterior limits are not presented in Figure (4.14) The compressive strength and Infiltration Rate of 28days of GPPC are analyzed by 1 linearly and non – linearly. Shown in the Figure 4.14 the curve has the best fitting effect and the R2 value is (0.9237) the better relationship between the flexural strength and the compressive strength of the 28 days GPPC can be expressed by

$$y = 6640.5e^{0.016x}$$

4.8a

$$y = 27887x^{-0.564}$$

4.8b

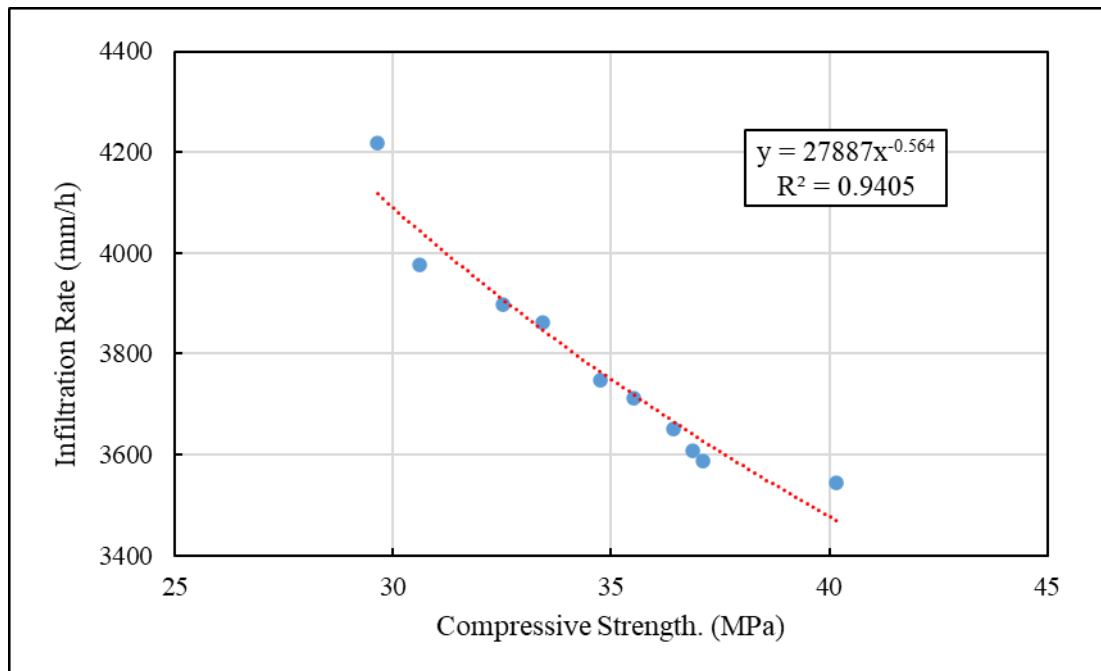


**Figure 4.10** Compressive strength and Infiltration Rate

#### 4.3.6 Void ratio and oven dry density

The density of pervious concrete is significant because it has a direct relationship with the void content, infiltration rate, and compressive strength. In line with ASTM C16887, density (unit weight) is measured in a standard yield pot. The delivered concrete's density (unit weight) must be within 80 kg/m<sup>3</sup> of the design density (unit weight). The void % needed by the hydraulic design must be compared to the plastic void content computed according to ASTM C1688. The empty content must be between 15 and 25 percent unless otherwise specified. Figure 4.7 shows the void ratio and oven dry density, the highest void ratio 21.22% was when oven dry density was 1853 kg/m<sup>3</sup> and the lowest void ratio 15.37% was when the oven dry density 1858 kg/m<sup>3</sup> (Khalil et al., 2019) reported that it can be seen that the higher void ratio the lowest is the oven dry density it can be seen that the higher void ratio the lowest is the oven dry density.

Conclusions The void ratio and oven dry density were measured by mechanical properties testing, the compressive strength and flexural strength were linearly fitted by axel program, and the internal and external limits were not displayed in these 10 groups of geopolymer grouting material Figure 4.15. The void ratio and oven dry density of 28days of GPPC are analyzed by linearly and non – linearly. As seen from Figure 4.15, the curve has the best fitting effect and the  $R^2$  value is (0.9137) the better relationship between the flexural strength and the compressive strength of the 28 days GPPC can be expressed by

$$y = 0.511x + 1842.4 \quad 4.9a$$

$$y = 1902.6x^{-0.009} \quad 4.9b$$

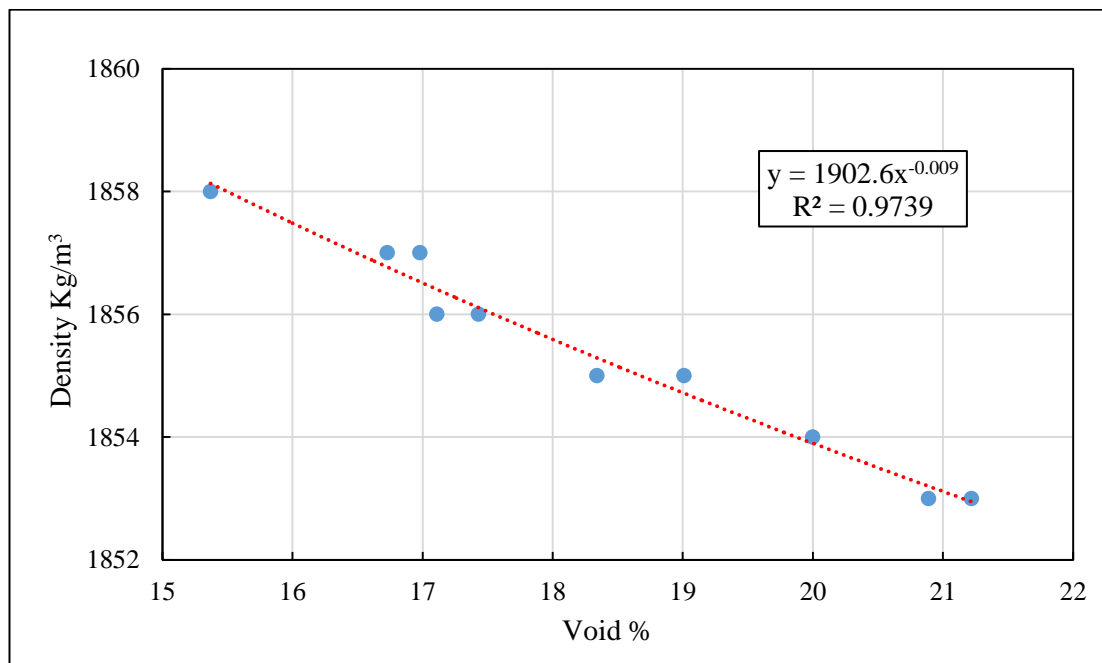


**Figure 4.11** Void Ratio and Oven Dray Density

### 4.3.7 Infiltration rate and void ratio

Figure 4.10 shows the infiltration rate. And the vacuum ratio, the higher the vacuum ratio. A high rate of infiltration can be observed. The higher the void ratio, the highest was the 4218 mm/h void rate when the void rate was 21.22% and the lowest was the 3545 mm/h void infiltration rate was when the void rate was 15.37% (Khalil et al., 2019; Arafa et al., 2017; Chokkalingam et al., 2007). , 2018) that it can be seen that the higher the infiltration rate, the higher the void ratio. Conclusions: In these ten

groups of geopolymer fillers, the infiltration rate and void ratio were determined, by testing the mechanical properties, the infiltration rate and void ratio were linearly fitted by Excel software, and the inner and outer limits were not shown in Figure (4.16).

The vacuum ratio and furnace Alk/GGBFS, for 28 days of GPPC are analyzed by linearity. As can be seen from Fig. 4.17, the curve has the best fitting effect and the value of R2 is (0.8786) The best relationship between bending strength and compressive strength for 28 days GPPC can be expressed by:

$$y = 6118.8e^{0.026x} \quad 4.10a$$

$$y = 904.67x^{0.4923} \quad 4.10b$$

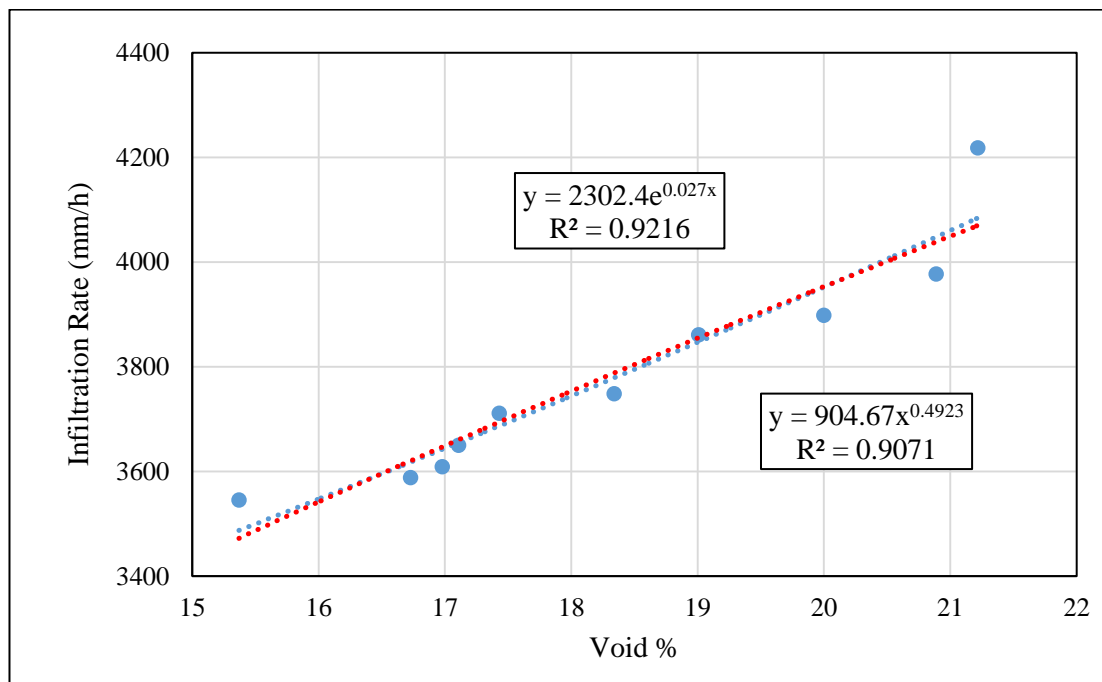


**Figure 4.12** Infiltration Rate and Void ratio

#### 4.3.8 Effects of types of compactions

Concrete compaction is one of the operations that has a significant impact on the compressive strength of concrete. Compressive strength is frequently low in non-dense concrete. (Mustafa et al., 2007). The Figure 4.17 and Table 4.4 shows the type of compaction method. It is found that the characteristic compressive strength by

vibration table is zero value because the vibration table cause segregation in geopolymer pervious concrete. Then the compressive strength by manual compaction was lower than compressive strength by jack hammer. There is no research on the influence of type of compaction on the compressive strength of GPPC, thus this is the first study to investigate at the effects of three different forms of compaction, such as tamping rods, vibration tables, and jack hammer tamping on a base plate.

Based on the result, it can be concluded that it is better to make a specimen of geopolymer pervious concrete compacted by jack hammer to obtain maximum compressive strength. The higher compressive strength compacted by jack hammer was 40.17 MPa while the compressive (Mustafa et al., 2007) strength compacted by manual compaction was 28.30 MPa.

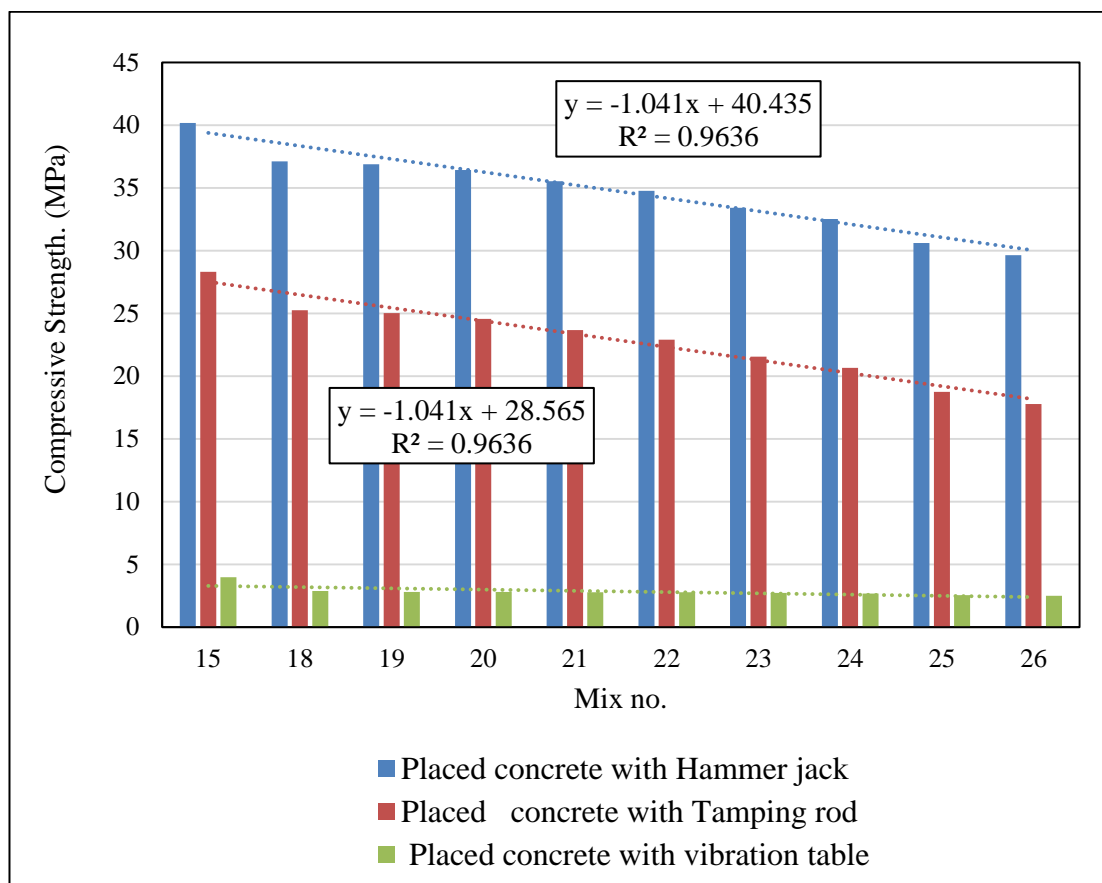


**Figure 4.13** Compressive Strength and Types of Compactions

**Table 4.8** Effect of type of compaction

Mix no.	Compressive Strength. (MPa)/placed concrete with Hammer jack	Compressive Strength. (MPa)/Placed concrete with Tamping rod	Compressive Strength. (MPa)/ placed concrete with vibration table
GPPC14-15	40.17	28.30	3.98
GPPC14-18	37.11	25.24	2.88
GPPC14-19	36.88	25.01	2.82
GPPC14-20	36.43	24.56	2.80
GPPC14-21	35.53	23.66	2.77
GPPC14-22	34.77	22.90	2.79
GPPC14-23	33.42	21.55	2.73
GPPC14-24	32.52	20.65	2.68
GPPC14-25	30.61	18.74	2.55
GPPC14-26	29.65	17.78	2.51

#### **4.4 Partial Replacement of GGBFS by Waste Products**

Geopolymerization of waste materials can help to address current environmental concerns such as natural resource depletion. The advantages of geopolymerization with waste material have been demonstrated (1.12). Despite the lower material reactivity of locally accessible waste materials compared to Fly Ash or GGBFS, it is important to focus on study of locally available waste materials, for environmental and sustainable development. In this paper different waste materials such as Erbil steel slag, Erbil steam condenser and fire clay bricks in powder form are utilized as a partial alternative for GGBFS slag to create geopolymer pervious concrete. The silica and alumina content in these waste materials are high. This indicates to their potential as a geopolymer mix preparation. The chemical composition of these waste products, notably the amounts of silica and alumina, determines their geopolymerization potential. The pervious concrete system's strength is dependent on the compressive strength of the pervious concrete and the strength of the soil

underneath it for support. The compressive strength of GPPC mixes generated utilizing GGBFS and several other locally waste materials at various replacement ratios is shown in Table No. (4.5). It can be seen that including all of these waste materials reduces the compressive strength of GPPC mixes; however, employing steel slag and steam condenser has given higher compressive strength than using fired clay bricks, and the compressive strength was around 24 MPa, indicating that mix no.1 to mix no.12 there is still have a potential capacity to support traffic loading.

**Table 4.9** Mix proportion of geopolymer pervious concrete (Erbil Steel Slag; Erbil Steam Condenser; Brick Powder)

Mix No.	GGBFS (%)	Compressive Strength MPa	Replacement material %		NaOH Molarity	Maximum size of aggregate
1	0	8.34	Erbil Steel Slag	100	12	14
2	25	11.98		75		
3	50	15.18		50		
4	75	24.11		25		
5	0	8.44	Erbil Steam Condenser	100		
6	25	11.98		75		
7	50	17.32		50		
8	75	25.31		25		
9	0	6.57	Brick Powder	100		
10	25	9.48		75		
11	50	11.81		50		
12	75	19.76		25		

**CHAPTER 5**  
**STRUCTURAL AND HYDROLOGICAL DESIGN BY PERVIOUS PAVE**  
**v1.0**

**5.1 Description**

Before it infiltrates into the subsoil, which may contain an underlying stone reservoir, a pervious concrete pavement absorbs and retains runoff. This pervious surface replaces traditional pavement by allowing stormwater to quickly infiltrate and be naturally treated. (Smith (Pervious concrete is made up of specifically formulated hydraulic cementitious ingredients, as well as uniform open graded coarse aggregate like sand and gravel. (ASTM 1999) C-33 or (3/8 inch) (10 mm), (3/4 inch-19 mm), to (1 inch-25 mm), and water. Pervious concrete has a large percentage of void space (15 percent or more) when properly planned and built, allowing it to handle runoff from any significant storm event. Figure 5.1 depicts a typical cross-section of pervious concrete pavement. Stormwater storage is supplied on level subgrades in the concrete surface layer (15 to 25% voids), the subbase (30 to 40% voids), and above the surface to the curb height 100 percent voids (Silva et al., 2013).

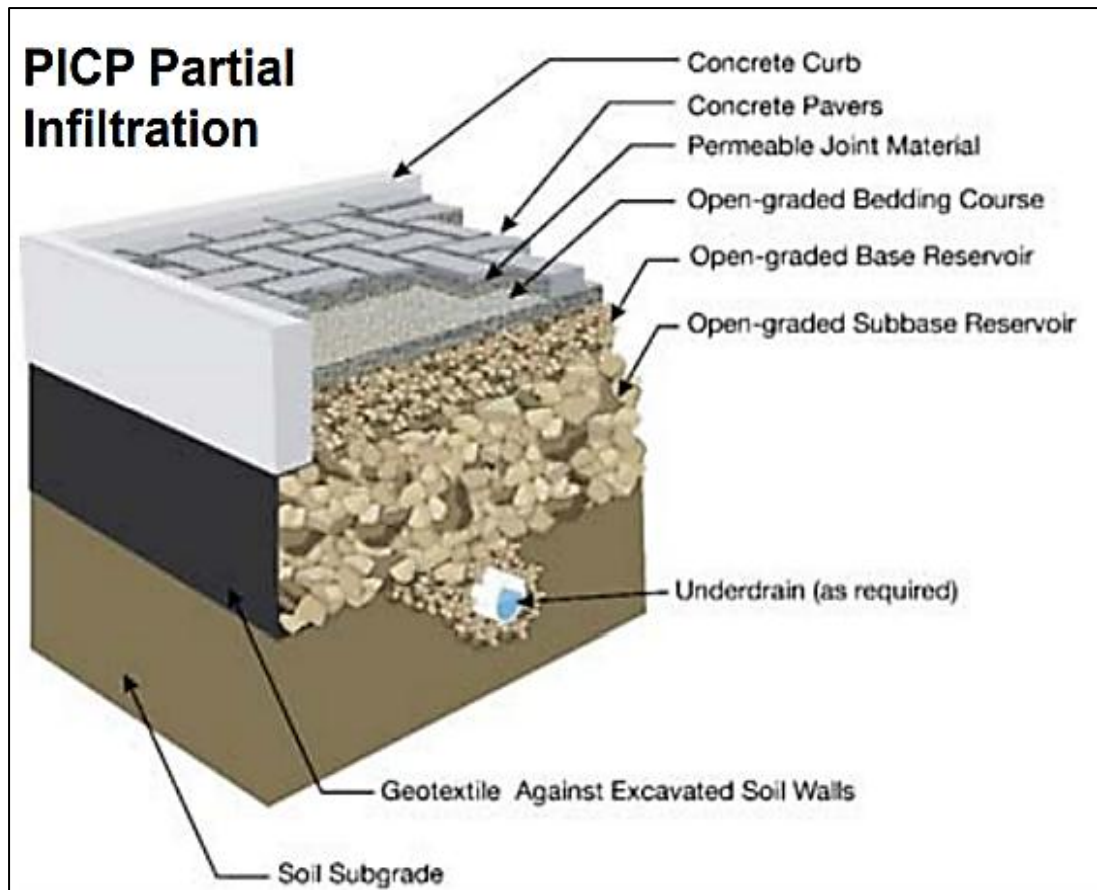


**Figure 5.1** Typical cross-section of pervious concrete paver units

## 5.2 Application

Pervious concrete pavement is appropriate for buildings (walkways, courtyards, etc.) and parking lots, as well as low-traffic routes. To reduce stormwater runoff, pervious concrete pavement could be used in the construction of highway shoulders and medians. It might also be used as a surface material to reduce tire noise, as well as hydroplaning, splash, and spray.



**Figure 5.2** Application Pervious concrete pavements

### 5.3 Limitations

- The parking areas are limited to auto parking and occasional trucks.
- If reinforcement is needed then epoxy coated bars should be used.
- Over vibration significantly reduces permeability of concrete.
- Runoff from adjacent areas onto pervious concrete needs to be prevented.
- It is still a new material that requires acceptance from cities and states.

### 5.4 Design theory

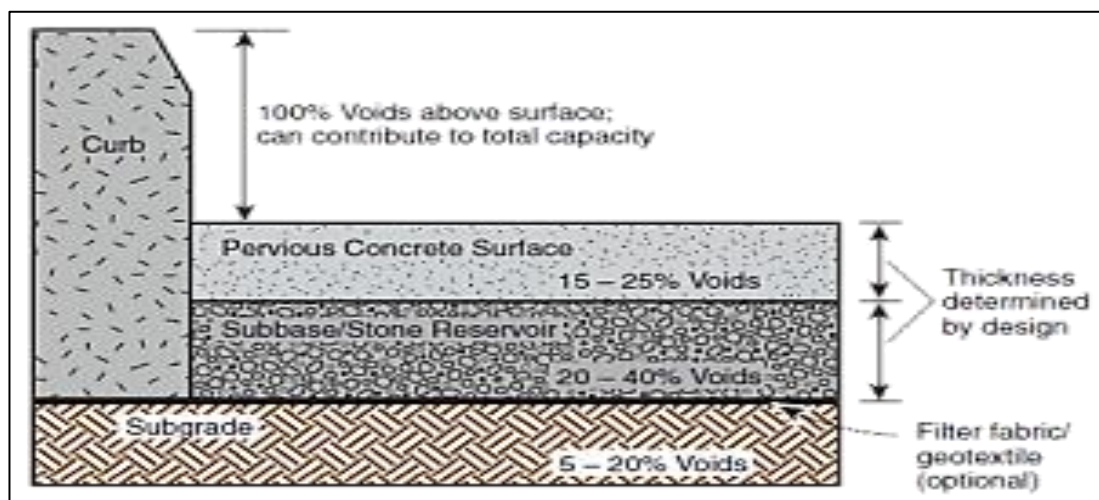


**Figure 5.3** Atypical section of the pervious concrete pavement.

This section can be modified to a mathematical model section as in Figure 5.4 to be used in the Pervious Pave v1.0 program and analysis of the results, where the design is focus on finding the thickness of pervious concrete pavement ( $h_p$ ) and open graded sub-base ( $h_s$ ) depending on engineering properties of the materials.

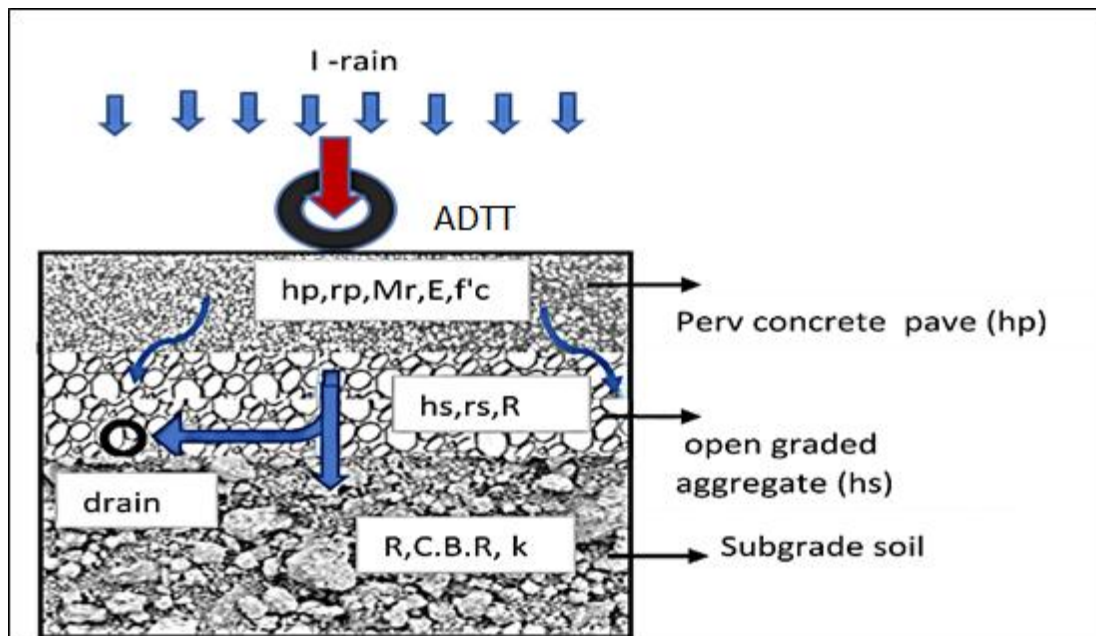


**Figure 5.4** Mathematical Model for Pervious Concrete Pavement

## 5.5 The Design process involves two design criteria

### 5.5.1 Structural design

Despite the fact that a number of studies have examined the fatigue behavior of pervious concrete Eqs. (5.1 and 5.2), issues like the difference in fatigue between laboratory specimens and full-sized slabs have made it challenging to adopt any existing pervious concrete fatigue models. Other investigations have shown that pervious and conventional concrete exhibit remarkably similar fatigue characteristics Eq (5.3) As a result, until a widely accepted fatigue equation for pervious concrete is created, Pervious Pave v1.0 employs the increased concrete fatigue model offered during the 2005 upgrade of Street Pave (5.1) The single failure criterion for the structural design of pervious concrete pavement, according to Equations for Structural Design in Pervious Pave v1.0, is fatigue. To compute overall fatigue damage, sum the cumulative damage caused by single, tandem, and tridem axle loads (FD total).

$$FD_{total} = FD_{single} + FD_{tandem} + FD_{tridem} \quad 5.1$$

where,

$FD_{total}$	= total fatigue damage, %
$FD_{single}$	= fatigue damage from single axle loads, %
$FD_{tandem}$	= fatigue damage from tandem axle loads, %
$FD_{tridem}$	= fatigue damage from tridem axle loads, %

Fatigue damage ( $FD$ ) for each axle type and load group in Equation 1 is computed per Miner's damage hypothesis (17):

$$FD = \frac{n}{N_f} \quad 5.2$$

where,

$n$	= number of load applications (calculated from the user inputted traffic data)
$N_f$	= allowable applications to failure

When the FD total reaches 100%, the limiting structural design requirement, PerviousPavev1.0 increases the pervious concrete pavement thickness while computing the FD total for each axle type and load group.

### 5.5.2 Hydrological design

This design approach can be utilized to assess the hydrologic needs for the construction combined with the structural design of the pavement. The required concrete slab thickness is determined by the structural design algorithm and is directly inputted into the hydrological design of the Pervious Pave v1.0 software. The thickness of the subbase/reservoir layer is then adjusted (increased) as necessary until the pervious concrete pavement structure satisfies the necessary stormwater management requirements. Utilizing this method ensures that both the structural design and stormwater requirements along the works are addressed. The minimum pervious concrete thickness required to support the design traffic over the pavement's lifetime is determined by the structural design approach. The thickness of the pervious concrete pavement is maintained throughout the hydrological design in order to maintain this situation. Pervious Pave v1.0 will take into account increasing the thickness of the subbase/reservoir layer, if necessary, or adding a subbase/reservoir layer, if one was not initially included in the structural design, to ensure that stormwater regulations are followed. If the hydrological design results in

a thicker subbase/reservoir layer section than was planned for in the structural design, the Pervious Pave v1.0 user will be informed and given the chance to re-run the structural design to determine whether a thinner pervious concrete pavement section is practical. One can specify how much water the pervious concrete pavement will drain.

$$V_w = \frac{(A_p + A_b) * I}{1000} \quad 5.3$$

were,

$V_w$  = volume of water, m<sup>3</sup>

$A_p$  = pervious concrete area, m<sup>2</sup>

$A_b$  = non-pervious area to be drained, m<sup>2</sup>

$I$  = rain intensity, mm

The capacity of the pervious concrete layer, the capacity of the subbase/reservoir layer, and any curb height that may contribute to the total capacity of the system (at 100 percent voids) are all taken into consideration when determining the total capacity of the system (at 100 percent voids):

$$h_p * r_p + r_s * h_s + h_{crub} = \frac{V * 1000}{A_p} \quad 5.4$$

$h_p$  = Thickness of pervious concrete pavement, mm

$r_p$  = void ratio of pervious concrete pavement, %

$h_s$  = thickness of subbase layer, mm

$r_s$  = void ratio of subbase layer, %

$h_{crub}$  = height of curb or height of allowable ponding, in.

From the viewpoint of a pavement engineer, site design considerations frequently influence the area to be paved (lane designs, parking lot size, etc.). The thickness of the subbase/reservoir layer can be estimated as follows with all other factors already provided by the user or computed beforehand from the structural design:

$$h_s = \frac{1}{r_s} \left( \frac{V_w * 1000}{A_p} - r_p * h_p - h_{crub} \right)$$

5.5

The detention period is then scrutinized to ensure that the structure and sub base layer of the pervious concrete pavement can manage the full amount of water in the specified time.

$$T_c = \frac{V_w * 1000}{A_p * k} \quad 5.6$$

k = permeability/infiltration rate of the sub-grade soil, mm/hr

T<sub>c</sub> = calculated detention time of water in pervious section

T<sub>max</sub> = maximum detention time (usually 24 hours)

If the computed detention period is shorter than the maximum detention time selected by the user, then the design subbase/reservoir layer thickness given by Equation 5 is sufficient for the volume of water to be handled by the paved area. If the computed detention period is longer than T<sub>max</sub>, the pervious concrete pavement area is insufficient for the soil to hold the design volume of water during the necessary detention time. If site constraints prevent this from being feasible, the non-pervious surface may need to be reduced, the pervious concrete area increased, or the necessary retention period revised... Finally, if the reservoir layer(s) are designed conservatively enough to hold the volume,

The detention period (as well as the rate of soil infiltration) is irrelevant as long as there is sufficient time between design storms for the water to be assimilated into the soil. Based on the maximum retention period, the pervious area needed if the paved surface is enlarged is:

$$A_p = \frac{V_w * 1000}{T_{max} * k} \quad 5.7$$

### 5.6 Design by Pervious Pave V1.0 Software

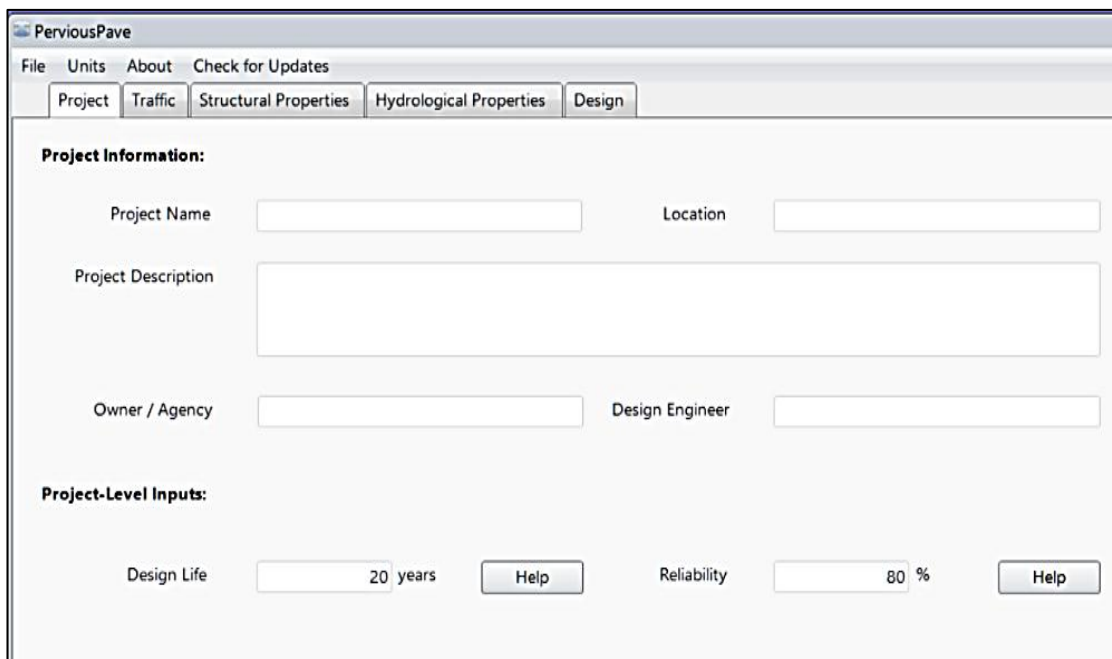
ACPA's Previous Pave is design software that supplies outcomes optimized for both structural and stormwater-management prerequisites by confining:

- The required subbase/reservoir thickness required to satisfy stormwater managing circumstances, based on the volume of water to be processed by the pavement within the maximum detention essential time. These requirements are based on procedure traffic, technique life, and other structural inputs. Previous Pave is obtainable as a free download and may be utilized without a license for up to 30 days. Behind the

30-day trial period, you will require to purchase a license to continue utilizing your copy of Pervious Pav.

### 5.6.1 Pervious pave software

The American Concrete Pavement Association (ACPA) has modified its design methodology for use in the structural design of pervious concrete pavements based on Street- Pav software, a thickness design approach for jointed plain concrete pavements. The user-friendly program Pervious-Pave v1.0 combines structural and hydrological design methods to produce the best results for both structural and stormwater management demands. Pervious-Pave v1.0's hydrological design method is based mostly on enhancements to the Los Angeles County method. Software for Pervious Pav v1.0 is capable of: Establishing the necessary minimum pervious concrete pavement thickness based on design traffic, design life, and other structural inputs, as well as the necessary subbase/reservoir thickened concrete stormwater management criterion based on the amount of water to be treated by the pavement within the necessary maximum detention period Pav v1.0 Figure 5.5 shows how the structural design determines the necessary slab thickness..



The screenshot displays the PerviousPave software interface. At the top, there is a menu bar with 'File', 'Units', 'About', and 'Check for Updates'. Below the menu bar are five tabs: 'Project', 'Traffic', 'Structural Properties', 'Hydrological Properties', and 'Design'. The 'Project' tab is currently selected. The main window is divided into two sections: 'Project Information:' and 'Project-Level Inputs:'. Under 'Project Information:', there are input fields for 'Project Name', 'Location', 'Project Description', 'Owner / Agency', and 'Design Engineer'. Under 'Project-Level Inputs:', there are input fields for 'Design Life' (set to 20 years) and 'Reliability' (set to 80 %). There are 'Help' buttons next to the 'Design Life' and 'Reliability' fields.

**Figure 5.5** show the screen menu of the Previous Pav v1.0

The soft gives its recommendation after end of the design, and the design details can be reported by the software Figure 5.6.

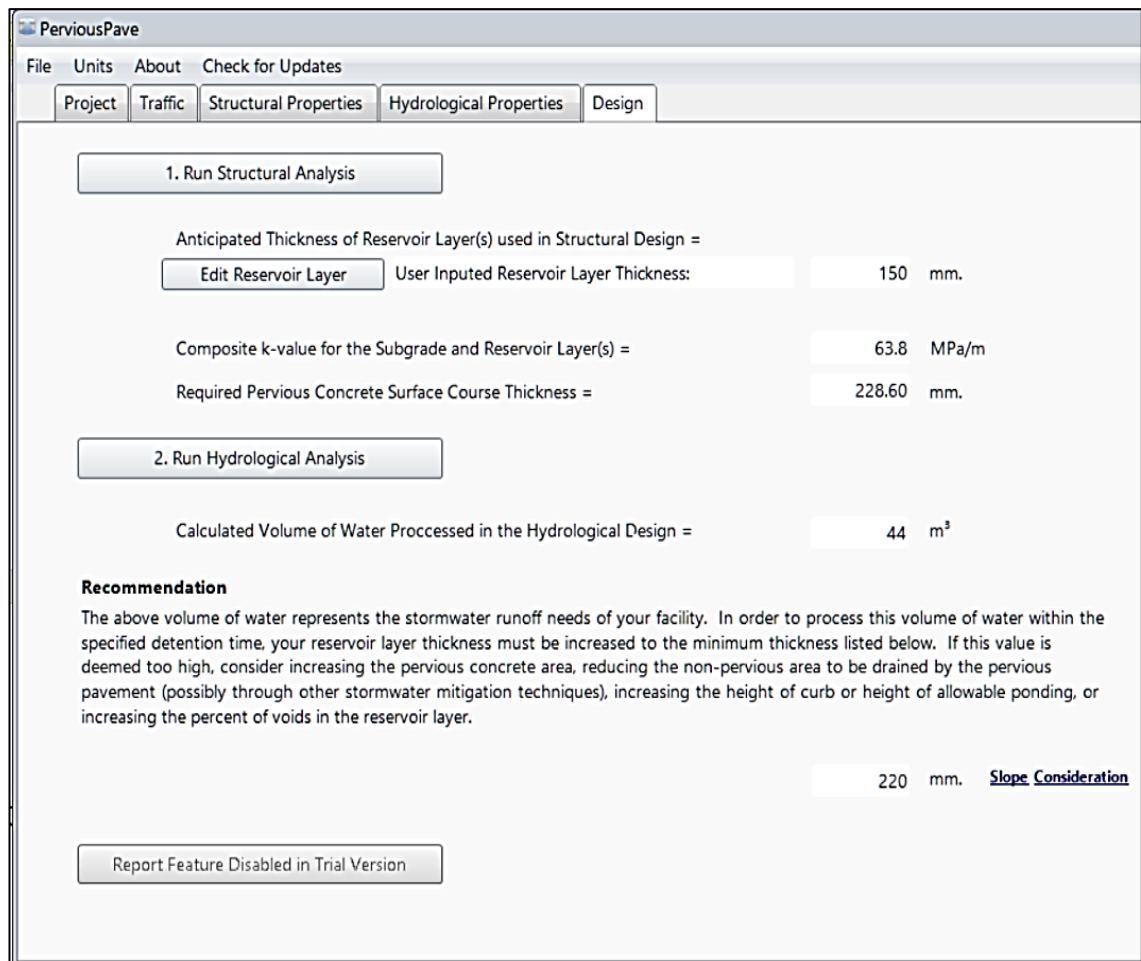


**Figure 5.6** Final step of design by Previous Pave v1.0

### 5.6.2 Research study

- A wide research study is performed from results of design by the software Pervious Pave v1.0, the results are confirmed by Excel using a mathematical mode as in Figure 5.7
- The study involved effect of the main factors in design of pervious concrete pavement among these factors:
  - compressive and rupture strength of pervious concrete ( $f_c$ ,  $M_r$ )
  - thickness of pave and sub base layer thickness ( $h_p$ ,  $h_s$ )
  - pervious concrete pave and subbase layer void ratio ( $r_p$ ,  $r_s$ )
  - rain intensity ( $I$ )
  - traffic load spectrum (average daily truck traffic ADTT value)

A part of laboratory test results on pervious concrete and open graded sub-base layer performed by the researcher Rafah Rasheed for her Ph. D degree are used as a base data in the software.

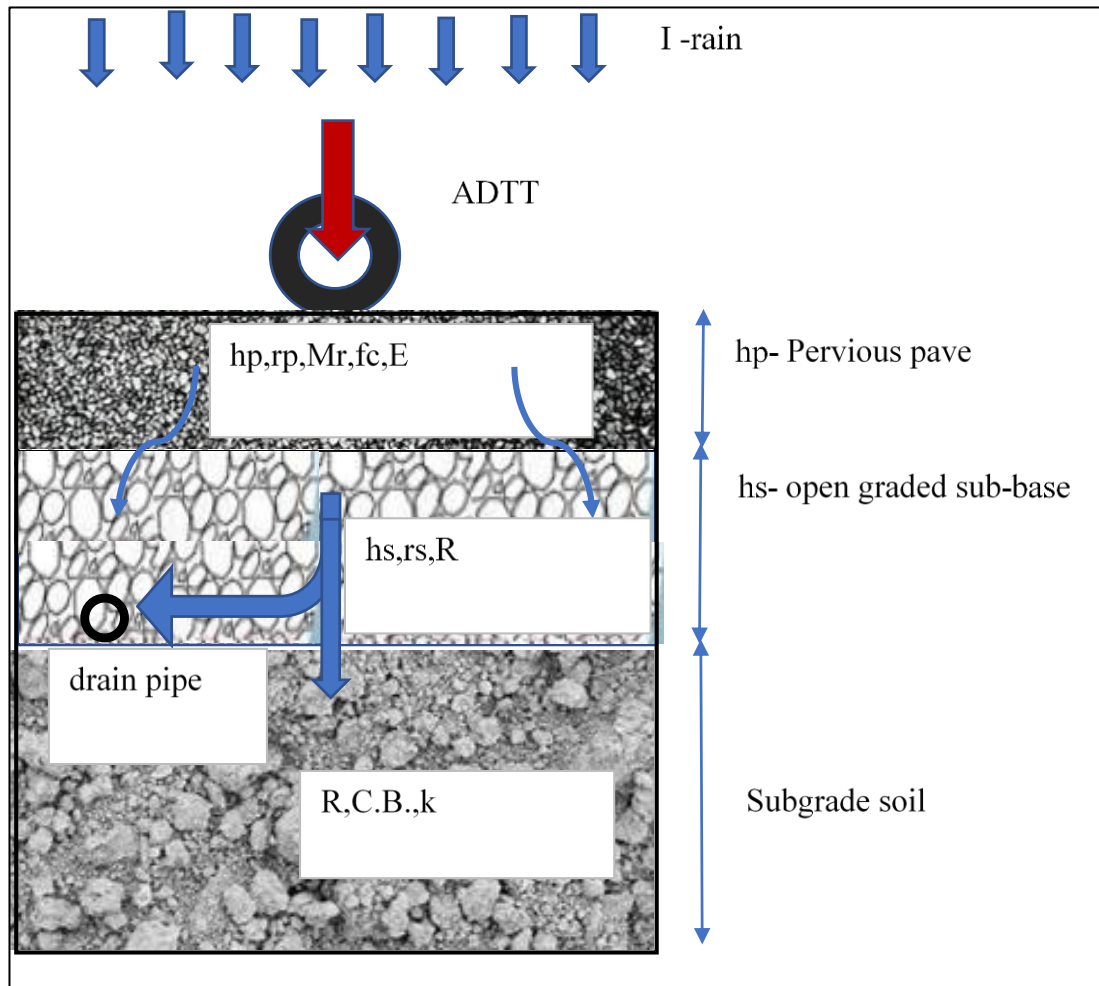


**Figure 5.7** Pervious concrete pave design for the study

### 5.6.3 Data base for the study

The following factors are studied:

- i-** Laboratory test results on pervious concrete samples: f c, rp, and Mr
- ii-** Traffic load spectrum
- iii-** Rain intensity

**Table 5.1** Laboratory test results on pervious concrete samples: fc, rp, and Mr

Compressive strength of pervious concrete	Rupture tensile strength	Void ratio
fc (MPa)	Mr (MPa)	rp (%)
40.17	3.37	15.37
36.43	2.89	16.73
34.77	2.74	17.11
32.52	2.11	18.34
30.00	1.80	20.00

**Table 5.2** Traffic load spectrum

Category	Application of Pervious Pave	ADDT	Truck on Design section %	Annual Truck Growth %	Design life (years)	Reliability %
A	Residential Pave /Parking lots	2	100	2	25	80
B	Collectors	50	100	2	25	90
C	Shoulders -minor Arterial	250	10	2	25	90
D	Shoulders -major Arterial	500	10	2	25	90

I= 30,40,50,60,70,80 mm

iv- The factors of constant value involved in software are below:

- area covered by pervious pave,  $A_p=500 \text{ m}^2$
- area of non-pervious zones,  $A_b =50 \text{ m}^2$
- infiltration rate of subgrade soil  $k=4 \text{ mm/hr}$  with pipes
- subgrade C.B.R =3 % silty clay soil
- open graded sub-base void ratio  $r_s= 40\%$  (for max size aggregate 20mm)
- resilient modulus of open graded sub- base  $R=170 \text{ mPa}$

The results found by Pervious Pave v1.0 are confirmed by Excel program, then are analyzed in the next article.

#### **5.6.4 Design steps by pervious pave v1.0**

The steps followed by the soft are as below:

- 1- Fix design life (years) and reliability % of the project
- 2- Select the application of the pervious concrete pave and the traffic load (ADTT)
- 3- Input structural data
  - C.B.R of subgrade soil in %
  - Resilient modulus of open graded layer (R)
  - 28-day rupture strength of the pervious concrete (Mr)
- 4- Input hydrological data
  - Site factor involving area of pervious and non-pervious zones (Ap and Ab)
  - Void ratio of pervious pave and open graded layer ( rp and rs )
  - Rain intensity (I) in mm average for 24hrs of 2 years
  - Maximum infiltration time Tmax (typically 24 hrs)
- 5- Run the design with structural analysis, where the Pervious Pave v1.0 first will do the structural analysis to find thickness of pervious pave and open graded layer (hp and hs)
- 6- Run the design with hydrological analysis, where the Pervious Pave v1.0 will find second value for thickness of open graded layer for hydrological requirements with giving recommendation
- 7- The value of thickness for pervious pave (hp) by structural analysis will be recommended for the design, while the largest value of thickness for open graded layer form the two analysis is recommended for the design.

The results by the Pervious Pave v1.0 software are collected in Excel sheet format

#### **5.6.5 Results analysis**

1. Pervious concrete (fc) vs pervious pave thickness(hp) and void ratio It is seen from Figure 5.8 that for all types of traffic as the compressive strength of the pervious concrete increases the pervious concrete pave decreases, and for

same compressive strength pervious pave thickness be higher as traffic load be heavier.

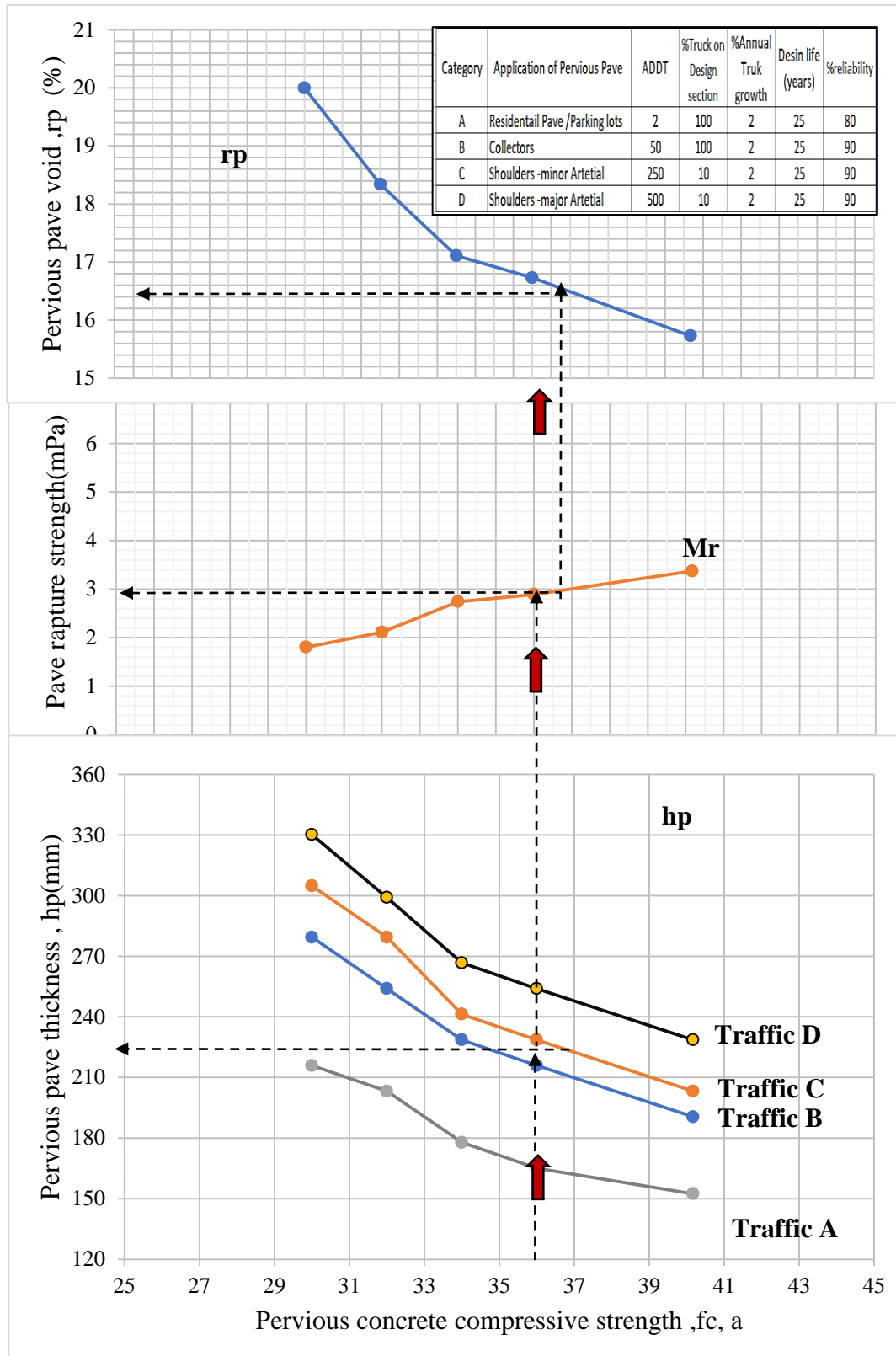


**Figure 5.8** Pervious pave and open graded sub-base thickness vs. pave concrete compressive strength for various traffic load

- Rain intensity (I) vs. open graded subbase thickness (hs) It is seen from Figure (5.9) that for all values of compressive strength, the open graded layer thickness increases as the intensity of rain increases, and has higher values

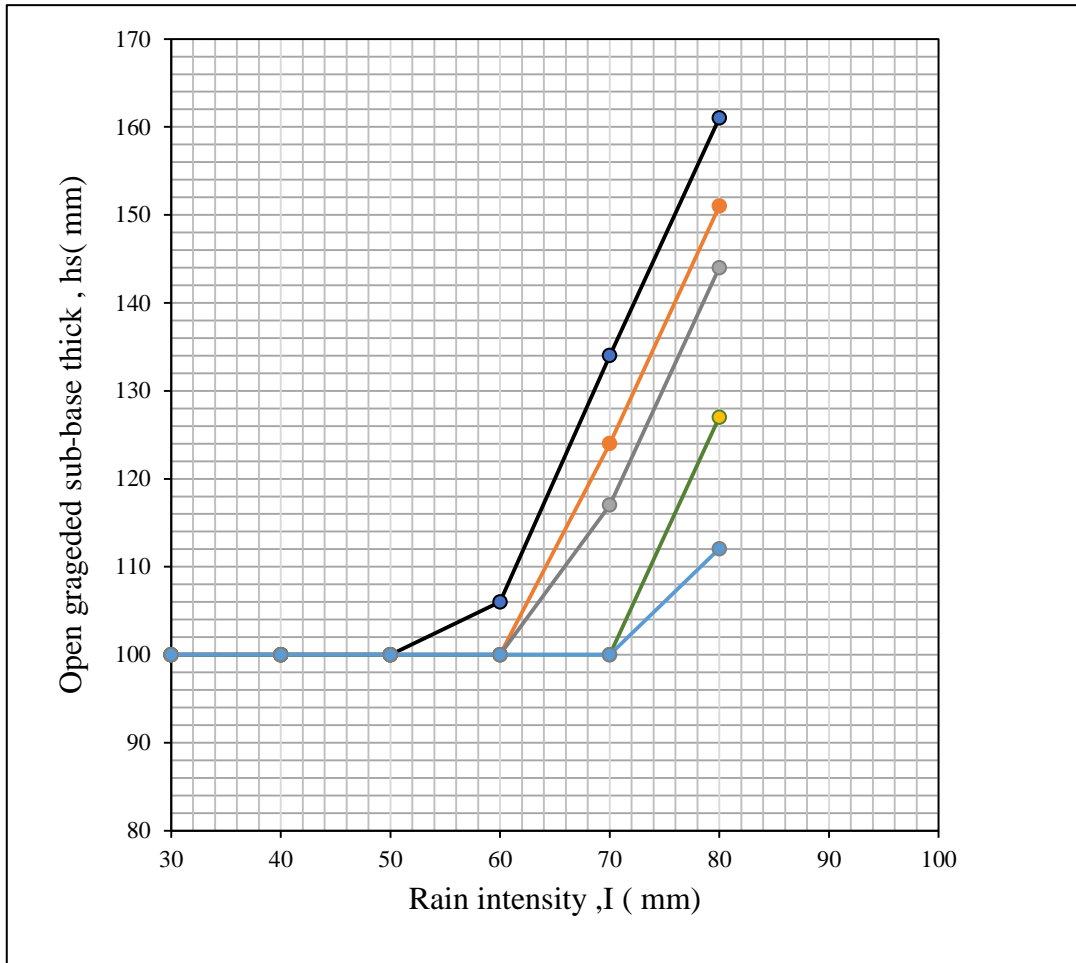


**Figure 5.9** Open graded layer thickness vs. rain intensity for various concrete compressive strength for parking lots area of Traffic A (ADTT=2)

- Traffic load spectrum (ADTT) vs. hp and hs, from Figure (5.10) and Figure (5.11) it is seen that as the traffic load becomes heavier the thickness of pervious concrete needed to be larger while for the open graded layer the case is inverse whereas the traffic load becomes heavier the thickness of pervious concrete needed to be smaller for higher compressive strength of pervious concrete

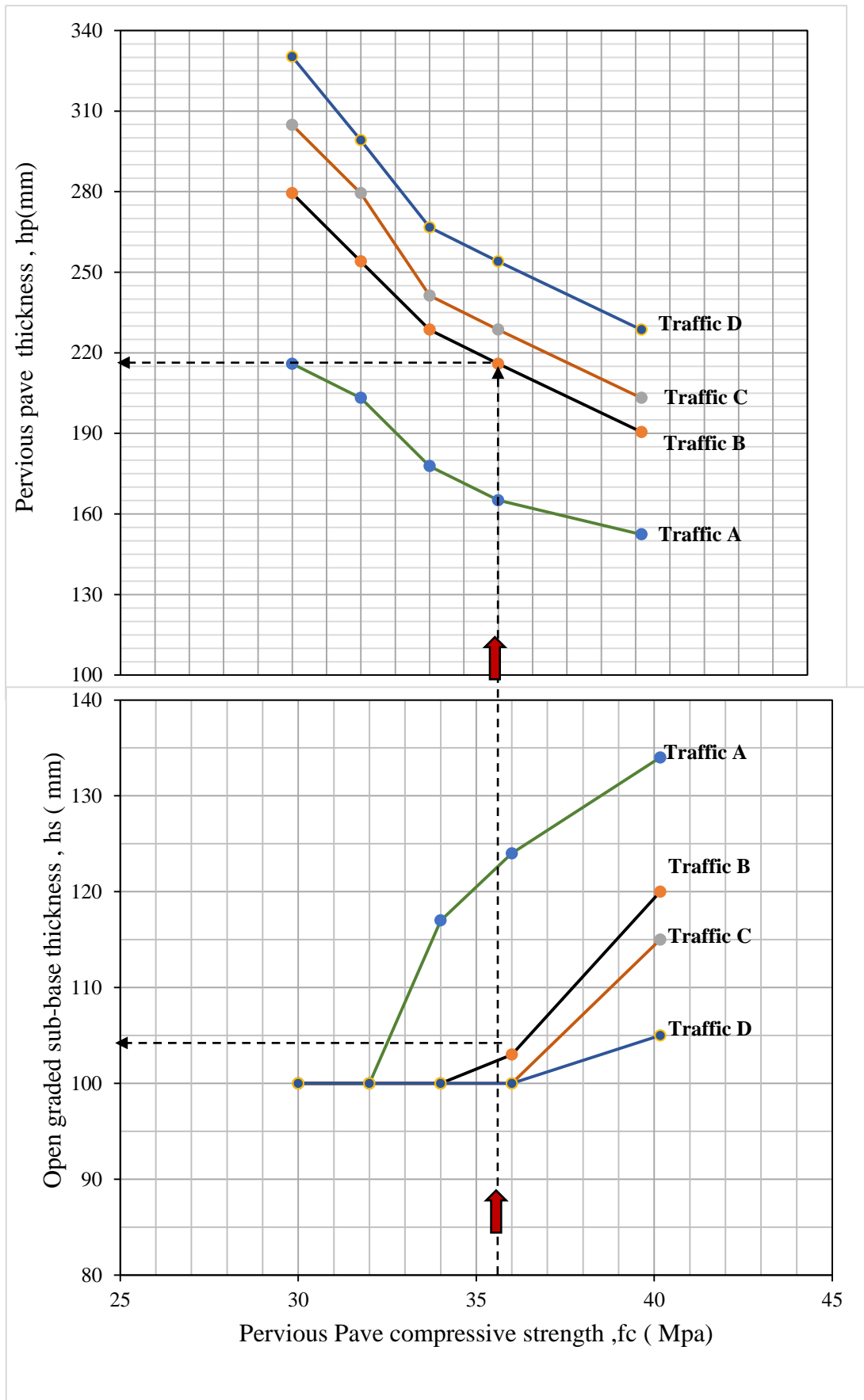


**Figure 5.10** Pervious pave and open graded sub-base thickness vs. pave concrete compressive strength for various traffic category and rain intensity 70 mm.

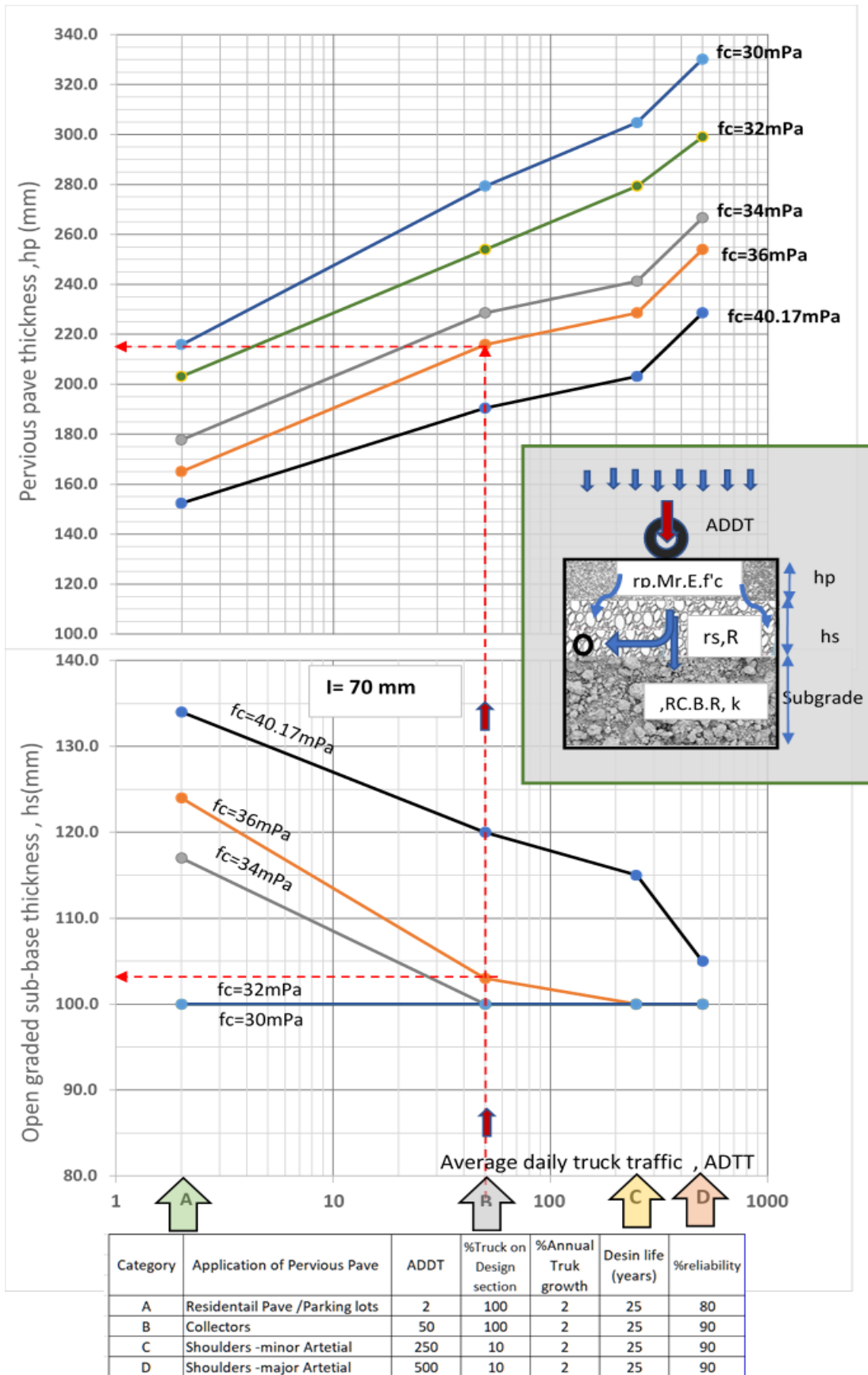


**Figure 5.11** Pervious pave and open graded sub-base thickness vs. pave concrete compressive strength for various traffic category under rain intensity 70 mm.

4. Entire water volume ( $V_w$ ) vs. rain intensity ( $I$ ) It is seen from fig. (5.12) that as the rain intensity increases the entire water volume that should be infiltrated linearly increases. In all cases the water volume should be equal or less to the sum of void volume of pervious concrete and open graded aggregate to insure storage of this water in the two layers during infiltration time by subgrade soil.
5. Infiltration time ( $T_c$ ) vs. rain intensity ( $I$ ) It is seen from fig. (5.12) that as the rain intensity increases the time needed for infiltration by subgrade soil increases, in any case the time of infiltration should not be larger than maximum time of 24 hours, otherwise additional drainage way must be selected like using drain by perforated pipe system at bottom of open graded aggregate layer.

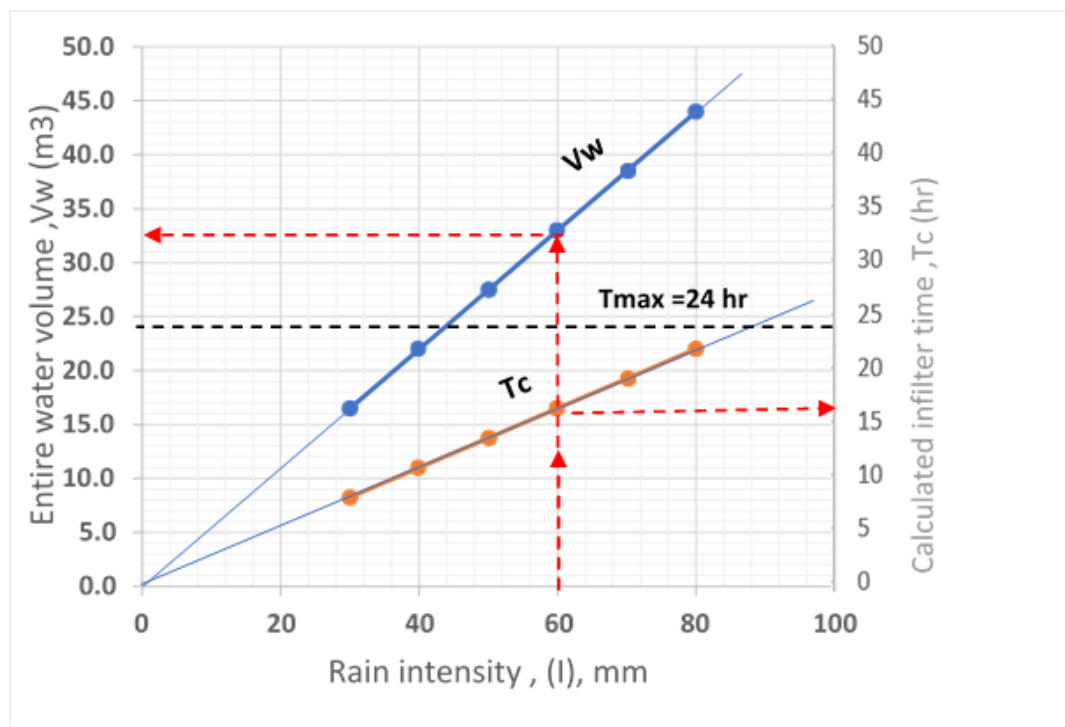


**Figure 5.12** Rain intensity vs. Entire water volume infiltrated and calculated infiltration time by soil and drain pipes.

### 5.7.6 Design chart

A design chart by Excel with aids of Pervious Pave v 1.0 is prepared to be used for design of pervious concrete pavement for wide range of variables as shown in 5.13

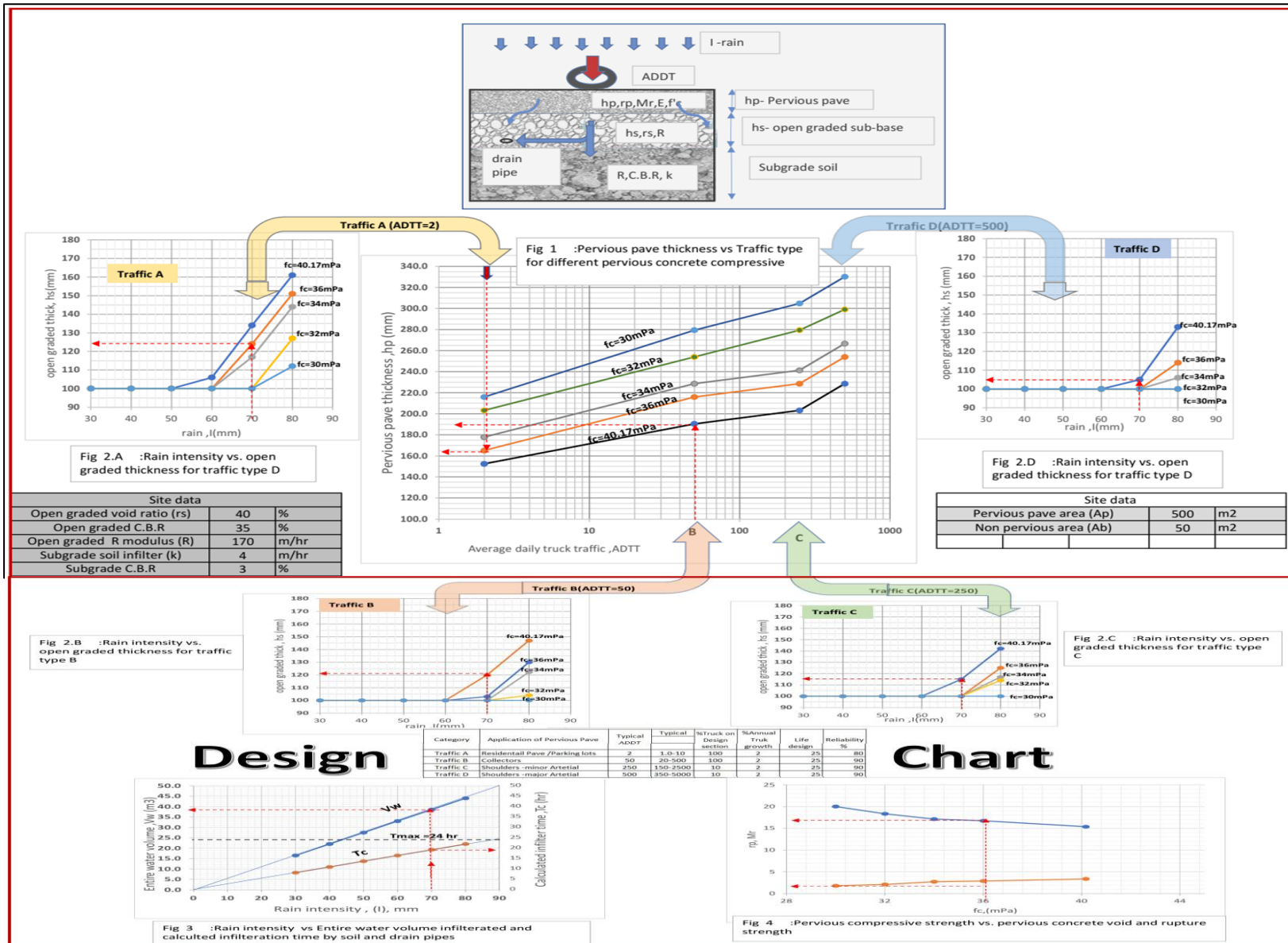
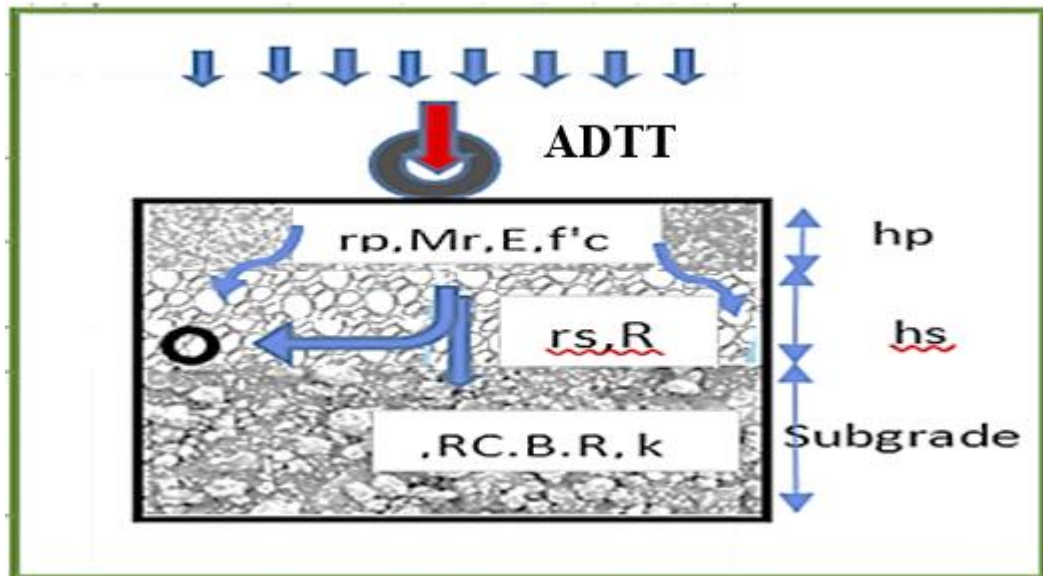


Figure 5.13 Design flow chart



**Figure 5.14** Mathematical model

### 5.7.7 Examples

It is necessary to design pavement for a site using pervious concrete with below data

Site: area of pervious pave =  $500 \text{ m}^2$ , area of non-pervious zone =  $50 \text{ m}^2$

Subgrade soil: infiltrer rate =  $4 \text{ mm/hr}$ , C.B.R = 3%

Open graded sub-base: 20 mm size aggregate of C.B. R= 35%, and void ratio =40%

Rain intensity: 70 mm, max infiltration time = 24 hours

Traffic type: Parking lots, ADTT= 2

Concrete compressive strength = 36 MPa

Requirements:

1-thickness of pervious concrete pavement  $h_p$

2-thickness of open graded sub-base

3-volume of infiltrated water

4-time for infiltration the water by the subgrade soil.

Solution: using design chart

Step 1: Find  $h_p$ :

from fig 5.13 for traffic A (Parking lots) with  $f_c = 36 \text{ MPa}$  we find that:

thick of pervious pave  $h_p = 165 \text{ mm}$

Step 2: find  $h_s$

from fig 5.13 for rain intensity,  $I = 70 \text{ mm}$  and  $f_c = 36 \text{ MPa}$  we find that;

thick of open graded  $h_s = 124 \text{ mm}$

Step 3: Volume of Infiltration water ( $V_w$ )

from fig. 5.13 for rain intensity,  $I=70 \text{ mm}$  we find that:  $V_w = 38 \text{ m}^3$

Step 4: Time of infiltration

from fig.5.13 for rain,  $I= 70 \text{ mm}$  we find calculated  $T_c= 19.5 \text{ hr}$  as this time is less than 24 hrs so the entire water can be infiltrated by the subgrade soil.

Ex2: find same requirement of Ex1 above, if  $f'_c= 40.17 \text{ Mpa}$  and  $I= 60 \text{ mm}$

$h_p= 153 \text{ mm}$ ,  $h_s = 106 \text{ mm}$ .

$V_w = 33 \text{ m}^3$ ,  $T_c= 16 \text{ hr}$  .

## CHAPTER 6

### CONCLUSIONS AND RECOMMENDATIONS

#### 6.1 Conclusions

In this chapter a summary of the research, conclusions and recommendations for future work are presented. Geopolymer pervious concrete can be considered as the decent eco-friendly alternative to cement and normal concrete for now and in the future. This study aimed at developing geopolymer pervious concrete mixtures that contain coarse aggregate. In order to achieve this goal, the study conducted in five phases. In the first- phase, the key factors affecting the performance of geopolymer pervious concrete were investigated; focusing on the aforementioned parameters using natural coarse aggregate (max. size 20 mm) then the results in order to reach decent mix proportions of the reference mix. In this step a total of 26 mixes were prepared with different proportions of materials. Out of this mechanical property (compressive strength).

In the second phase, the key factors affecting the performance of geopolymer pervious concrete were investigated; focusing on the aforementioned parameters using natural coarse aggregate (max. size 14 mm) then the results in order to reach decent mix proportions of the reference mix. In this step a total of 26 mixes were prepared with different proportions of materials. Out of this mechanical property (compressive strength).

For economic purposes, the Erbil slag, Erbil slag steam condenser and Brick Powder was used instead of imported slag in the third, fourth and fifth phase, and natural coarse aggregate (maximum size 14 mm) was used, which resulted in a total of four mixes with varied proportions of components. This mechanical feature is derived from (compressive strength). It was not employed because of its low compressive strength.

Ten experimental mixtures were chosen from the 64 above based on two factors. The first was to examine the compressive strength and the second we adopted on the

shape. When choosing the ten mixtures, we conducted tests on them flow test, void ratio, density, compressive strength, splitting test, flexure test, Modulus of Elasticity and Infiltration Rate, In this section, the curing regimes.

The experimental results and the output of the statistical analysis can lead to the following conclusions:

1. The optimal molarity of NaOH for the preparation of GPPC has been determined to be between 12 and 14, this value is dependent on other parameters, most notably the sodium silicate-to-sodium hydroxide solution ratio.
2. To earn a desired strength and pervious property in GPPC, the Alkali/GGBFS ratio should be between 0.25 and 0.35, which is similar to the w/c ratio in conventional pervious concrete, and the GGBFS content should be between 325 and 350 kg/m<sup>3</sup>.
3. Gravel with a 20 mm particle size was found to be inadequately strong. The optimal gravel size for the production of high-strength pervious concrete has been determined to be 14 mm. Reduced maximum size increases compressive strength but decrease pervious properties
4. Combining Erbil steel slag, Erbil steam condenser, and fire clay bricks in powdered form as a partial substitution for GGBFS reduces compressive strength; however, using steel slag and steam condenser has given higher compressive strength than using fired clay bricks, with compressive strength of 24 MPa at a 25% replacement level, indicating that these mixes still have the ability to support traffic loading.
5. It has been observed that the type of compaction has a considerable effect on the qualities of the geopolymer pervious concrete produced. Because the mix is sticky and highly stiff, tamping with a jack hammer on the concrete surface through a base plate is recommended.
6. The compressive strength increases as the percentage of voids decreases. With each 1% increase in air void volume resulting in a 5% reduction in strength.
7. It was discovered that when compressive strength increased, tensile splitting strength increased as well. The best fit exponential equation revealed an

increasing rate of tensile splitting strength as compressive strength increased. And it accounted for roughly 19 percent of the compressive strength.

8. The higher the compressive strength, the greater the elasticity modulus. The best fit an exponential equation showed increasing rate of elastic modulus with increase in compressive strength.
9. Flexure strength increases as compressive strength increases. The best fit exponential equation demonstrated an increasing rate of flexural strength as compressive strength increased. Approximately It was around 15% of the compressive strength.
10. A linear relationship exists between flexural strength and tensile splitting strength; basically, tensile splitting strength is approximately 20% more than flexural strength for GPPC
11. The lower the infiltration rate, the stronger the compressive strength. Both linear and nonlinear equations can be used to express it.

$$y = 6640.5e^{0.016x} \tag{6.1a}$$

$$y = 27887x^{-0.564} \tag{6.1b}$$

12. The higher the void ratio, the higher the density of the oven dry. Both linear and nonlinear equations can be used to express it.

$$y = 0.511x + 1842.4 \tag{6.2a}$$

$$y = 1902.6x^{-0.009} \tag{6.2b}$$

13. The larger the void ratio, the higher the rate of infiltration. Both linear and nonlinear equations can be used to express it.

$$y = 6118.8e^{0.26x} \tag{6.3a}$$

$$y = 904.67x^{0.4923}$$

6.3b

Pervious Pave v1.0 is very suitable and applicable soft for design pervious concrete pavement.

14. Wide number of variables can be included in the soft considering traffic, engineering properties of pervious concrete and open graded layer, hydrological factors, geotechnical data of subgrade and open graded layer.
15. The design results by the software were very dependable and coincidence with design values from theoretical equations.
16. Design charts depending on results from the software are performed which can be used as a guide for design of pervious concrete pavement.

## **6.2 Recommendations**

1. Sun bathing curing is a new type of curing which must be studied more in the future for different environments and different geographical locations.
2. Fire resistance of geopolymer pervious concrete.
3. Durability of geopolymer pervious concrete.
4. Only GGBFS was employed as a precursor in this study to make geopolymer. Rice husk, silica fume, PFA, and metakaolin are some of the other materials that could be studied further.
5. Microcracks in geopolymer mortars were investigated, in addition to the relationship between strength and nano-crystallization particles in geopolymer mortars.
6. To evaluate the impact of environmental circumstances, formwork type, and structural factors on the temperature increase in the mix, more research is needed.

## REFERENCES

- Açikgenç, M., Alyamaç, K. E., and Ulucan, Z. Ç., (2015). Relationship between Steel Fiber-Reinforced Concrete Splitting Tensile and Flexural Strengths. *The International Conference on the Regeneration and Conservation of Concrete Structures (RCCS)* At: Nagasaki, Japan P (4-6).
- Ahmed, H. Q., Jaf, D. K., and Yaseen, S. A. (2020). Comparison of the flexural performance and behaviour of fly-ash-based geopolymer concrete beams reinforced with CFRP and GFRP bars. *Advances in Materials Science and Engineering*. vol. 2020, 1-15 <https://doi.org/10.1155/2020/3495276>
- Andersen, C. T., Foster, I. D., and Pratt, C. J. (1999). The role of urban surfaces (permeable pavements) in regulating drainage and evaporation: development of a laboratory simulation experiment. *Hydrological processes*, 13(4), 597-609.
- Arafa, S. A., Ali, A. Z. M., Rahmat, S. N., and Lee, Y. L. (2017). Optimum mix for pervious geopolymer concrete (GEOCRETE) based on water permeability and compressive strength. In *MATEC Web of Conferences* (Vol. 103, p. 01024). EDP Sciences.
- ASTM, C. (1999). Standard specification for concrete aggregates. *Philadelphia, PA: American Society for Testing and Materials*.
- Awal, A. A., Ibrahim, M. H. W., Ali, A. Z. M., and Hossain, M. Z. (2017). Mechanical properties and thermal behaviour of two-stage concrete containing palm oil fuel ash. *GEOMATE Journal*, 12(32), 166-175.
- Balaguru, P., Kurtz, S., and Rudolph, J. (1997). Geopolymer for repair and rehabilitation of reinforced concrete beams. St Quentin, France, *Geopolymer Institute*, 5.
- Bone, B. D., Barnard, L. H., Boardman, D. I., Carey, P. J., Hills, C. D., Jones, H. M., and Tyrer, M. (2004). Review of scientific literature on the use of stabilisation/solidification for the treatment of contaminated soil, solid waste and sludges (SC980003/SR2). *The Environment Agency, Bristol*, 1-375.
- Cahill, T., Adams, M., and Marm, C. (2003). Porous asphalt: The right choice for porous pavements. *HMAT: Hot Mix Asphalt Technology*, 8(5).
- Chandrappa, A. K., and Biligiri, K. P. (2016). Pervious concrete as a sustainable pavement material—Research findings and future prospects: A state-of-the-art review. *Construction and building materials*, 111, 262-274.

- Chen, Y., Wang, K., Wang, X., and Zhou, W. (2013). Strength, fracture and fatigue of pervious concrete. *Construction and Building Materials*, 42, 97-104.
- Chindapasirt, P., Chareerat, T., and Sirivivatnanon, V. (2007). Workability and strength of coarse high calcium fly ash geopolymer. *Cement and concrete composites*, 29(3), 224-229.
- Chindapasirt, P., Hatanaka, S., Chareerat, T., Mishima, N., and Yuasa, Y. (2008). Cement paste characteristics and porous concrete properties. *Construction and Building materials*, 22(5), 894-901.
- Chokkalingam, R. B., Subbu, P., Raj, T., and Sawant, S. (2018). Properties of geopolymer pervious concrete made with GGBS. *International Journal of Engineering and Technology*, 7(4.5), 693-695.
- Chopra, M., Wanielista, M., and Stuart, E. (2010). Chapter 12 in Statewide Stormwater Rule. *Revised Draft Applicant's Handbook., Florida Department of Environmental Protection.*
- Chung, D. D. L. (2002). Piezoresistive cement-based materials for strain sensing. *Journal of Intelligent Material Systems and Structures*, 13(9), 599-609.
- Conceição, L., Cláudio S., (2019). Avaliação de parâmetros físico-químicos na produção de geopolímeros em vulcânico e silicato de sódio alternativo. MSc thesis
- Crouch, L.K., Jordan P., and Ryan H. (2007). Effects of aggregates on the static modulus of elasticity of pervious Portland cement concrete. *Journal of materials in civil engineering*, (19) 561-568.
- Davidovits J (2008) Geopolymer chemistry and applications. *Geopolymer Institute 5th ed*
- Davidovits, J. (2002). years of successes and failures in geopolymer applications. Market trends and potential breakthroughs. In Geopolymer 2002 conference (Vol. 28, p. 29). Saint-Quentin, France; Melbourne, Australia: *Geopolymer Institute.*
- Davidovits, J., (1989). Geopolymers and geopolymeric materials. *Journal of thermal analysis* (35) 429-441.
- Davidovits, J., (1994) Global warming impact on the cement and aggregates industries. *World resource review* (6) 263-278.
- Davidovits, J., and Morris, M., (1988). The pyramids: An enigma solved. *In.: Hippocrene Books.*
- Davidovits, Joseph. (2005). Geopolymer, green chemistry, and solutions for sustainable development: *proceedings of the 2005 World Congress on Geopolymer* (Geopolymer Institute).

- Deo, Omkar, Narayanan Materials Science Neithalath, and Engineering: A. (2010). 'The influence of random pore structural features on the compressive behavior of pervious concretes has been quantified. ', 528: 402-412.
- Diaz, EI, EN Allouche, and Sven Eklund. (2010). 'Factors affecting the suitability of fly ash as source material for geopolymers', *Fuel*, 89: 992-996.
- Duxson, P., Lukey, G. C., Separovic, F., and Van Deventer, J. S. J. (2005). Effect of alkali cations on aluminum incorporation in geopolymeric gels. *Industrial and Engineering Chemistry Research*, 44(4), 832-839.
- Duxson, P., Provis, J. L., Lukey, G. C., and Van Deventer, J. S. (2007). The role of inorganic polymer technology in the development of 'green concrete'. *cement and concrete research*, 37(12), 1590-1597.
- Eduok, E. (2016). *Thermal properties of geopolymer materials* (Master's thesis, University of Stavanger, Norway).
- Faris, M. A., Abdullah, M. M. A., Sandu, A. V., Ismail, K. N., Moga, L. M., Neculai, O., and Muniandy, R. (2017). Assessment of alkali activated geopolymer binders as an alternative of portland cement. *Mater. Plast*, 54(1), 145-154.
- Fernandez-Jimenez, A. M., Palomo, A., and Lopez-Hombrados, C. (2006). Engineering properties of alkali-activated fly ash concrete. *ACI Materials Journal*, 103(2), 106.
- Fernández-Jiménez, A., García-Lodeiro, I., and Palomo, A. (2007). Durability of alkali-activated fly ash cementitious materials. *Journal of Materials Science*, 42(9), 3055-3065.
- Fernández-Jiménez, Ana, JG Palomo, F Cement Puertas. (1999). 'Alkali-activated slag mortars: mechanical strength behaviour', 29: 1313-1321.
- GangaRao, Hota VS, Narendra Taly, and PV Vijay. (2006). Reinforced concrete design with FRP composites (CRC press).
- García-Lodeiro, I., Palomo, A. Y., and Fernández-Jiménez, A. (2007). Alkali-aggregate reaction in activated fly ash systems. *Cement and Concrete Research*, 37(2), 175-183.
- Gee, Kenneth H.(1979). "The potential for slag in blended cements." In Proceedings, 14th International Cement Seminar, Rock Products, 55-53.
- Glukhovskiy, Y. D., Rostovskaja, G. S. and Rumyna, G. V., (1980). High-strength Slag-Alkaline Cements. *Int. Cong. Chem. Cem., Geophysics and Space Physics*, Vol. (13) 164-168.

- Haddad, R. H., and Alshbuol, O. (2016). Production of geopolymer concrete using natural pozzolan: A parametric study. *Construction and Building Materials*, 114, 699-707.
- Hardjito, D., Cheak, C. C. and Carrie H., (2008). Strength and setting times of low calcium fly ash-based geopolymer mortar. *Modern applied science*, (2) 3-11.
- Haselbach, L. M., Srinivas V., and Felipe. (2006). Permeability forecasts for sand-clogged pipes Pavement systems made of Portland cement and pervious concrete. *Journal of environmental management Montes* (81) 42-49.
- Hassan, M. S., Al-Azawi, Z. M ., Muntadher (2016). Complementary Effect of Heat Treatment and Steel Fibers on Mechanical and Microstructural Properties of High-Performance Concrete. *Arabian Journal for Science Taher, and Engineering* (41) 3969-3981.
- Huang, B., Xiang H. W., Edwin (2010). Laboratory evaluation of permeability and strength of polymer-modified pervious concrete *Construction Burdette, and Building Materials*. (24) 818-23.
- Huang, B., Xiang H., W., and Burdette, E. M., (2010). Permeability and strength of polymer-modified pervious concrete were assessed. *Construction and Building Materials*, (24) 818-823.
- Ibrahim, A., Enad M., Mohammed Y., and Patibandla V. C., (2014). Experimental study on Portland cement pervious concrete mechanical and hydrological properties. *Construction and Building Materials*, (50) 524-529.
- Imbabi, M. S., Collette C., and Sean. (2012). Trends and developments in green cement and concrete technology. *International Journal of Sustainable Built Environment McKenna*. (1)194-216.
- Jaber, A., Gorgis, I., and Hassan, M. (2018). Relationship between splitting tensile and compressive strengths for self-compacting concrete containing nano-and micro silica. In *MATEC Web of Conferences* (Vol. 162, p. 02013). EDP Sciences.
- Jamal, A.S., (2019). Development of Mixtuer Proportion and Properties of Lightweight Aggregate Geopolymer Concrete. *MSc thesis*, Salahaddin University - Erbil.
- Jiminez, A. M. F., Lachowski, E. E., Palomo, A., and Macphee, D. E. (2004). Microstructural characterisation of alkali-activated PFA matrices for waste immobilisation. *Cement and Concrete Composites*, 26(8), 1001-1006.
- Juenger, MCG, Frank Winnefeld, J Lt Provis, and JH Ideker. (2011). Advances in alternative cementitious binders. *Cement and Concrete Research*, (41) 1232-1243.

- Keerthan, M. (2017) Experimental Study on Fly Ash based Geopolymer Concrete with Replacement of Sand by GBS. *Int. Journal of Engineering Research and Application*, (7), 57-61.
- Kevern, J., Wang, K., Suleiman, M. T., and Schaefer, V. R. (2005). Mix design development for pervious concrete in cold weather climates. In *Proceedings of the 2005 Mid-Continent Transportation Research Symposium*. 1-11
- Kevern, J. T., Schaefer, V. R., and Wang, K. (2009). Evaluation of pervious concrete workability using gyratory compaction. *Journal of Materials in Civil Engineering*, 21(12), 19.
- Kevern, John Tristan. (2008). Advancements in pervious concrete technology. *PhD Thesis* (Iowa State University).
- Khale, D., and Rubina. (2007). 'Mechanism of geopolymerization and factors influencing its development: a review. *Journal of materials science Chaudhary* (42) 729-46.
- Khalil, W. I., Qais J. F., and Haider T A. (2019). Properties of Metakaolin Based Pervious Geopolymer Concrete. In *IOP Conference Series: Materials Science and Engineering*, 022056. IOP Publishing.
- Khan, M. I., Rafat R. S., (2011). 'Utilization of silica fume in concrete: Review of durability properties. *Conservation, and Recycling* (57) 30-35.
- Kim, H. K., and Lee, H. K. (2010). Acoustic absorption modeling of porous concrete considering the gradation and shape of aggregates and void ratio. *Journal of Sound and Vibration*, 329(7), 866-879.
- King, D. (2012, August). The effect of silica fume on the properties of concrete as defined in concrete society report 74, cementitious materials. In *37th Conference on our world in concrete and structures, Singapore* (pp. 29-31).
- Kong, D. L., and Sanjayan, J. G. (2008). Damage behavior of geopolymer composites exposed to elevated temperatures. *Cement and Concrete Composites*, 30(10), 986-991.
- Kong, Daniel LY, Jay G Sanjayan, and Kwesi Sagoe-Crentsil. (2007). 'Comparative performance of geopolymers made with metakaolin and fly ash after exposure to elevated temperatures', *Cement and Concrete Research*, 37: 1583-1589.
- Kriven, Waltrud M, and Jonathan L Bell. (2004). "Effect of alkali choice on geopolymer properties." In *Proceedings of the 28th International Conference on Advanced Ceramics and Composites*, 99-104.

Kumar, Chandan, Krishna Murari, and CR Sharma. (2014). 'Strength Characteristics of Low Calcium Fly Ash Based Geopolymer Concrete', International Organization of Scientific Research (IOSR) Journal of Engineering (2014). ISSN (e): 2250-3021.

Lavanya, G., and Jegan, J. (2015). Evaluation of relationship between split tensile strength and compressive strength for geopolymer concrete of varying grades and molarity. *Int. J. Appl. Eng. Res*, 10(15), 35523-35527.

Li, Zongjin, and Wenlai Li. (2003). "Contactless, transformer-based measurement of the resistivity of materials." In.: Google Patents. US 6,639,401 B2

Lian, C., and Zhuge, Y. (2010). Optimum mix design of enhanced permeable concrete—an experimental investigation. *Construction and Building Materials*, 24(12), 2664-2671.

Luck, J. D., Stephen R W., Mark S. C., and Stephen F. H. (2008). 'Solid material retention and nutrient reduction properties of pervious concrete mixtures. *Biosystems engineering*, (100) 401-408.

Luck, Joe D, Stephen R Workman, Mark S Coyne, and Stephen F. (2009). 'Consequences of manure filtration through pervious concrete during simulated rainfall events. *Biosystems Engineering Higgins* (102) 417-23.

Madheswaran, C.K., Ambily, P. S., Lakshmanan N., Dattatreya, D. K. and Sathik, S. A. (2014). Shear Behavior of Reinforced Geopolymer Concrete Thin-Webbed T-Beams, *ACI materials journal*, 111.

Mahboub, K. C., Canler, J., Rathbone, R., Robl, T., and Davis, B. (2009). Pervious concrete: Compaction and aggregate gradation. *ACI Materials Journal*, 106(6), 523.

Malayali, A. B., and Chokkalingam, R. B. (2018). Mechanical properties of geopolymer pervious concrete. *International Journal of Civil Engineering and Technology*, 9, 2394-2400.

Malayali, A. B., Chokkalingam, R. B., and Singh, M. V. (2019, October). Experimental study on the compressive strength and permeable properties of GGBS based geopolymer pervious concrete. In *IOP Conference Series: Materials Science and Engineering* (Vol. 561, No. 1, p. 012004). IOP Publishing.

Malayali, A. B., Chokkalingam, R. B., Krishnan, T. H., and Nagaselvam, P. I. O. P. (2020, June). Effect of molar content on GGBS based geopolymer pervious concrete. In *IOP Conference Series: Materials Science and Engineering* (Vol. 872, No. 1, p. 012146). IOP Publishing.

McDonald, M., and Thompson, J. L. (2006). Sodium silicate a binder for the 21st century. *National silicates and PQ Corporation of Industrial Chemicals Division*.

- ME, M. U. L. B., and Shimpale, M. P. M. (2019). Experimental Investigation of Fly Ash Based Geopolymer Concrete. *International Research Journal of Engineering and Technology* (6) 1307-1313
- Meininger, R. C. (1988). No-fines pervious concrete for paving. *Concrete International*, 10(8), 20-27.
- Mindess, S., Young, J. F., and Darwin, D. (1981). Hydration of Portland Cement. *Chapter-4, Concrete, 1st ed, Prentice-Hall, Inc, Englewood, Cliffs, New Jersey.*
- Morsy, M. S., Alsayed, S. H., Al-Salloum, Y., and Almusallam, T. (2014). Effect of sodium silicate to sodium hydroxide ratios on strength and microstructure of fly ash geopolymer binder. *Arabian journal for science and engineering*, 39(6), 4333-4339.
- Mustafa Tuncan, Ö. A., Ramyar, K., and Karasu, B. (2007). Effect Of Compaction On Assessed Concrete Strength. In *The IV. Ceramic, Glass, Enamel, Glaze and Pigment Seminar with International Participation (SERES 2007)*.
- Nath, P., and Sarker, P. K. (2014). Effect of GGBFS on setting, workability and early strength properties of fly ash geopolymer concrete cured in ambient condition. *Construction and Building materials*, 66, 163-171.
- Nawy, Edward G. (2008). Concrete construction engineering handbook (*CRC press*).
- Neithalath, N., Weiss, J., and Olek, J. (2006). Characterizing enhanced porosity concrete using electrical impedance to predict acoustic and hydraulic performance. *Cement and Concrete Research*, 36(11), 2074-2085.
- Olivia, M., and Nikraz, H. (2012). Properties of fly ash geopolymer concrete designed by Taguchi method. *Materials and Design (1980-2015)*, 36, 191-198.
- Pacheco-Torgal, F., Castro-Gomes, J., and Jalali, S. (2008). Alkali-activated binders: A review. Part 2. About materials and binders manufacture. *Construction and building materials*, 22(7), 1315-1322.
- Palomo, A., Grutzeck, M. W., and Blanco, M. T. (1999). Alkali-activated fly ashes: A cement for the future. *Cement and concrete research*, 29(8), 1323-1329.
- Park, S. B., Lee, B. J., Lee, J., and Jang, Y. I. (2010). A study on the seawater purification characteristics of water-permeable concrete using recycled aggregate. *Resources, Conservation and Recycling*, 54(10), 658-665.
- Park, S. B., and Tia, M. (2004). An experimental study on the water-purification properties of porous concrete. *Cement and concrete research*, 34(2), 177-184.
- Piemonti, A., Conforti, A., Cominoli, L., Sorlini, S., Luciano, A., and Plizzari, G. (2021). Use of iron and steel slags in concrete: state of the art and future perspectives. *Sustainability*, 13(2), 556.

Popovics, Sandor. (1982). *Fundamentals of Portland Cement Concrete: Fresh concrete book* (Wiley).

Provis, J. L., Lukey, G. C., and van Deventer, J. S. (2005). Do geopolymers actually contain nanocrystalline zeolites A reexamination of existing results. *Chemistry of materials*, 17(12), 3075-3085.

Puertas, F., and Fernández-Jiménez, A. (2003). Mineralogical and microstructural characterisation of alkali-activated fly ash/slag pastes. *Cement and Concrete composites*, 25(3), 287-292.

Rahmat, S. N., Ali, A. Z. M., Ibrahim, M. H. W., and Alias, N. A. (2017). Oil and grease removal from commercial kitchen waste water using carbonised grass as a key media. In *MATEC Web of Conferences* (Vol. 87, p. 01010). EDP Sciences.

Ramadoss, P., and Nagamani, K. (2006). Investigations on the tensile strength of high-performance fiber reinforced concrete using statistical methods. *Computers and Concrete*, 3(6), 389-400.

Rangan, B Vijaya. (2008). 'Fly ash-based geopolymer concrete'. handbook

Revie, R Winston. (2011). Uhlig's corrosion handbook (John Wiley and Sons).

Safari, S. (2016). Early-age mechanical properties and electrical resistivity of geopolymer composites (*Doctoral dissertation*, Brunel University London).

Sathonsaowaphak, A., Chindaprasirt, P., and Pimraksa, K. (2009). Workability and strength of lignite bottom ash geopolymer mortar. *Journal of Hazardous Materials*, 168(1), 44-50.

Shen, J. G., Guo, C. Y., Chen, M., Yu, J. K., and Jiang, M. F. (2006). Utilization of metallurgical slag as resource materials in China. *Developments in Chemical Engineering and Mineral Processing*, 14(3- 4), 487-493.

Siddique, Rafat. (2008). *Waste materials and by-products in concrete* (Springer Science and Business Media), Handbook.

Silva, L. A., Borges, W. R., Cunha, L. S., Branco, M. G. C., Farias, M. M., and Mayne, P. W. (2013). Use of GPR to identify metal bars and layer thickness in a rigid pavement. *Geotech. Geophys. Site Charact*, 4, 1341-1346.

Škvára, František, Tomáš Jílek, and Lubomír Ceram.-Silik Kopecký. (2005). 'Geopolymer materials based on fly ash', (49) 195-204.

Sonebi, Mohammed, Mohamed Bassuoni, and Ammar Yahia. (2016). 'Pervious concrete: mix design, properties and applications', *RILEM Technical Letters*, (1)109-15.

Song, X. (2007). Development and performance of class F fly ash based geopolymer concretes against sulphuric acid attack (*Doctoral dissertation*, UNSW Sydney).

- Srinivasan, V., Pazhani, K. C., Kumar, S. S., and Bharatkumar, B. H. (2017). Geopolymer Concrete a Sustainable Building Materials for Rural Housing. *J. Environ. Nanotechnol*, 6(2), 14-19.
- STMFH (2013a). ", Standard Test Method for Flow of Hydraulic Cement Mortar, ASTM International, *West Conshohocken*, PA, 2013,." In ASTM C1437-13.
- Sumajouw, DMJ, D Hardjito, SE Wallah, and BV Journal of materials science Rangan. (2007). 'Fly ash-based geopolymer concrete: study of slender reinforced columns', 42: 3124-3130.
- Sumajouw, M.D.J. and Rangan, B.V.(2006). Low-Calcium fly ash-based geopolymer concrete: Reinforced beams and columns. Curtin University of Technology. *Report*
- Sumanasooriya, Milani S, and Narayanan Neithalath.( 2011). 'Pore structure features of pervious concretes proportioned for desired porosities and their performance prediction', *Cement and concrete composites*, 33: 778-787.
- Sun, Z., Lin, X., and Vollpracht, A. (2018). Pervious concrete made of alkali activated slag and geopolymers. *Construction and Building Materials*, 189, 797-803.
- Swain, B., Mishra, C., Kang, L., Park, K. S., Lee, C. G., and Hong, H. S. (2015). Recycling process for recovery of gallium from GaN an e-waste of LED industry through ball milling, annealing and leaching. *Environmental research*, 138, 401-408.
- Szostak, R. (1989). Molecular Sieves: Principles of Synthesis and Identification. *Part of the book series: Van Nostrand Reinhold Electrical/Computer Science and Engineering Series* (NRECSSES).
- Tangchirapat, W., Jaturapitakkul, C., and Chindaprasirt, P. (2009). Use of palm oil fuel ash as a supplementary cementitious material for producing high-strength concrete. *Construction and Building Materials*, 23(7), 2641-2646.
- Temuujin, J., Williams, R. P., and Van Riessen, A. V. (2009). Effect of mechanical activation of fly ash on the properties of geopolymer cured at ambient temperature. *Journal of materials processing technology*, 209(12-13), 5276-5280.
- Tennis, P. D., Leming, M. L., and Akers, D. J. (2004). Pervious concrete pavements (No. PCA Serial No. 2828). *Skokie, IL: Portland Cement Association*.
- Tho-In, T., Sata, V., Chindaprasirt, P., and Jaturapitakkul, C. (2012). Pervious high-calcium fly ash geopolymer concrete. *Construction and Building Materials*, 30, 366-371.
- Tomosawa, F., and Noguchi, T. (1993, June). Relationship between compressive strength and modulus of elasticity of high-strength concrete. In Proceedings of the Third International Symposium on Utilization of High-Strength Concrete (Vol. 2, pp. 1247-1254). Lillehammer, Norway: Norwegian Concrete Assn.

- Tyner, J. S., Wright, W. C., and Dobbs, P. A. (2009). Increasing exfiltration from pervious concrete and temperature monitoring. *Journal of environmental management*, 90(8), 2636-2641.
- Valiev, M., and Kosimov, H. International Journal of Recent Technology and Engineering (IJRTE) ISSN: 2277-3878. *Locomotive Diesel Engine Excess Air Ratio Control Device*, 8.
- Van Jaarsveld, J. G. S., Van Deventer, J. S. J., and Schwartzman, A. (1999). The potential use of geopolymeric materials to immobilise toxic metals: Part II. Material and leaching characteristics. *Minerals Engineering*, 12(1), 75-91.
- Van Jaarsveld, JGS, JSJ Van Deventer, and GC Lukey.( 2003). 'The characterisation of source materials in fly ash-based geopolymers', *Materials Letters*, 57: 1272-1280.
- Wallah, S. E., Hardjito, D., Sumajouw, D. M., and Rangan, B. V. (2005). Performance of fly ash based geopolymer concrete under sulfate and acid exposure. In *Geopolymer, Green Chemistry and Sustainable Development Solutions: Proceedings of the World Congress Geopolymer* (Vol. 153).
- Wang, H., Li, H., and Yan, F. (2005). Synthesis and mechanical properties of metakaolinite-based geopolymer. *Colloids and Surfaces A: Physicochemical and Engineering Aspects*, 268(1-3), 1-6.
- Xie, Z., and Xi, Y. (2001). Hardening mechanisms of an alkaline-activated class F fly ash. *Cement and Concrete Research*, 31(9), 1245-1249.
- Xu, Hua, and JSJ Van Deventer.( 2000). 'The geopolymerisation of alumino-silicate minerals', *International journal of mineral processing*, 59: 247-266.
- Yang, Jing, and Guoliang Jiang. 2003. 'Experimental study on properties of pervious concrete pavement materials', *Cement and Concrete Research*, 33: 381-386.
- Zakaria, Nor Azazi, A Ab Ghani, Rozi Abdullah, L Mohd Sidek, AH Kassim, and Anita Ainan. (2004). "MSMA—a new urban stormwater management manual for Malaysia." In *international conference “ICHE*.
- Zende, R., and Mamatha, A. (2015). Study on fly ash and GGBS based geopolymer concrete under ambient curing. *Journal of Emerging Technologies and Innovative Research*, 2(7), 3082-3087.